# Riparian Buffers, Floodplain Management, and Subsurface Phosphorus Transport in Alluvial Floodplains in the Ozark Plateau

# FINAL REPORT

**Output 16.4.1 of *Program to Improve the Adoption Rates and Efficiency of Best Management Practices to Protect Oklahoma Waters from Nonpoint Source Pollution***

**OCC Task 08-146**
**FY 2007-2008 319(h) Project 16**
**EPA Grant C9-996100-14**

Submitted to:

Oklahoma Conservation Commission

Submitted by:


Dr. Garey A. Fox[1], Associate Professor, Project PI
Dr. Daniel E. Storm[1], Professor, Project Co-PI
Dr. Todd Halihan[2], Project Co-PI
Dr. Chad J. Penn[3], Assistant Professor, Project Co-PI
Dr. Glenn Brown[1], Professor, Project Co-PI
Mr. Derek M. Heeren[1], Research Engineer
Mr. Ronald B. Miller[1], Graduate Research Assistant
Mr. Aaron R. Mittelstet[1], Research Engineer

[1]Department of Biosystems and Agricultural Engineering
[2]School of Geology
[3]Department of Plant and Soil Sciences
Oklahoma State University
Stillwater, OK


July 20, 2010

## AKNOWLEDGEMENTS

We would like to thank the Oklahoma Conservation Commission and Environmental Protection Agency Region VI for their generous funding and support of this project. The authors acknowledge Dan Butler, Bill Berry, Sharon Beck, and Shannon Tate for providing access to the alluvial floodplain properties. Amanda K. Fox, Stillwater, OK, is acknowledged for her assistance with the Matlab software. The authors also acknowledge Wayne Kiner and the Biosystems and Agricultural Engineering Laboratory staff, Oklahoma State University, for fabrication and essential machine maintenance. The following individuals from Oklahoma State University are thanked for their assistance with field and laboratory work: Tim Sickbert, Jorge Guzman, Dr. Maria Chu-Agor, Grant Graves, Katie Morgan, Jesi Lay, Sharla Lovern, Jason Walker, and Elliot Rounds.

**This report was prepared as part of a research study of preferential flow paths and their occurrence at sites in the Illinois River and Honey Creek basins conducted by Oklahoma State University. It was paid for in whole or in part with funds provided by the U.S. Environmental Protection Agency as administered by the Oklahoma Conservation Commission as authorized by Mike Thralls, executive director. Copies have been deposited with the Publication Clearinghouse of the Oklahoma Department of Libraries.**

# TABLE OF CONTENTS

Title Page ……1
Acknowledgements ……..2
Table of Contents ……..3
Executive Summary ……..4
Chapter 1: Detailed Description of Alluvial Floodplain Sites ……13
Chapter 2: Geophysical Mapping of Preferential Flow Paths ……..21
Chapter 3: Subsurface Heterogeneity and Transient Storage ……43
Chapter 4: Phosphorus Concentrations in PFP and non-PFP Groundwater ……..63
Chapter 5: Comparison of Subsurface and Surface Runoff P Transport ……75
Appendix A: Quality Assurance Report ……84
Appendix B: USDA NRCS Web Soil Survey Maps ……85
Appendix C: FEMA 2009 Floodplain Maps ……..94

# EXECUTIVE SUMMARY

## Overview

Eutrophication due to excess nutrients is currently a major issue in eastern Oklahoma and western Arkansas. Eutrophication can be detrimental to waterways and costly to remediate. In this region of concentrated poultry production, high phosphorus (P) poultry feed is imported and poultry, which is low in P, is exported. What remains in the region is nutrient rich poultry litter, which is bulky and expensive to export. Therefore, the poultry litter is applied to nearby pastures as an inexpensive fertilizer, and over time results in elevated soil test phosphorus (STP) with an increasing risk of P loss to streams and reservoirs. There has been a major focus on implementing conservation practices in the region to decrease P reaching the streams. Some conservation practices include the use of riparian buffers to filter surface runoff and fences to keep cattle out of the streams. Both of these can be effective in decreasing P in surface runoff, but may not help with subsurface P transport. Scientists and engineers need to identify critical nutrient source areas and transport mechanisms within a catchment in order to protect and enhance drinking water systems, recreation activities, and aquatic ecosystems. While surface runoff is considered to be the primary transport mechanism for P, subsurface transport through coarse subsoil to gravel bed streams may be significant and represent a source of P not alleviated by current conservation practices (e.g., riparian buffers). Subsurface transport may be important due to local or regional conditions, even for a highly sorbing contaminant such as P.

The study area is in the Ozark ecoregion, which is characterized by karst topography such as caves, springs, sinkholes and losing streams. The erosion of limestone has left a residuum of chert gravel, producing gravel-bed streams and coarse alluvial aquifers overlain by a mantle of gravelly loam or silt loam (Figure 1). Topsoil depth in the floodplains ranged from 1 to 300 cm in the Oklahoma Ozarks, and generally increased with increasing stream order. Previous work at a site in eastern Oklahoma found preferential flow paths (PFPs) within the gravel subsoil with an estimated hydraulic conductivity of 140 to 230 m $d^{-1}$. It is hypothesized that these PFPs, if there is connectivity to the soil surface, can provide a rapid P transport mechanism through the alluvial groundwater system to the stream.

Key results from this project include the following: Subsurface geophysics was used to map PFPs at four floodplain sites, showing zones of high hydraulic conductivity within each alluvial floodplain. Water table elevation data showed PFPs acting as groundwater flow convergence or divergence zones, with their activity depending on stream stage. In PFPs that were activated and connected to the stream, total P concentrations approached the P level in the stream during flood events. Subsurface P load estimates, using Monte Carlo simulations, showed that the alluvial aquifers had a capacity for subsurface P transport, bypassing riparian buffers. If P leaching through the topsoil is also significant, these subsurface flow paths may be a rapid and efficient method of transporting P from fertilizer at the soil surface to the stream. This could have significant implications for how riparian floodplains are managed in the Ozark ecoregion.

## PFP Mapping

PFP mapping is a non-invasive method to determine the nature and extent of the PFPs in the Ozark ecoregion. Previous field experiments have documented a PFP affecting alluvial groundwater flow in an alluvial floodplain and that water flow in the PFP was transmitted at rates

that limited sorption of P. The implication of these findings depends partly on the frequency and distribution of similar preferential flow features. To this end, multi-electrode electrical resistivity imaging (ERI) was completed at four floodplain sites (Pumpkin Hollow, Honey Creek, Flint Creek, and Barren Fork Creek) in the Ozark ecoregion. Electrical resistivity is a soil property that depends on particle size, surface electrical properties, pore saturation, and the ionic content of pore fluids, and generally has a positive correlation with hydraulic conductivity. ERI was effective at locating zones of high hydraulic conductivity in the alluvial floodplains, with results showing significant subsurface heterogeneity at each site (Figure 1).

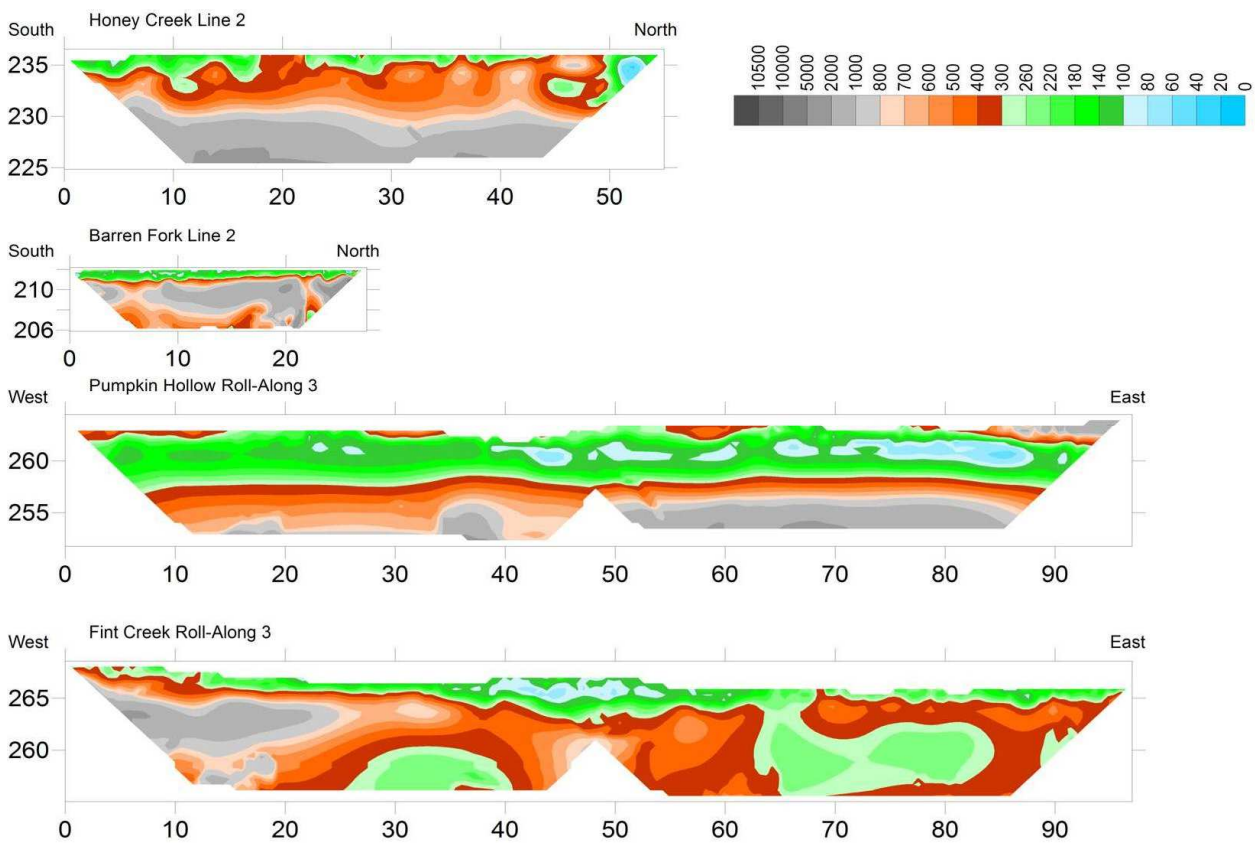


Figure 1. Example resistivity profiles from each floodplain site. All sites show horizontal distribution of high resistivity lenses in the vadose zone near the soil surface.

Borehole permeameter tests using an apparatus specifically designed for gravel subsoils were used to estimate saturated hydraulic conductivity (*K*) in the vadose zone. A relationship was derived to relate *K* with electrical resistivity (Figure 2), making it possible to make three dimensional grids of *K* based on ERI data. The median and mean *K* at the Barren Fork Creek site were 71 m $d^{-1}$ and 94 m $d^{-1}$, respectively, with a maximum value of 1750 m $d^{-1}$. At the Honey Creek site, the median and mean *K* were 50 m $d^{-1}$ and 52 m $d^{-1}$, respectively, with a maximum value of 105 m $d^{-1}$. Among the four sites, maximum electrical resistivity and hydraulic conductivity generally increased as stream order increased.

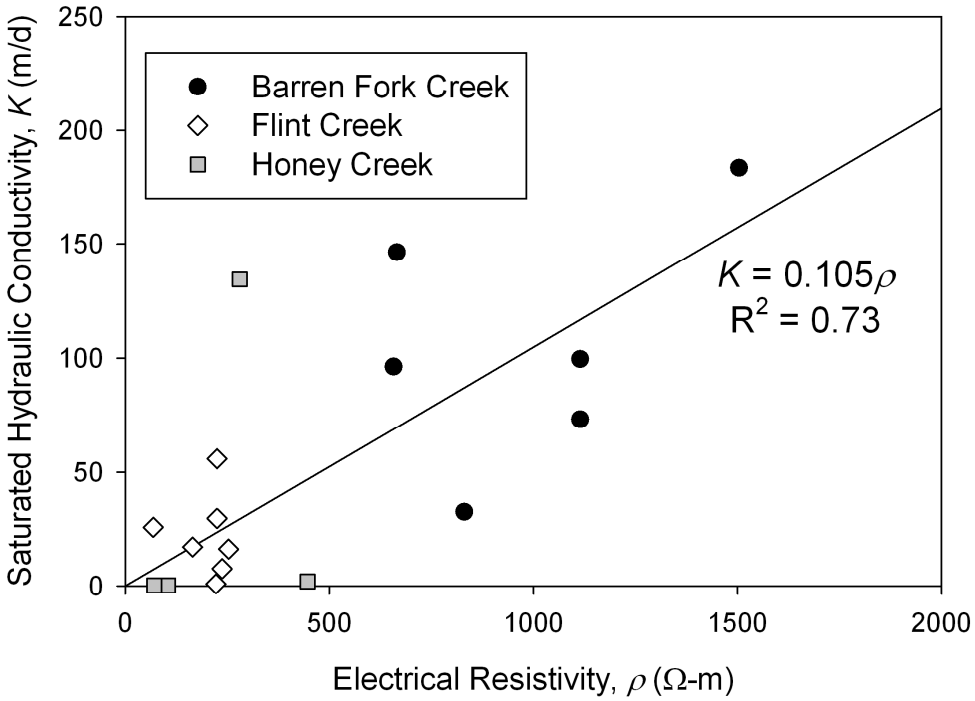


Figure 2. Correlation between electrical resistivity and saturated hydraulic conductivity at Flint Creek, Honey Creek and Barren Fork Creek field sites.

## Aquifer Heterogeneity and Transient Storage

Water table elevation data were used to further characterize the heterogeneity of *K* in the alluvial aquifers. The alluvial system is often considered homogeneous due to convenience, yet a better understanding is necessary for estimating flow and contaminant transport in alluvial systems. Based on the correlation between resistivity and *K*, monitoring wells were installed in both PFP and non-PFP subsoils at the Honey Creek and Barren Fork Creek field sites. Loggers were placed in 24 wells at each site, recording water pressure and temperature at five minute intervals over a period of six weeks, including multiple high flow events. The effect of aquifer heterogeneity and transient storage on groundwater flow patterns was observed to be dependent on changes in stream stage. Divergence of the water table gradient (Figure 3) was used as an indicator of heterogeneity in *K*, and changes in flow direction (Figure 4) were used as an indication of transient storage. It is also hypothesized that highly conductive alluvial systems are transient storage zones for nutrients, acting as a sink during high flow and a source during base flow. The procedures in this project provide methodologies for quantifying subsurface heterogeneity, focused recharge/discharge, and transient storage in groundwater for alluvial floodplains.

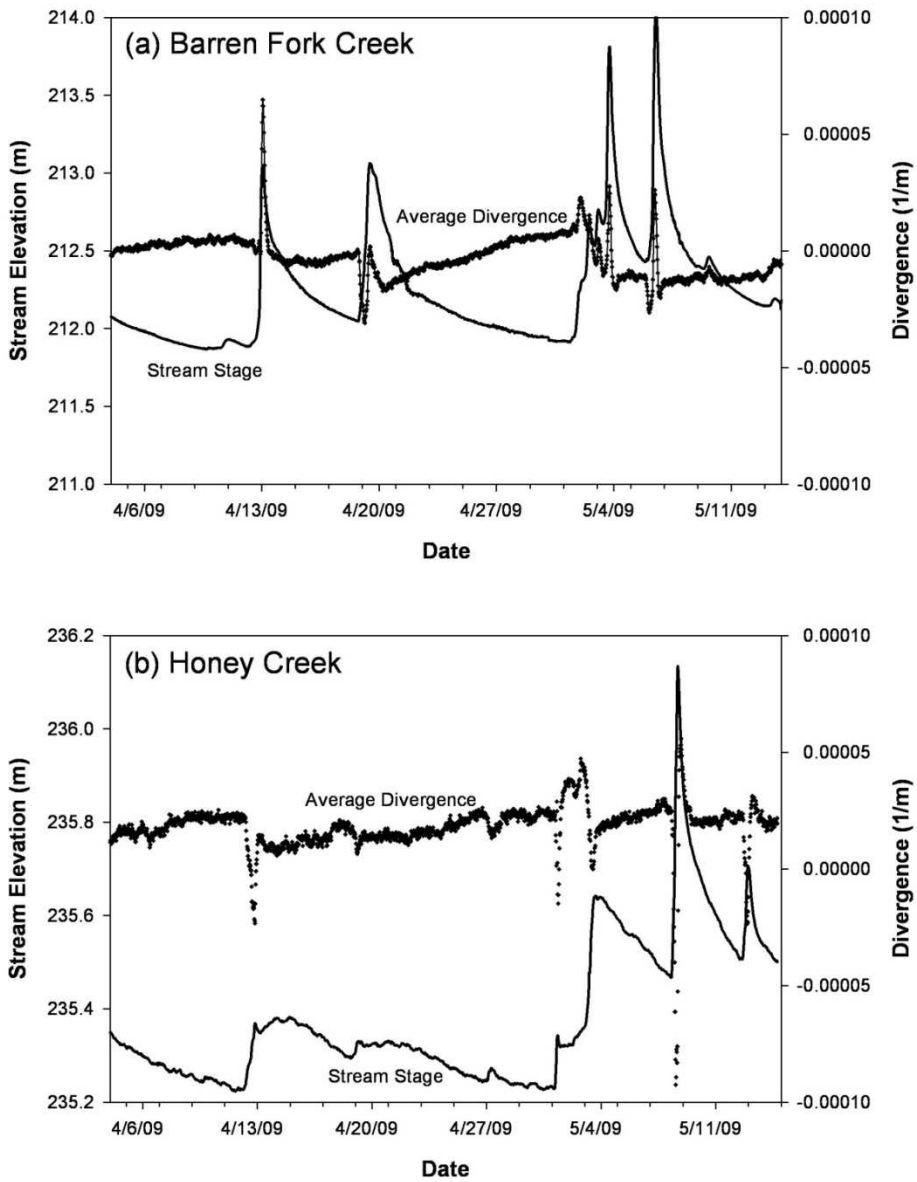


Figure 3. Divergence data for the Barren Fork Creek site (a) and the Honey Creek site (b).

The PFPs appeared to act as flow divergence zones allowing stream water to quickly enter the groundwater system, or as flow convergence zones draining a large groundwater area. Divergence correlated closely with stream stage, with maximum divergence or convergence (Figure 3) occurring with maximum rates of change in stream stage. Flow directions in the groundwater changed considerably between base and high flows (Figure 4), suggesting that the floodplains acted as a transient storage zone, rapidly storing and releasing water during the passage of a storm hydrograph. Such transient storage may have a direct impact on the transport of in-stream contaminant loads as the stream water interacts with the alluvial groundwater along floodplains throughout the watershed. Assumptions of uniform, homogeneous stream/aquifer interaction and only localized, near-streambed hyporheic interactions were not appropriate in the studied alluvial floodplains. In fact, the Barren Fork

Creek was a losing stream at the study site, even during base flow and falling limb conditions. We hypothesize a flow pattern where water regularly left the stream at one point within the study area, traveled through the aquifer, and reentered further downstream outside of the study area. Also, groundwater models of these alluvial floodplains should account for the non-random nature of heterogeneity in hydraulic conductivity, as well as the fact that some PFPs may only become activated after a minimum stream stage is reached.

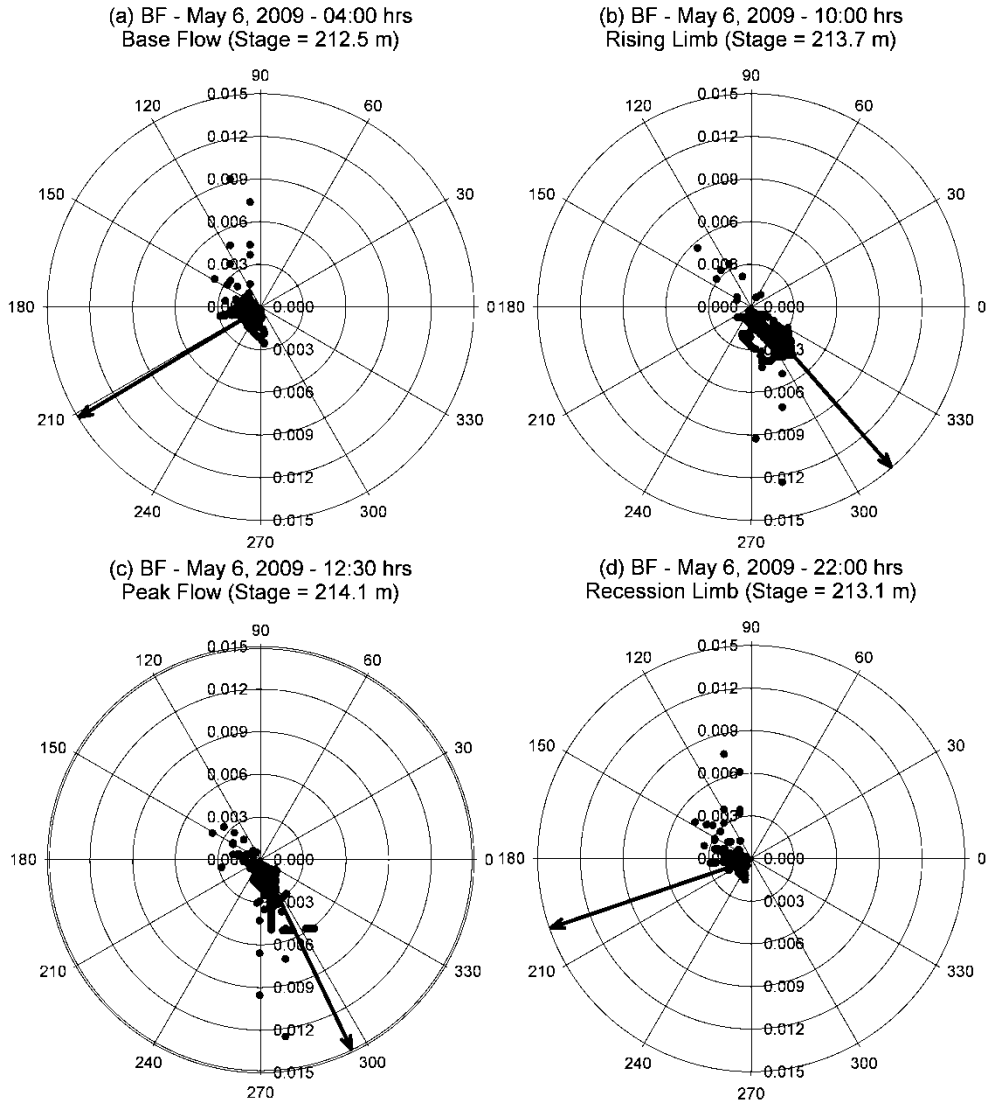


Figure 4. Polar plots of the hydraulic gradients at the Barren Fork Creek field site on May 6, 2009, during the passage of a hydrograph: (a) base flow, (b) rising limb, (c) peak flow, and (d) falling limb. The polar plots are constructed with the magnitude and direction of the groundwater gradient for all points in the floodplain grid, with the arrow indicating the direction of the average groundwater gradient.

## Alluvial Aquifer Phosphorus Concentrations

Phosphorus concentrations in the alluvial systems were documented during multiple high flow events at each site (Figure 5-6). It is hypothesized that PFPs, if connected to the soil surface, provide a rapid and efficient method of transporting P to the receiving stream. Water samples were obtained from the observation wells and the stream and analyzed for total P to document concentration gradients over time. During baseflow conditions, groundwater P concentrations were typically 0.01 to 0.04 mg/L and 0.02 to 0.06 mg/L at the Barren Fork Creek and Honey Creek field sites, respectively. During high flow events, the maximum P concentrations measured in the groundwater were as high as 0.20 mg/L at the Barren Fork Creek site and 0.25 mg/L at the Honey Creek field site.

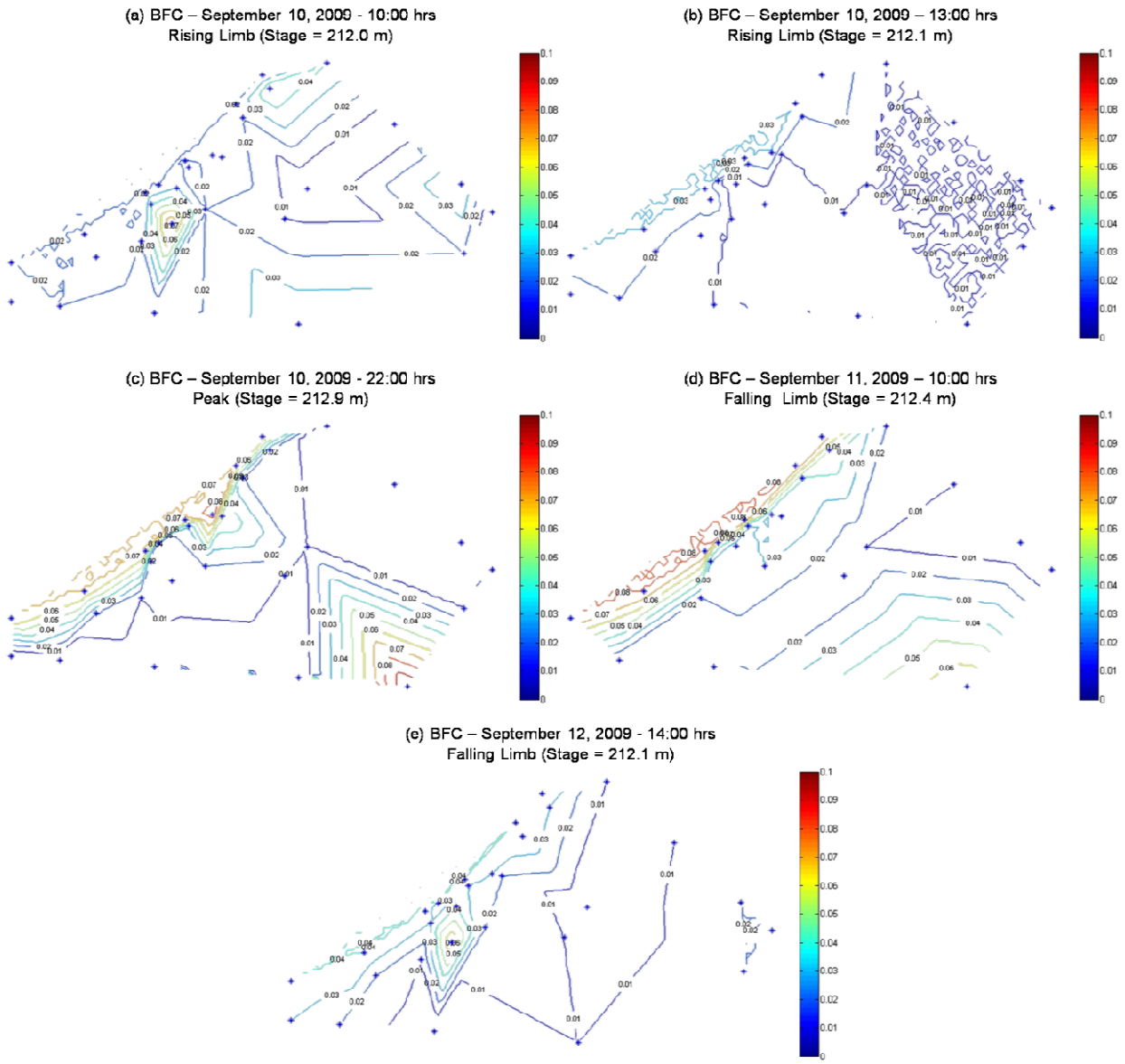


Figure 5. Total phosphorus concentration (mg/L as P) contour plots for the Barren Fork Creek (BFC) site for the September 10, 2009 high flow event.

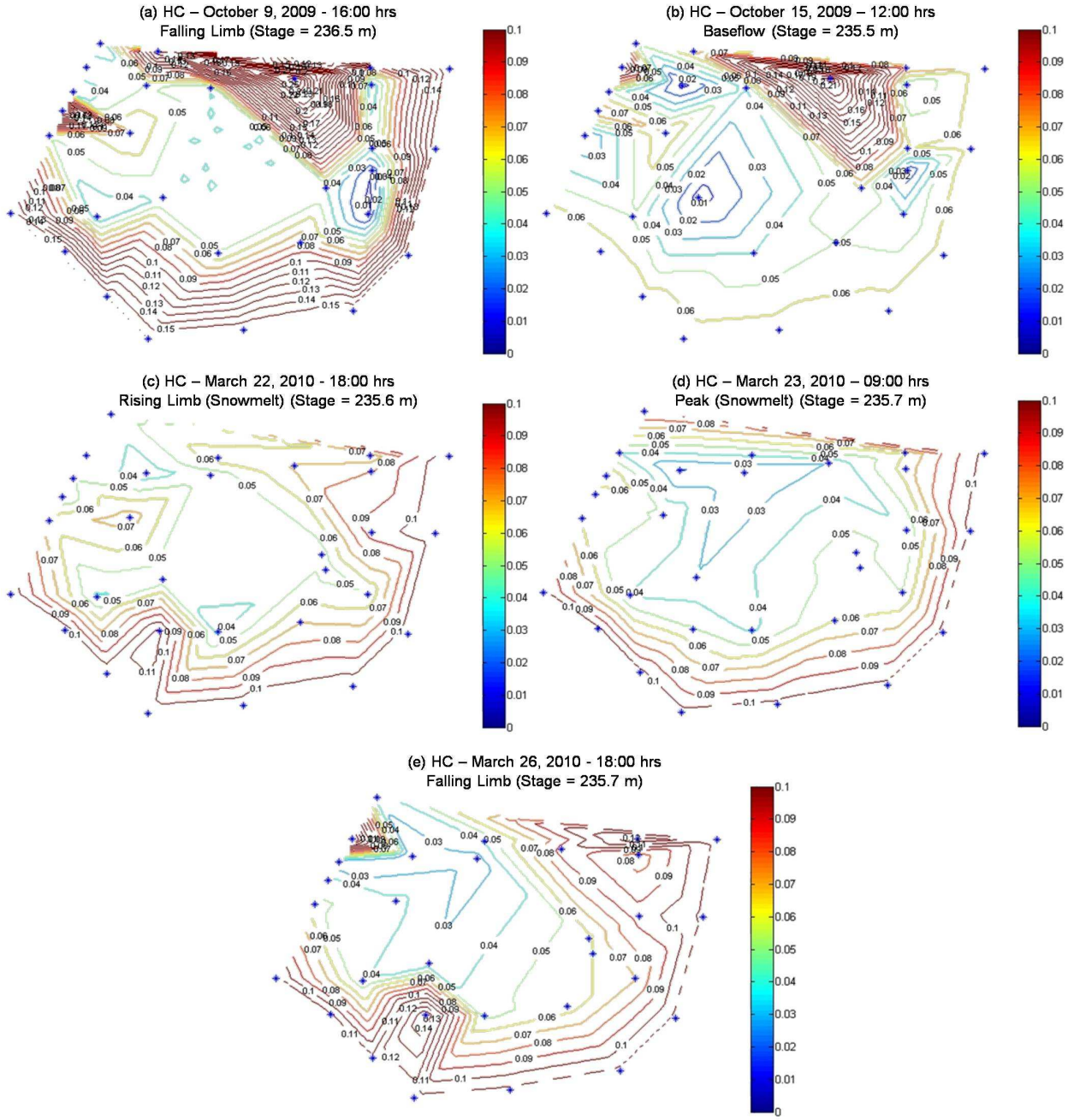


Figure 6. Total phosphorus concentration (mg/L as P) contour plots for Honey Creek (HC) for the October 9, 2009 and March 23 and March 25, 2010 flow events.

P concentrations were generally highest where stream water was entering the groundwater system, and decreased with distance down-gradient from the stream. Even though total P concentrations generally decreased as stream water moved through the aquifer due to sorption and dilution, transient storage was occurring in the alluvial aquifer as seen in the significant levels of P leaving the study area (and presumably re-entering the stream).

In the PFPs, rapid transport of P occurred in the groundwater system with concentrations at or near the P concentration in the creeks during larger storm events when the PFPs were activated. Without properly locating observation wells within the pathways, general groundwater monitoring may have never indicated this preferential flow. This demonstrated that the PFPs were capable of transporting high concentrations of P through the subsurface, bypassing riparian buffers. The pathways with rapid P transport did not necessarily correlate to subsurface zones of high hydraulic conductivity. Pathways of high hydraulic conductivity must be hydraulically activated (i.e., stream stage above a minimum elevation) for preferential flow to occur and must be connected to a source of P (e.g., surface water) for preferential transport of P to occur. High P levels at the soil surface would be another possible source for preferential transport, but that transport mechanism was not studied in this project.

## Surface and Subsurface Phosphorus Loads

The groundwater P concentrations, *K*, depth and width of the aquifers, groundwater gradient, and the number of days per year the subsurface transport was active were used to quantify the subsurface P transport capacity through a boundary with one PFP (estimated based on the annual subsurface P load). Using Monte Carlo simulations based on statistical distributions of the above parameters, the subsurface transport capacity was estimated and compared to the surface runoff P based on simulations by PPM Plus for the current land management practices and soil P levels at the sites (i.e., no litter application or cattle grazing), as shown in Figure 7. At the Barren Fork Creek field site, the mean subsurface P load in the non-PFPs and a single PFP was 0.12 kg $yr^{-1}$, or approximately 25% of the P loads from surface runoff. At the Honey Creek site, the mean subsurface P transport capacity was 0.02 kg $yr^{-1}$ or 3% of P load from surface runoff based on current site conditions (Figure 7). Simulations were also performed based on intensive pasture management typical for the region with poultry litter application and cattle grazing. These scenarios resulted in total P surface runoff of 14.0 kg $yr^{-1}$ at the Barren Fork and 9.8 kg $yr^{-1}$ at Honey Creek, an order of magnitude greater than the estimated subsurface P transport capacities estimated in this project for the current site conditions.

Though the total P capacity was relatively small in the single PFP due to the small area and number of days active, it may provide rapid transport from the surface to the aquifer and from the aquifer to the stream. In areas where there is a larger number or area of PFPs or during years where the PFPs remain active for longer periods of time, the PFPs may provide larger P transport capacities. The Honey Creek site had a smaller P transport capacity due to a smaller cross-sectional area (e.g., depth of the aquifer) and *K* than the Barren Fork Creek site. As stream order increases, the significance of subsurface P capacity and PFPs may also increase. At larger stream orders, the depth of the aquifer and *K* generally increase due to larger gravel deposits. For example, compared to the Barren Fork Creek, the Illinois River may have a deeper aquifer, higher *K*, and larger PFPs, and therefore higher subsurface P capacity.

Subsurface P transport capacity was significant relative to the surface runoff based on current site conditions. These results indicated that the subsurface P capacity of alluvial floodplains through with a single PFP in the Ozark ecoregion was at least $10^{-2}$ to $10^{-1}$ kg $yr^{-1}$, although the capacity may be higher in cases where the subsurface is connected to a larger source of P. Further work is needed to address sites with poultry litter application and cattle grazing, quantifying P leaching through the topsoil resulting in potentially higher subsurface P loads. If P leaching through the topsoil is significant, these subsurface flow paths may be a rapid and efficient method of transporting P from fertilizer at the soil surface to the stream. This could have significant implications for how riparian floodplains are managed in the Ozark ecoregion.

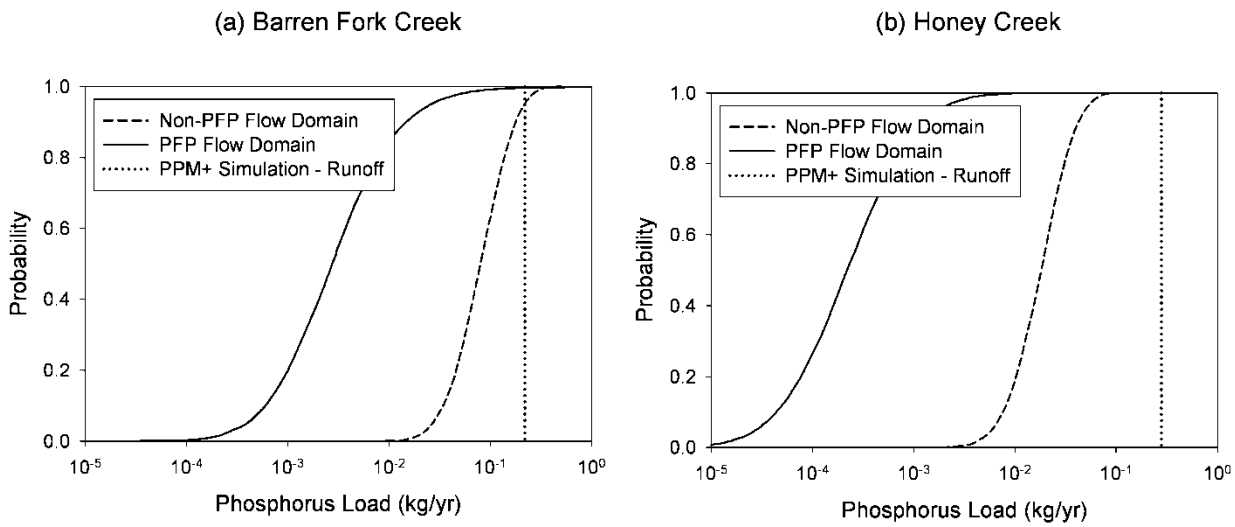


Figure 7. Total phosphorus load capacity of subsurface with a single PFP based on Monte Carlo simulations and surface runoff total phosphorus loads based on PPM Plus simulations at the Barren Fork Creek and Honey Creek field sites. PFP = preferential flow pathways; non-PFP = non-preferential flow.

# CHAPTER 1
# DETAILED DESCRIPTION OF ALLUVIAL FLOODPLAIN SITES

## Overview

The riparian floodplain sites were located in the Ozark region of northeastern Oklahoma. The Ozark ecoregion of Missouri, Arkansas, and Oklahoma is characterized by karst topography, including caves, springs, sink holes, and losing streams. The erosion of carbonate bedrock (primarily limestone) by slightly acidic water has left a large residuum of chert gravel in Ozark soils, with floodplains generally consisting of coarse chert gravel overlain by a mantle of gravelly loam or silt loam (Figure 1.1). Topsoil depth in the floodplains ranged from 1 to 300 cm in the Oklahoma Ozarks, and generally increased with increasing stream order. Common soil series include Elsah (frequently flooded, 0-3% slopes) in floodplains; Healing (occasionally flooded, 0-1% slopes) and Razort (occasionally flooded, 0-3% slopes) in floodplains and low stream terraces; Britwater (0-8 % slopes) on high stream terraces; and Clarksville (1-50%) on bluffs. A typical soil pedon (USDA Soil Survey) is shown in Table 1.1.

Table 1.1. Typical pedon for Razort gravelly loam, which is common in the floodplains of the Ozark ecoregion of Oklahoma and Arkansas.

| Horizon | Depth (cm) | Soil Type |
|---|---|---|
| A | 0-30 | Gravelly loam |
| Bw | 30-109 | Gravelly loam |
| C | 109-152 | Very gravelly loam |

For phosphorus (P), the primary transport mechanism from source areas into surface water systems has been considered to be surface runoff, with subsurface transport considered to be negligible (Turner and Haygarth, 2000). However, local or regional conditions, such as those found in the Ozark Plateau, can lead to conditions where subsurface transport is important. Previous work (Fuchs et al., 2009), conducted at the Barren Fork Creek site, demonstrated that subsurface transport of injected phosphorus during three tracer tests was significant in a localized preferential flow path (PFP). It is hypothesized 1) that PFPs, if connected to the soil surface, provide a fast and efficient method of subsurface P transport, and 2) that subsurface gravel may act as a transient storage zone, providing a P sink during high flow and a P source during baseflow.

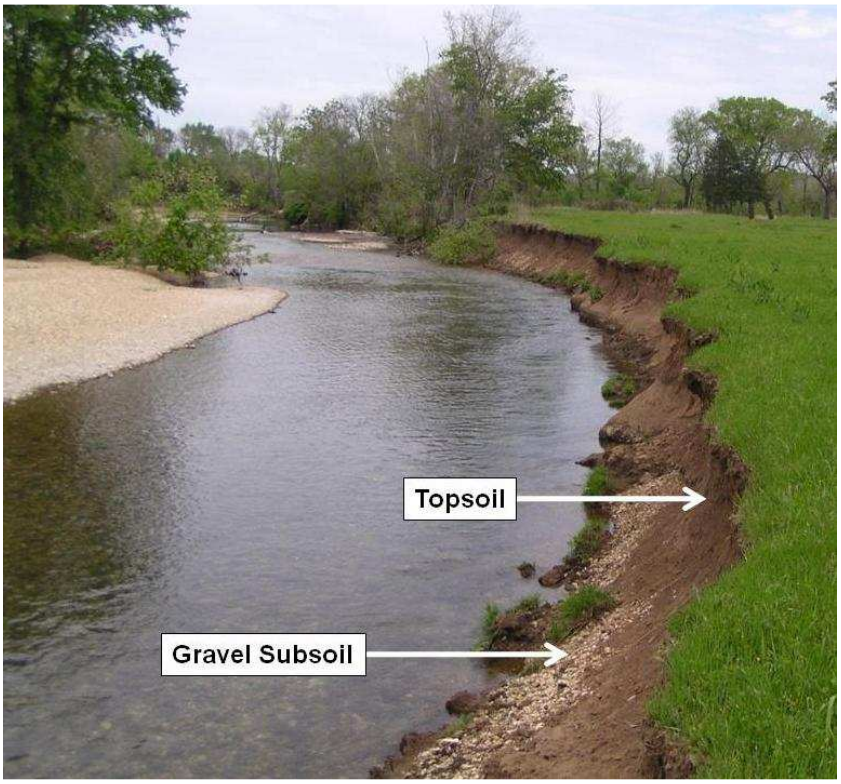


Figure 1.1. Floodplains in the Ozark ecoregion generally consist of coarse chert gravel overlain by a mantle (1-300 cm) of topsoil.

In order to better characterize the presence and activity of PFPs in the Ozark Plateau, four riparian floodplain sites were selected (Figure 1.2) based on riparian buffer widths, spatial location in the basin (i.e., headwater versus low-gradient), small versus large floodplains, and differences in floodplain management (Table 1.2).

Table 1.2. Land use and watershed characteristics of riparian floodplain sites.

| Site | Watershed Area ($km^2$) | Median Daily Discharge ($m^3 s^{-1}$) | Land Use |
|---|---|---|---|
| Barren Fork Creek | 845 | 3.6 | Hay field |
| Flint Creek | 300 | 1.6 | Riparian forest, hay field |
| Honey Creek | 150 | 0.54 | Riparian forest, hay field |
| Pumpkin Hollow | 15 | Intermittent | Pasture |

Figure 1.2. Location of riparian floodplain sites in the Ozark ecoregion of Oklahoma.

## Barren Fork Creek Site

The Barren Fork Creek site, five miles east of Tahlequah, Oklahoma, in Cherokee county (Figures 1.3 and 2.6, latitude: 35.90°, longitude: -94.85°), is located just downstream of the Eldon U.S. Geological Survey (USGS) gage station (07197000). A tributary of the Illinois River, the Barren Fork Creek has a median daily flow of 3.6 $m^3 s^{-1}$ and an estimated watershed size of 845 $km^2$ at the study site. Historical aerial photographs of the site demonstrate the recent geomorphic activity including an abandoned stream channel that historically flowed in a more westerly direction than its current southwestern flow path (Figure 1.3).

Fuchs et al. (2009) described some of the soil and hydraulic characteristics of the Barren Fork Creek floodplain site. The floodplain consists of alluvial gravel deposits underlying 0.5 to 1.0 m of topsoil (Razort gravelly loam, Appendix B). Topsoil infiltration rates are reported to range between 1 and 4 m/d based on USDA soil surveys (USDA, 1970). The gravel subsoil, classified as coarse gravel based on the Wentworth (1922) scale, consists of approximately 80% (by mass) of particle diameters greater than 2.0 mm, with an average particle size ($d_{50}$) of 13 mm. Estimates of hydraulic conductivity for the gravel subsoil range between 140 and 230 m $d^{-1}$ based on falling-head trench tests (Fuchs et al., 2009). Soil particles less than 2.0 mm in the gravelly subsoil consist of secondary minerals, such as kaolinte and noncrystalline Al and Fe oxyhydroxides. Ammonium oxalate extractions on this finer material estimated initial phosphorus saturation levels of 4.2% to 8.4% (Fuchs et al., 2009).

Figure 1.3. Aerial photos for 2003 (left) and 2008 (right) show the southward migration of the stream toward the bluff and the large deposits of gravel in the current and abandoned stream channels. The study site is the hay field in the south-central portion of each photo (red arrow).

The floodplain site is a hay field with occasional trees (Figure 1.4). The field has a Soil Test Phosphorus (STP) of 33 mg/kg (59 lb/ac) and has not received fertilizer for several years. The southern border of the floodplain is a bedrock bluff that rises approximately 5 to 10 m above the floodplain elevation and limits channel migration to the south. The floodplain width at the study site is 20 to 100 m from the streambank (based on the 100 year floodplain, FEMA, 2009, Appendix C); however, water was observed 200 m from the streambank (to the bluff) during a 6 year recurrence interval flow event with (Figure 1.4).

Figure 1.4. The Barren Fork site is a hay field (left). The site becomes completely inundated during large flow events (right).

## Flint Creek Site

The Flint Creek site, eight miles west of West Siloam Springs, Oklahoma, in Delaware County (Figures 1.5 and 2.8, latitude: 36.20°, longitude: -94.71°), is located immediately upstream of

the USGS gage station (07196000) near Kansas, OK. Also a tributary of the Illinois River, Flint Creek has a median daily flow of 1.6 $m^3$ $s^{-1}$ and an estimated watershed area of 300 $km^2$ at the study site.

Figure 1.5. The Flint Creek site is west of the creek (left) and includes both riparian forest and a hay field (right).

The Flint Creek site is a hay field with a riparian buffer composed of an average of 50 m of forest. The 100 year floodplain (FEMA, 2009, Appendix C) extends 120 to 160 m from the streambank (just across the road). The riparian area is primarily Elsah very gravelly loam, with the rest of the site composed of Healing silt loam and Britwater gravelly silt loam (Appendix B). The Flint Creek site is located on the outside of a bend in an eroded area, leaving a view of subsoil layering (Figure 1.6).

Figure 1.6. Similar to the Barren Fork Creek, Flint Creek is ladened with large gravel bars (left). The streambank profile shows complex layering (right).

## Honey Creek Site

The Honey Creek site, five miles southeast of Grove, Oklahoma, in Delaware County (Figures 1.7, 1.8, and 2.7, latitude: 36.54°, longitude: -94 .70°), is located immediately downstream of an USGS gage station (07189542) and is a tributary of the Grand Lake O' the Cherokees. A smaller order stream, Honey Creek has a median daily flow of 0.54 $m^3 s^{-1}$ and an estimated 150 $km^2$ watershed at the study site.

Figure 1.7. The Honey Creek site was located within a meander bend.

The Honey Creek site is located at the edge of a tree farm. Having received poultry litter in the past, the STP is 60 mg/kg (106 lb/ac). The study area includes a hayfield and a riparian area composed of an average of 50 m of forest. From the streambank at the southern tip of the meander bend, the 100 year floodplain (FEMA, 2009, Appendix C) extends 230 m (to the bluff). The entire study area is a Razort gravelly loam (Appendix B), with a topsoil thickness of 0.1 to 0.5 m. Located on the inside of a bend, the area is likely to be aggradational. Just downstream, a stream restoration project was recently completed, including a small dam that backs up water part way around the bend.

Figure 1.8. Honey Creek displays algae growth during base flow (left) and turbid water during high flow (right).

## Pumpkin Hollow Site

The Pumpkin Hollow site, 12 miles northeast of Tahlequah, Oklahoma, in Cherokee County (Figures 1.9 and 2.9, latitude: 36.02°, longitude: -94.81°) has an estimated watershed area of 15 $km^2$. A small tributary of the Illinois River, Pumpkin Hollow is an ephemeral stream in its upper reaches. During March at the floodplain site, the stream was dry in some places but emerged in pools or short flowing reaches elsewhere.

Figure 1.9. Pumpkin Hollow is a narrow valley ascending from the Illinois River to the plateau.

The Pumpkin Hollow site is pasture for cattle (Figure 1.10). The entire floodplain is 120 to 130 m across (FEMA, 2009, Appendix C). The study area was a combination of Razort gravelly loam and Elsah very gravelly loam (Appendix B), with a topsoil thickness ranging from 1 to 3 cm.

Figure 1.10. The Pumpkin Hollow site in spring (left) and winter (right). The thickness of the topsoil layer above the gravel aquifer is minimal.

# CHAPTER 2
# GEOPHYSICAL MAPPING OF PREFERENTIAL FLOW PATHS

## Abstract

In the Ozark ecoregion of Oklahoma, Arkansas and Missouri, the erosion of carbonate bedrock (primarily limestone) by slightly acidic water has left a residuum of chert gravel, producing gravel-bed streams and floodplains generally consisting of coarse chert gravel overlain by a mantle (1 to 300 cm) of gravelly loam or silt loam. Previous work has documented the occurrence of preferential flow paths (PFP) in an alluvial floodplain. Field experiments have shown that the PFP affected alluvial groundwater flow in the floodplain and that water flow in the PFP was transmitted at rates that limited sorption of phosphorus. The implication of these findings depends partly on the frequency and distribution of similar preferential flow features. To this end, four floodplain sites were chosen for comparative mapping. The sites were located in the Ozark region of northeast Oklahoma and had similar underlying geology but differed in watershed area, land cover, and stream order. Subsurface features at the sites were mapped using electrical resistivity imaging (ERI). Vadose zone hydraulic conductivity was measured at three sites using a direct-push borehole permeameter. The ERI profiles at each site showed that the subsurface was heterogeneous and areas of high electrical resistivity formed discrete, possibly continuous features in the vadose zone. Interpolations, based on variograms of resistivity, showed that resistivity within the alluvial aquifers formed patterns that were often linked to geomorphic processes. Hydraulic conductivity within the alluvial aquifers was estimated by applying an empirical linear relationship between electrical resistivity and hydraulic conductivity. Since all of the alluvial floodplain sites were gravel dominated systems, the sites were similar enough that the linear relationship between electrical resistivity and hydraulic conductivity was not site-specific. The positive slope of the relationship suggested that areas of continuous high resistivity could also act as zones of preferential flow within the aquifer under suitable hydrologic conditions. Among the sites, maximum electrical resistivity and hydraulic conductivity generally increased with increasing watershed area.

## Introduction

The chert-bearing carbonate geology of the Ozarks produces complex hydrologic flow patterns influenced by caves, sinkholes, springs, and also streams with beds and banks dominated by coarse chert gravel (Jacobson and Gran, 1999). However, in some parts of the Ozarks, stream and reservoir water quality is threatened, partly as a result of changes in land use that have increased nutrient concentrations and loads (Menjoulet et al., 2009).

Alluvial floodplains are complex and dynamic landforms resulting from channel migration, fluvial erosion and sediment deposition, producing both vertical and horizontal spatial heterogeneity (Bridge, 2003). Previous work has documented complex subsurface flow patterns for gravel-dominated floodplains in the Ozarks. Using an array of monitoring wells designed to capture subsurface flow from an injection trench to a nearby stream, Fuchs et al. (2009) found a preferential flow path (PFP) that transported water bearing a conservative tracer (Rhodamine WT) and phosphorus (P) in a discrete direction in subsurface alluvial gravels. The tracer concentration found in the wells within the PFP (2 to 3 m from the trench) was similar to the

concentration in the trench, while non-PFP wells located a similar distance from the trench had greatly reduced concentrations. The rate of transport in the PFP was found to overwhelm the potential for P sorption, allowing P to travel from the injection trench and along the PFP in relatively undiminished concentrations (Fuchs et al., 2009). Larger-scale transport experiments have also demonstrated the influence of the PFP, acting in accordance with the larger groundwater system dynamics, on conservative tracer transport (Heeren et al., 2010b).

Subsurface PFPs are undetectable by visual inspection of the surface and thus mapping PFPs requires an indirect method. Electrical resistivity imaging (ERI) has been used to measure two- and three-dimensional profiles below the surface in near-surface applications. Auton (1992) and Beresnev et al. (2002) have used ERI for gravel prospecting, Gourry et al. (2003) and Green et al. (2005) for mapping buried paleochannels, and Smith and Sjogren (2006) for geologic investigation of glacial deposits. Baines et al. (2002) and Bersezio et al. (2007) are among those who have used ERI to map floodplain fluvial sediments, while Crook et al. (2008) used ERI to map the sedimentary structure of the active streambed itself.

Researchers have noted that both Darcy's Law of flow in porous media and Archie's Law of resistivity (Archie, 1942) depend on the porosity of the matrix material, and theorized a relationship between the electrical resistivity of a porous media and its water transmitting characteristics (Lesmes and Friedman, 2005). Since the hydraulic properties of aquifers are difficult to accurately measure across large areas and ERI offers a relatively rapid and inexpensive window into the subsurface, this relationship has been sought as a way to estimate the hydraulic conductivity of aquifers. However, the relationship is not straightforward. Mazac et al. (1985) noted that previous work showed both positive and negative correlations between resistivity and hydraulic conductivity. Similarly, Dam et al. (2000) notes that while a general relationship between electrical resistivity and hydraulic conductivity has not been found, site-specific empirical relationships can be effectively determined.

Evaluating the importance of subsurface PFPs for planning and environmental modeling requires understanding their material nature and spatial distribution at the field and watershed scales. The objectives of this project were two-fold: (1) to assess the presence of potential high hydraulic conductivity PFPs in several alluvial floodplains sites, and (2) derive three-dimensional hydraulic conductivity maps to better aid in understanding the movement of water and potential contaminants within the alluvial aquifers.

## Materials and Methods

### *Floodplain Field Sites*

The Ozark ecoregion of Missouri, Arkansas, and Oklahoma (Figure 2.1) is characterized by karst topography, including caves, springs, sink holes, and losing streams. The erosion of carbonate bedrock (primarily limestone) by slightly acidic water has left a large residuum of chert gravel in Ozark soils, with floodplains generally consisting of coarse chert gravel overlain by a mantle of gravelly loam or silt loam that ranges in thickness from 0.1 to 3 m. Topsoil depth in the floodplain generally increased with increasing stream order. Common soil series in the region include Elsah (frequently flooded, 0 to 3% slopes) in floodplains; Healing (occasionally flooded, 0 to 1% slopes) and Razort (occasionally flooded, 0 to 3% slopes) in floodplains and low stream terraces; Britwater (0 to 8 % slopes) on high stream terraces; and Clarksville (1 to 50%) on bluffs. Four sites were selected on a variety of streams within the Ozark region of northeastern Oklahoma (Figure 2.1). Watershed size and land use varied at each site (Table 2.1).

Figure 2.1. Location of the selected floodplain sites in northeastern Oklahoma.

Table 2.1. Land use and watershed characteristics of the studied floodplain sites.

| Site | Watershed Area ($km^2$) | Median Daily Discharge[1] ($m^3 s^{-1}$) | Primary Land Use |
|---|---|---|---|
| Barren Fork Creek | 845 | 3.6 | Hay field |
| Flint Creek | 300 | 1.6 | Riparian forest, hay field |
| Honey Creek | 150 | 0.54 | Riparian forest, hay field |
| Pumpkin Hollow | 15 | Intermittent | Pasture |

[1]Source: U.S. Geological Survey

### *Electrical Resistivity Imaging*

Electrical Resistivity Imaging (ERI) is a geophysical method commonly used for near-surface investigations which measures the resistance of earth materials to the flow of DC current between two source electrodes. The method is popular because it is efficient and relatively unaffected by many environmental factors that confound other geophysical methods. According to Archie's Law (Archie, 1942), earth materials offer differing resistance to current depending on grain size, surface electrical properties, pore saturation, and the ionic content of pore fluids.

Normalizing the measured resistance by the area of the subsurface through which the current passes and the distance between the source electrodes produces resistivity, reported in ohmmeters ( Ω-m), is a property of the subsurface material (McNeill, 1980). Mathematical inversion of the measured voltages produces a two-dimensional profile of the subsurface showing areas of differing resistivity (Loke and Dahlin, 2002, Halihan et al., 2005).

ERI data were collected using a SuperSting R8/IP Earth Resistivity Meter (Advanced GeoSciences Inc., Austin, TX) with a 56-electrode array. The ERI surveys at the four sites occurred between June 2008 and March 2009. Fourteen lines were collected at the Barren Fork Creek site, five at the Honey Creek site, four at the Flint Creek site, and three at the Pumpkin Hollow site. One line at the Barren Fork Creek site and all of the lines at Flint Creek and Pumpkin Hollow were “roll-along” lines that consisted of sequential ERI images with one-quarter overlap of electrodes. The profiles at the Barren Fork Creek site employed electrode spacing of 0.5, 1.0, 1.5, 2.0 and 2.5 m with associated depths of investigation of approximately 7.5, 15.0, 17.0, 22.5 and 25.0 m, respectively. All other sites utilized a 1-m spacing. The area of interest in each study site was less than 3 m below the ground surface and thus well within the ERI window. The resistivity sampling and subsequent inversion utilized a proprietary routine devised by Halihan et al. (2005), which produced higher resolution images than conventional techniques.

The OhmMapper (Geometrics, San Jose, CA), a capacitively-coupled dipole-dipole array, was effectively deployed at the relatively open Barren Fork Creek site for large scale mapping. The system used a 40 m array (five 5 m transmitter dipoles and one 5 m receiver dipole with a 10 m separation) that was pulled behind an ATV. Two data readings per second were collected to create long and data-dense vertical profiles. The depth of investigation was limited to 3 to 5 m. Positioning data for the ERI and OhmMapper were collected with a TopCon HyperLite Plus GPS with base station. Points were accurate to within 1 cm.

### *Three-Dimensional Interpolation*

The ERI profiles were collected to assess the heterogeneity within the subsurface of the alluvial floodplains. The profiles themselves were two-dimensional and provided insight into only a small proportion of the subsurface. Interpolation between the ERI lines can provide insight into the possible distribution of resistivity across the entire floodplain study area. Variograms are a representation of spatial variation created by measuring the sum of squared differences of data pairs separated by every possible distance within the data set (Isaaks and Srivastava, 1989). The variogram components included the “nugget” or latent error of the estimate and the “range or the maximum distance for covariance between data points”. The variogram also included the angle and shape of anisotropy, which provided insight into the directionality of the closest relationship within the data. This was important in the context of PFPs since the angle of anisotropy could correspond to the flow direction within connected PFPs. A mathematical model (i.e., linear, quadratic, polynomial, exponential, etc.) fit to the variogram used the spatial variation within the data to interpolate values for the unsampled area. The variograms were generated using Surfer 8 (Golden Software, Golden, CO). Each site was modeled by selecting ERI data from a single elevation or horizontal “slices”. Slices were generated from the vadose zone of each site by estimating the baseflow water table elevation and then fitting as many slices as possible at 1 m increments. Several variograms were generated for each slice and used to interpolate the elevation “slice”. The resulting grid with the lowest standard deviation of variance was selected.

### *Saturated Hydraulic Conductivity*

At three of the field sites (Barren Fork Creek, Honey Creek, and Flint Creek), hydraulic conductivity (*K*) was measured using a modification of existing borehole permeameter techniques (Miller et al., 2010). The alluvial gravels encountered at the study sites required a cased hole to prevent collapse and powerful drilling techniques to reach the intended depths. To circumvent this shortfall, a slotted casing was devised that could be driven to a specific depth (Figure 2.2). The screen section consisted of an 8.25-cm pipe section with 27 vertical slots (0.002 m wide by 0.2 m long) arranged in three groups with solid (unslotted) sections in between. This arrangement was chosen to provide the pipe strength to resist the forces necessary to penetrate the coarse gravels at each site. The screened area was 0.01 $m^2$ with a ratio of open area to total area of 21%. The screen section allowed hydraulic conductivity testing of discrete depths of the floodplain vadose zone. A Geoprobe Systems (Salina, KS) 6200 TMP (trailer-mounted probe) direct-push drill rig was used to push the array of 8.25-cm diameter pipe sections to specified depths in the alluvial floodplain at each site.

Figure 2.2. Modified 0.082 m (3.25 inch) Geoprobe Systems pipe with screened sections in driving position. Screen consists of 27 0.002 m x 0.2 m slots arranged in three groups with three solid sections between to preserve pipe integrity for driving through coarse gravel strata.

The *K* testing consisted of driving the screened section to the desired depth, installing a vented pressure transducer at the bottom of the well, placing a water inflow pipe on the open end of the pipe, and pumping water into the well from a 3.8 $m^3$ portable tank. Testing in the well was initiated after the well reached a constant head (pseudo steady-state), usually after 10 to 15 minutes, and monitored with a pressure transducer. When necessary, flow into the well was adjusted with an in-line gate valve. Tests lasted approximately 15 minutes after reaching steady state, during which head in the well and level in the tank were recorded continuously. The flow into the well ($Q$, $m^3$ $s^{-1}$) was calculated using a stage/volume relationship for the tank and the total elapsed time for the test.

The *Q* and stage data were converted to hydraulic conductivity using the U. S. Bureau of Reclamation Gravity Permeability Method 2 test for permeability of unsaturated material (USBR, 1985). The method required a graphical determination to choose between three equations designed for use in unsaturated (Zone 1), partially saturated (Zone 2) and saturated (Zone 3) conditions. The equations, which are in conventional units, for the hydraulic conductivity were as follows:

Zone 1:
$$K_{fs} = \frac{Q}{C_u r_e H} \tag{2.1}$$

Zone 2:
$$K_{fs} = \frac{2Q}{\left[\left(C_s + 4\frac{r_1}{r_e}\right) r_e\right]\left(T_u + H - A\right)} \tag{2.2}$$

Zone 3 (below WT):
$$K_{fs} = \frac{Q}{\left(C_s + 4\frac{r_1}{r_e}\right) r_e H} \tag{2.3}$$

where $K_{fs}$ is field saturated hydraulic conductivity (ft $s^{-1}$), *Q* was discharge through the pipe ($ft^3$ $s^{-1}$), $C_u$ was an unsaturated conductivity coefficient, $C_s$ was a saturated conductivity coefficient, $r_e$ was effective radius (bore radius) of the well (ft), $r_1$ was the outside radius of casing (ft), *H* was the steady-state depth in the well (ft), and $T_u$ was the difference between depth to steady-state water surface and the depth to water table (ft). The test method required that the degree of saturation of the material be estimated graphically based on the relationship between the ratio of well head depth/water table depth and the percent of unsaturated stratum. The values for $C_s$ and $C_u$ were then graphically estimated based on the ratio of the head in the well to the effective radius of the well and the length of the screen section to the effective radius, respectively. The test was valid for test conditions where the saturated thickness (*S*, ft), was less than 5*l*, where *l* is the length of the screen section (ft); *l* greater than or equal to $10r_1$; and *Q/a* less than or equal to 0.10, where *a* was the perforated area of the screen ($ft^2$). Some tests, especially those with the highest *Q* into the permeameter, failed these requirements and were removed from further analysis. Approximately 20 measurements of $K_{fs}$ from the three field sites satisfied the above-mentioned criteria.

Each test produced a value of field saturated hydraulic conductivity, $K_{fs}$, which can be less than saturated hydraulic conductivity (*K*), especially in fine-grained soils with high capillarity. The gravel-dominated strata tested in this study had low capillarity and thus the measured $K_{fs}$ was assumed to approximate the actual *K*.

The *K* value was assumed to occur at the depth of the screen for each test. Depth and the test position on the ERI line were used to determine the resistivity from the formation that was influencing the *K* measurement. The electrical resistivity value was determined by averaging the four inverted resistivity values closest to that point. An empirical relationship was derived between *K* and electrical resistivity. Distributions of *K* within the three alluvial aquifers were estimated by transforming resistivity values from the three-dimensional ERI interpolations.

# Results and Discussion

## *Electrical Resistivity Imaging Results*

The ERI profiles showed heterogeneity of resistivity at each site as evidenced by the strong positive skew of resistivity values and the large number of extreme values seen in the resistivity boxplots (Table 2.2, Figure 2.3). The Barren Fork Creek site contained the most extreme resistivity range and the highest mean and maximum values, while the Honey Creek site had the highest median value.

Table 2.2. Descriptive statistics for vadose zone resistivity at the four study sites. All values are electrical resistivity in Ω-m.

| | Mean | Standard Deviation | Minimum | Median | Maximum |
|---|---|---|---|---|---|
| Barren Fork Creek | 534 | 829 | 10.9 | 276 | 19100 |
| Flint Creek | 239 | 185 | 32.8 | 187 | 2500 |
| Honey Creek | 351 | 228 | 3.0 | 313 | 2430 |
| Pumpkin Hollow | 387 | 351 | 57.7 | 263 | 3110 |

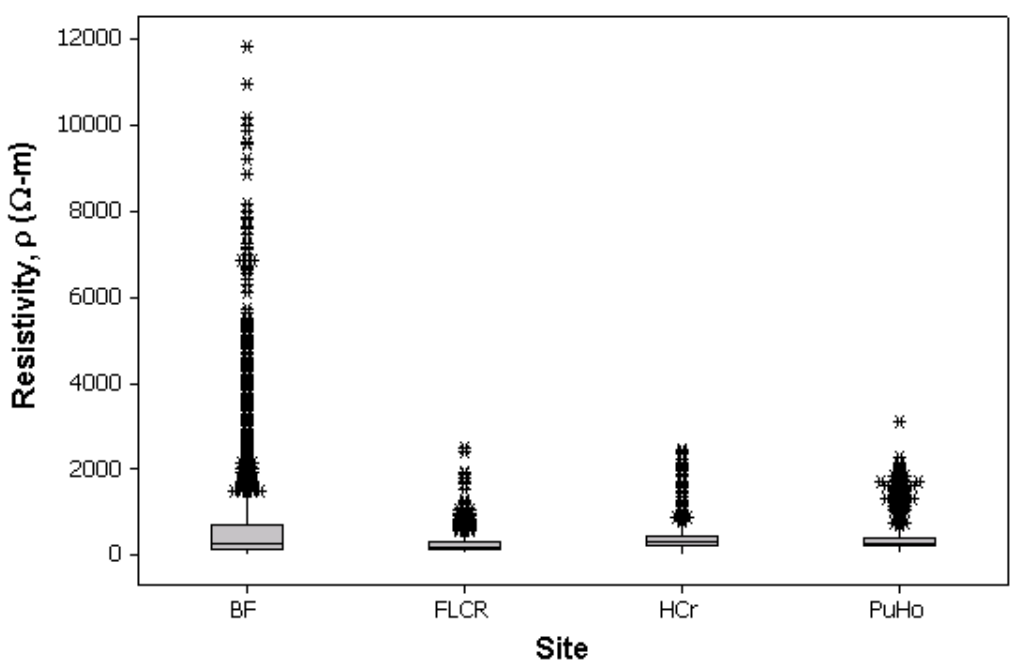


Figure 2.3. Boxplot of vadose zone resistivity at each site. BF = Barren Fork Creek, FLCR = Flint Creek, HCr = Honey Creek, and PuHo = Pumpkin Hollow.

The ERI profiles suggested that the resistivity was distributed heterogeneously with discrete areas of high and low resistivity (Figure 2.4). An increase in resistivity with depth was observed at all sites with the highest resistivities (> 5000 Ω-m) occurring at least 5 m below ground surface. These high values were consistent with the range of resistivity for limestone ($1 \times 10^3$ to $1 \times 10^7$ Ω-m), and was interpreted as competent bedrock. Lower resistivity layers above the bedrock corresponded to gravel or weathered limestone (i.e., epikarst). Indirect evidence for this interpretation comes from the Honey Creek site where push-probe installation of monitoring wells encountered refusal at depths above the zone interpreted as bedrock (Chapter 3; Heeren et al., 2010a).

Among the sites, maximum electrical resistivity generally increased with increasing watershed area (Table 2.2). It is hypothesized that larger order streams would have sediment transport capacities capable of moving larger particle sizes, producing higher resistivities in stream deposited gravel. However, the relationship between stream or watershed characteristics and resistivity was not always consistent, since the factors influencing fluvial geomorphology varied among the sites. For example, Pumpkin Hollow had the smallest area but the second highest mean and maximum resistivity. This was likely due to gravel transported onto the floodplain from nearby plateau surfaces, with the hillslopes able to transport larger gravel than the stream. Site-specific characteristics were also important at the Flint Creek site. While both the Barren Fork Creek and Honey Creek sites were dominated by their resident streams, the Flint Creek floodplain may have been primarily constructed by a smaller, seasonal tributary (6.2 $km^2$ watershed area), resulting in a low mean resistivity compared to Flint Creek's watershed area (300 $km^2$).

The depth of most interest for this project was the vadose zone or the area above the baseflow water table. This was the zone that controlled interaction between the ground surface and alluvial groundwater. Heterogeneity of resistivity within this zone was of particular interest because it could indicate the presence of PFPs. The sites, except Pumpkin Hollow, possessed a pattern of discrete high resistivity features within this zone, although the size and range of resistivities for these features varied. A detailed description of resistivity patterns within the zone of interest for each site follows. Field experience at the sites allows resistivities less than 100 Ω-m to be generally interpreted as fine-grained soils, 100 to 250 Ω-m as soil with gravel, 250 to 1000 Ω-m as gravel with fines, and >1000 Ω-m as clean gravel.

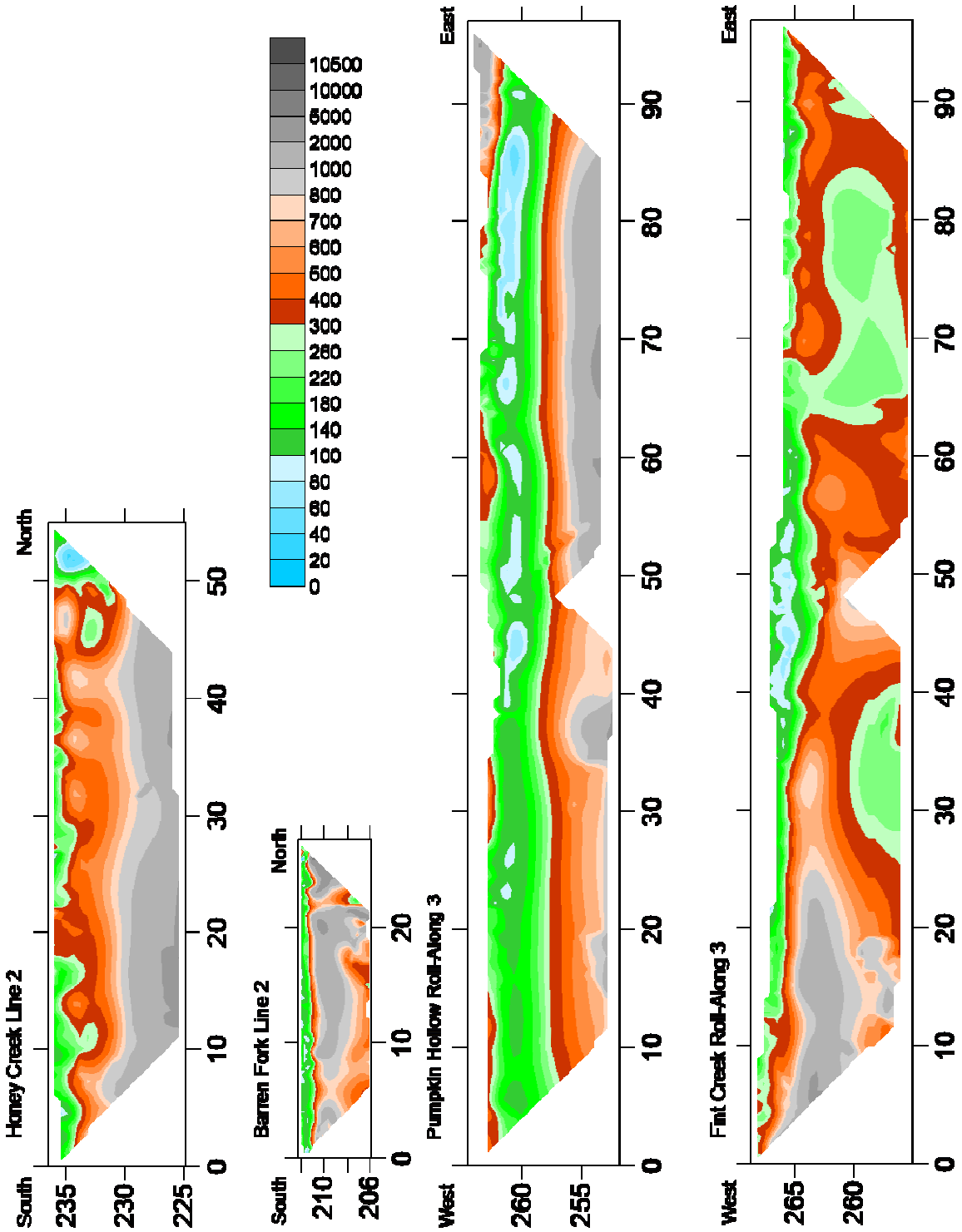


Figure 2.4. Example resistivity profiles from each site. All sites show horizontal distribution of high resistivity lenses in the vadose zone near the soil surface. Shallow depth to bedrock is evident in Honey Creek and Pumpkin Hollow profiles but the depth of investigation is too shallow to capture bedrock at the Flint Creek and Barren Fork Creek sites. The horizontal layer of low-resistivity at Pumpkin Hollow is interpreted as soil layer buried by gravel from nearby slopes. The y-axes are elevation above mean sea level (m); the x-axes are lateral distance (m).

### *Barren Fork Creek*

Resistivity at the Barren Fork Creek site appeared to conform generally to surface topography with higher elevations having higher resistivity, although the net relief was minor (~1 m). This was most evident in the OhmMapper resistivity profiles which covered most of the floodplain and which revealed a pattern of high and low resistivity that trended SW to NE (Figure 2.5). More precise imaging with reduced spatial coverage was obtained with the ERI. The area around the PFP was clearly imaged with the roll-along and cross lines 1 to 5 (0.5 to 1 m electrode spacing), as shown in Figure 2.6. This feature appeared be 1 to 2 m thick, trended SW to NE (similar to the pattern seen in the OhmMapper survey), dipped slightly down to the SW, and ranged in width from 3 to 5 m. Other high resistivity features seen in the OhmMapper survey were detected by the longer ERI lines; for example, a relatively high resistivity feature was observed at 30 m on line 11, 70 m on line 13, 80 m on line 12, and then again at 70 m on lines 7 and 8 (Figure 2.6). This feature formed an angle of about 50° from an EW line, but because of the wider electrode spacing, those profiles had less resolution so the dimensions of the feature were not as clear (Figure 2.6).

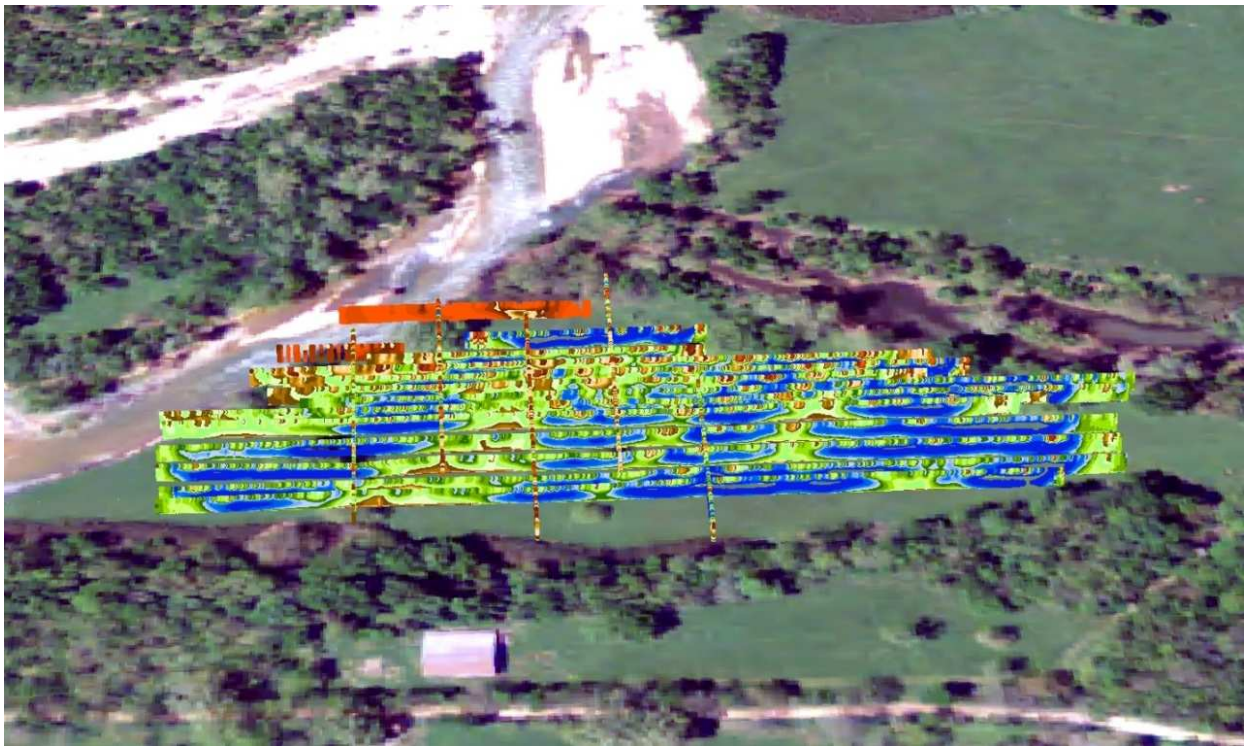

Figure 2.5. OhmMapper coverage of the Barren Fork Creek alluvial floodplain showing SW to NE trends of low (blue) and high (orange) resistivity. View is to the North and subsurface resistivity profiles are displayed above the aerial image for visualization purposes. Modified from Heeren et al. (2010b).

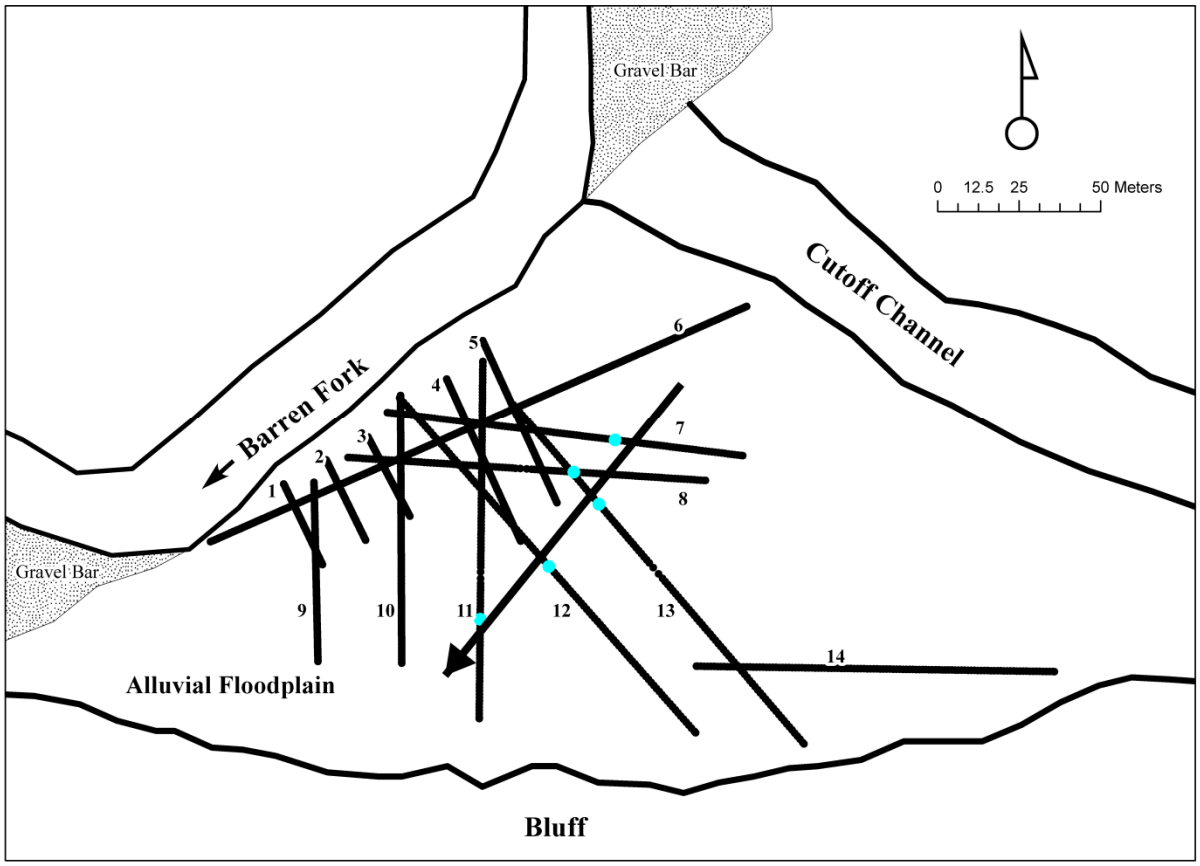


Figure 2.6. High resistivity feature locations on ERI lines at the Barren Fork Creek site (shown in blue). The orientation of the arrow representing potential connections in high resistivity was similar to high resistivity features seen in OhmMapper profiles (Figure 2.5).

The linear nature and NE-SW directional trend of these surface features, roughly parallel to the stream, suggested that they might be old stream channels and lateral gravel bars buried by floodplain sediment. Evidence that some of the high resistivity features within these floodplains were likely to be gravel bars was derived from ERI evidence where an ERI profile from an exposed mid-channel gravel bar at this site suggested resistivities in the same range as those in the PFP area (1000 to 5000 Ω-m). Also, gravel material collected from the surface of the bar was similar in particle-size distribution to material from the streambank at the PFP, with the percent of soil less than 2.0 mm diameter in the PFP and the gravel bar approximately 6% and 13% by mass, respectively (Heeren et al., 2010b). This comparison became available due to severe streambank migration which revealed a section of the PFP.

### *Honey Creek*

The baseflow water table at the Honey Creek site was at an elevation of approximately 234 m. The ground surface elevation was between 235 and 236 m. Four ERI profiles (1 m electrode spacing and 12.5 m profile depth) were collected with a general S-N orientation. Resistivity within the zone of interest ranged from less than 10 to 2400 Ω-m, with a mean of 351 Ω-m. Similar to the Barren Fork Creek site, it was observed that areas of high resistivity within the

zone of interest at Honey Creek appeared in discrete units 2 to 5 m wide and about 1 m thick and were associated with high topographic features. However, the ERI profiles were not spaced close enough to conclusively determine connectivity between the high resistivity features (Figure 2.7). Considering that the site was located on the inside of a meander bend, an area considered to be an aggradational point bar (Bridge, 2003), the high resistivity features may be sequential deposits that retain the curvilinear shape of the meander bend (Figure 2.7). The stream was presently depositing coarse gravel on the point bar and thus it was reasonable to assume that historic deposits contained gravel as well.

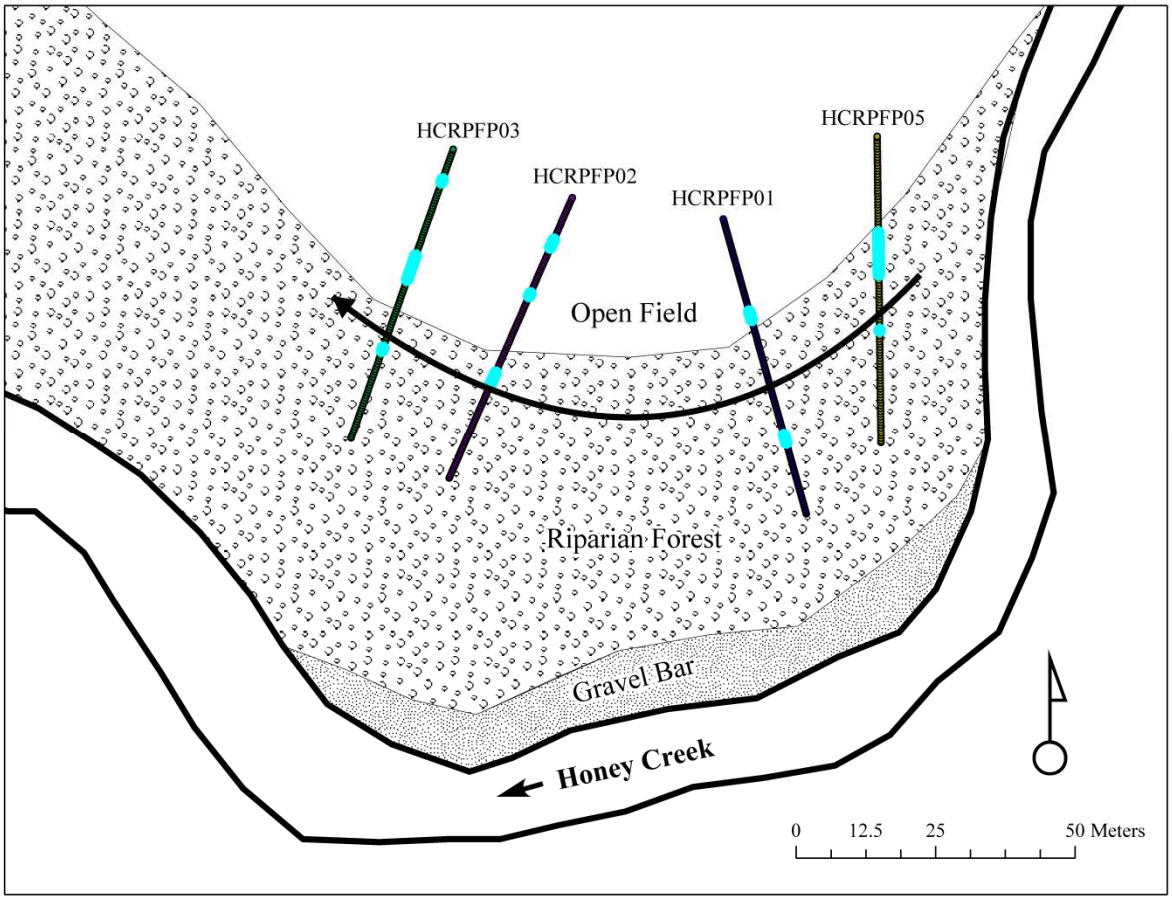


Figure 2.7. High resistivity feature locations on ERI lines at the Honey Creek site (shown in blue). The curved line represents the potential connection in high resistivity.

### *Flint Creek*

The Flint Creek site occupied a narrow floodplain currently being eroded. Five separate ERI profiles, including three composite roll-along lines were collected. Each line was oriented orthogonal to the creek and as close to W-E as possible considering the riparian forest cover. Each profile had a 1 m electrode spacing and 12.5 m depth of investigation. The general alluvial floodplain surface elevation was about 267 m and the water table elevation about 265 m, so the area of interest extended approximately 2 m in depth. The range of resistivity found in the ERI profiles within the alluvial interest area was 33 to 2500 Ω-m, with a mean of 239 Ω-m, and a distribution similar to the Honey Creek site (Figure 2.3). The vertical distribution of resistivity at the Flint Creek site was unique among sites studied because the profiles showed considerable

variation in resistivity with depth. For instance, line 1 resulted in high resistivity close to the surface, which was likely to be a bedrock similar to an outcrop directly across the stream, while roll-along lines 2-3, 5-6 and 4-7 all showed a marked decrease in resistivity at the bottom of the profile suggesting that the bedrock seen in line 1 had dipped strongly to the north (Figure 2.8). Except line 1, the profiles had discrete areas of high resistivity ranging from 10 m in width in the northern lines to 1 m in lines 2-3. The high resistivity was likely due to gravel lenses within the floodplain, although the source may not be Flint Creek itself but rather a tributary that crosses the floodplain in the vicinity of line 8 (Figure 2.8).

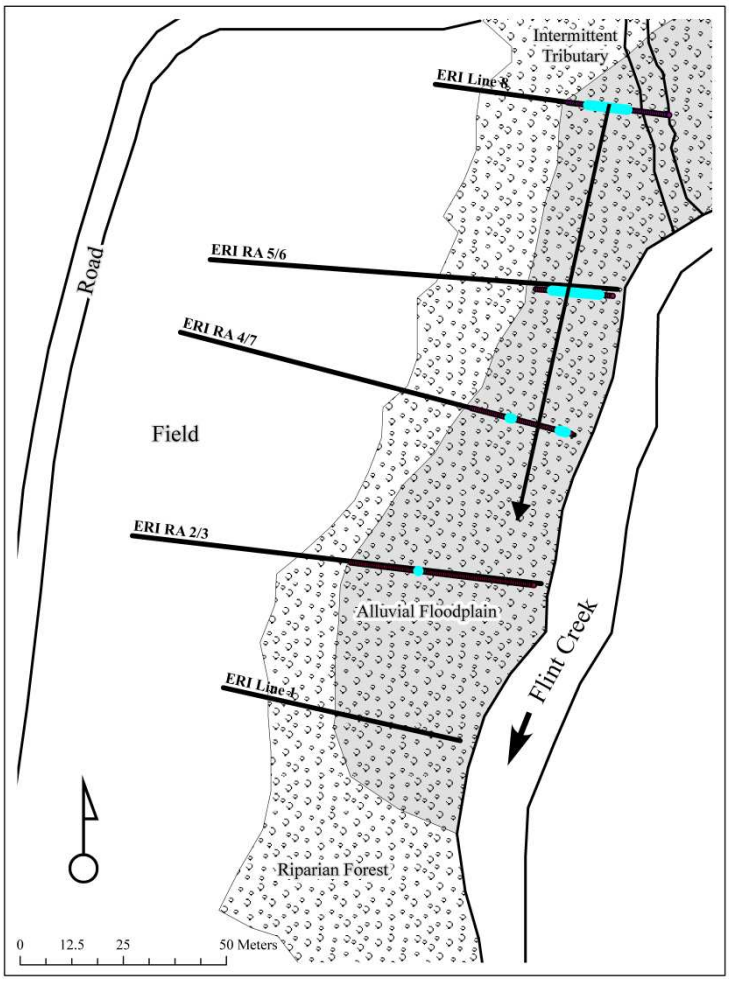


Figure 2.8. High resistivity feature locations on ERI lines at the Flint Creek site (shown in blue). The line with an arrow represents potential high resistivity connection and the direction of flow.

### *Pumpkin Hollow*

Pumpkin Hollow differed from the other streams because it was a headwater stream with a smaller watershed area. The valley at the study site was approximately 200 m wide and the roll-along lines spanned nearly the entire valley width, crossing Pumpkin Hollow Creek at about the midpoint of the line. The ERI survey at Pumpkin Hollow consisted of three lines oriented W-E with 1 m electrode spacing, 12.5 m depth, and 97 m (lines 1-2 and 3-4) or 139 m (line 5-6-7) length (Figure 2.9).

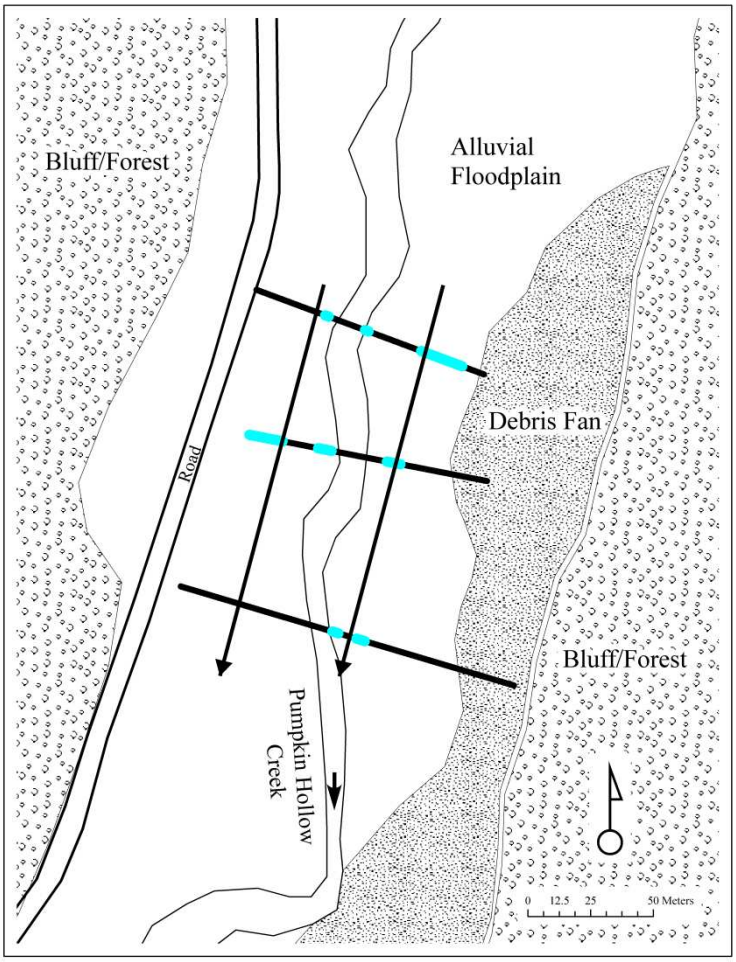


Figure 2.9. High resistivity feature locations on ERI lines at the Pumpkin Hollow site are shown in blue. Arrows represent potential connections between them and the direction of flow.

The Pumpkin Hollow ERI profiles also had a unique configuration consisting of a low resistivity layer between a high resistivity surface layer and high resistivity at depth (Figure 2.4). The surface layer was dominated by gravel underlying only 1 to 3 cm of topsoil. Observations at the site included the close proximity of large gravel debris fans originating from nearby upland areas. Jacobson and Gran (1999) noted similar pulses of gravel in Ozark streams in Missouri and Arkansas originating from 19$^{th}$ and early 20$^{th}$ century deforestation of plateau surfaces, implying that a possible interpretation of the low resistivity layer in the ERI profiles was a soil layer buried by gravel from the nearby plateau surfaces. The streambed elevation was approximately 262 m with the general floodplain surface being about 1 m above that elevation. Pumpkin Hollow was not actively flowing through the study site although flow was evident within 1 km downstream, suggesting that significant amounts of water were likely flowing within the gravel streambed as groundwater. The area of interest included the elevations above 262 m (note that the mean elevation was 262.9 m and that the maximum elevation 265 m occurred at the valley edge) and was therefore thin compared to the other study sites. The resistivity at Pumpkin Hollow ranged from 58 to 3110 Ω-m with a mean of 387 Ω-m. The mean and maximum values were ranked second behind only Barren Fork Creek and were additional

evidence that the floodplain was dominated by gravel. Like the other sites, the Pumpkin Hollow resistivity suggested a pattern of discrete areas of high resistance that indicated PFPs (Figure 2.9). These were generally associated with topographic high areas and appeared to have the potential to direct flow down-valley parallel to the stream.

### *Three-Dimensional Interpolation*

The variograms generated for each site showed both variations among sites but also occasional variation between elevations within a site (Table 2.3). The anisotropy angle for variograms at the Barren Fork Creek was consistent with depth and generally corresponded to the PFP pattern detected on the ERI profiles. The anisotropy angles for the Pumpkin Hollow interpolations also were fairly consistent with depth and were also similar to the angle determined from the ERI profiles. The variograms at the Flint Creek and the Honey Creek sites both showed different angles with depth. The variety of anisotropy angles for the Flint Creek and the Honey Creek sites were possibly due to the presence of many similar features which can be linked at different angles indicating the presence of layers with different geomorphic origins.

Table 2.3. Variogram model information for each of the selected alluvial floodplain sites.

| | Elevation (m) | Standard Deviation | Nugget Effect | Model | Anisotropy Angle (degrees) | Range (m) |
|---|---|---|---|---|---|---|
| Barren Fork Creek | 209 | 2060 | 6.88E+06 | Power | 46 | 1 |
| | 210 | 564 | 1.19E+06 | Power | 50 | 1 |
| | 211 | 213 | 1.63E+05 | Power | 50 | 2 |
| Honey Creek | 234 | 99 | 4.97E+04 | Power | 44 | 1 |
| | 235 | 111 | 2.50E+04 | Linear | 139 | 2 |
| Flint Creek | 265 | 90 | 8.70E+03 | Exponential | 65 | 10 |
| | 266 | 85 | 3.14E+03 | Power | 130 | 30 |
| Pumpkin Hollow | 262 | 66 | 2.00E+00 | Exponential | 85 | 17 |
| | 263 | 353 | 6.20E+03 | Quadratic | 97 | 78 |

Three elevation “slices” at the Barren Fork Creek were spaced at 1 m depth intervals designed to include the area between the baseflow water table (209 m) and the soil layer (211 m). The Barren Fork Creek surface interpolations show the high resistivity near the PFP and the low and high pattern that corresponded to surface topography (Figure 2.10). The resistivity consistently increased with depth so that high resistivity was typically continuous just above the water table.

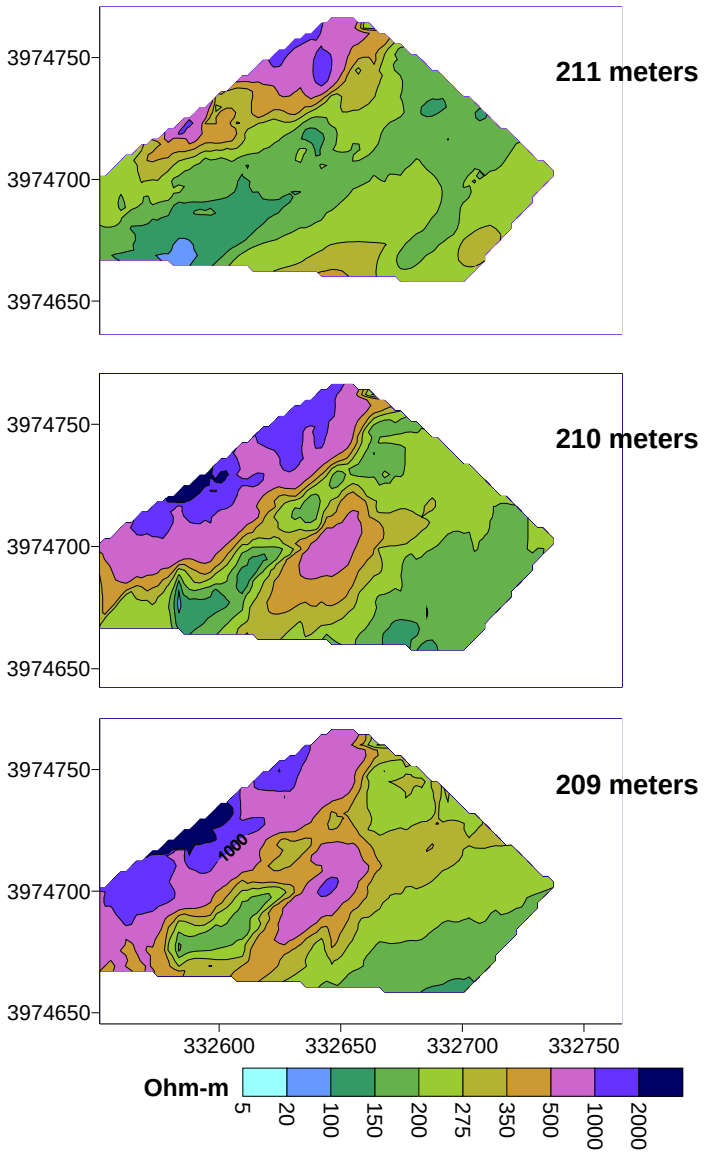


Figure 2.10. Interpolated ERI surfaces for elevation slices at the Barren Fork Creek site. North is top of image. The Barren Fork Creek flows southwest along the top left edge. The interpolated surfaces are trimmed to the existing field of monitoring wells at the study site. Axes (m) are Northings and Eastings (UTM Zone 15N).

The Honey Creek site interpolations showed only a slight pattern of increase with depth with the highest connectivity among high resistivity occurring at higher elevations within the floodplain (Figure 2.11). The interpolated resistivity did not follow the curvilinear pattern that would be likely within point bar sediments, but that result could be explained due to the large area with little data at the apex of the curve, and because the variogram-based interpolation connected the existing points linearly.

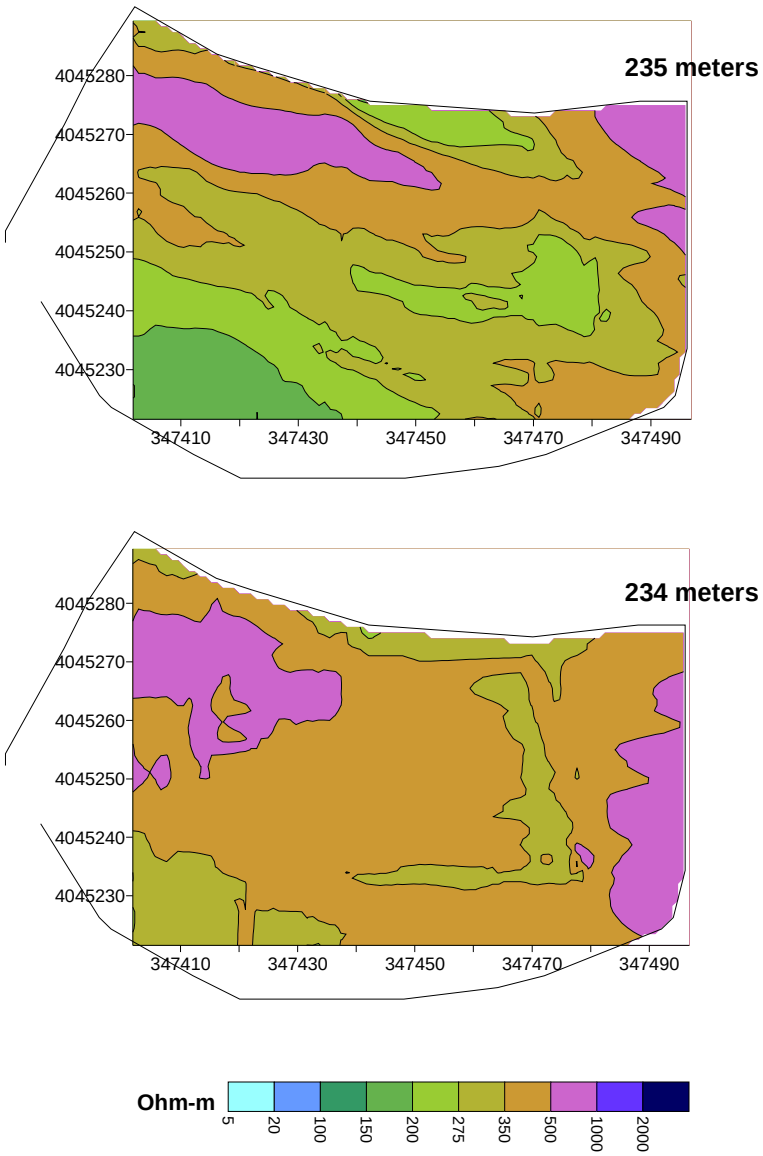


Figure 2.11. Interpolated ERI surfaces for elevation slices at the Honey Creek site. North is at the top of the image. Honey Creek flows westerly about 50 m south along the arc at the bottom. Axes (m) are Northings and Eastings (UTM Zone 15N).

The Flint Creek interpolation showed that resistivity increased with depth (Figure 2.12). The interpolations also showed a change in patterns: at the shallower depth there was a strong pattern across the alluvial floodplain to the stream while the deeper interpolation showed the longitudinal pattern parallel to the stream seen on the ERI profiles.

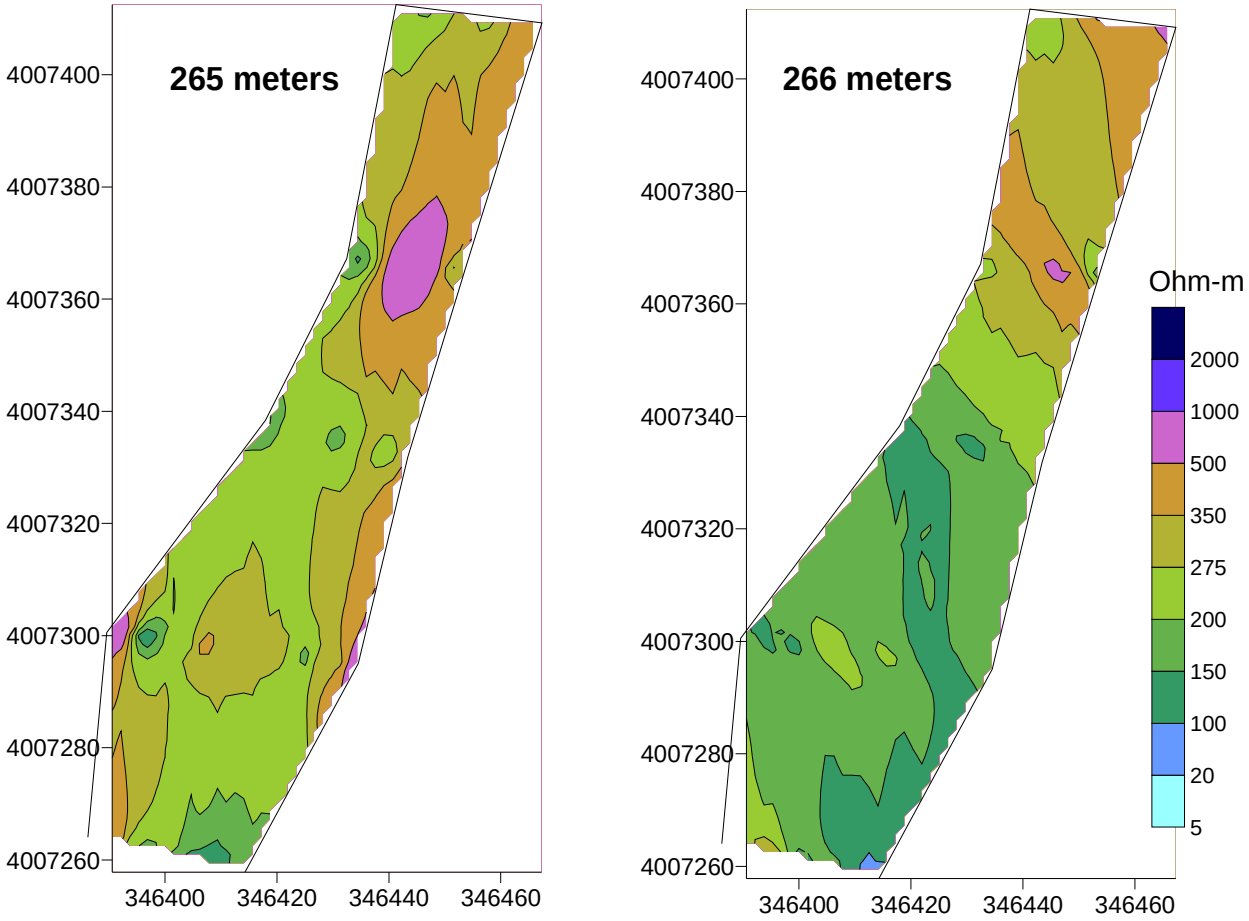


Figure 2.12. Interpolated ERI surfaces for elevation slices at the Flint Creek site. North is at top of image. Flint Creek flows south on the east edge of site. Axes (m) are Northings and Eastings (UTM Zone 15N).

The Pumpkin Hollow interpolations showed a decrease in resistivity with depth that was most likely associated with the feature previously interpreted as a buried soil surface (Figure 2.13). The high resistivity in the shallower interpolation showed a longitudinal pattern parallel to the stream similar to that seen in the ERI profiles.

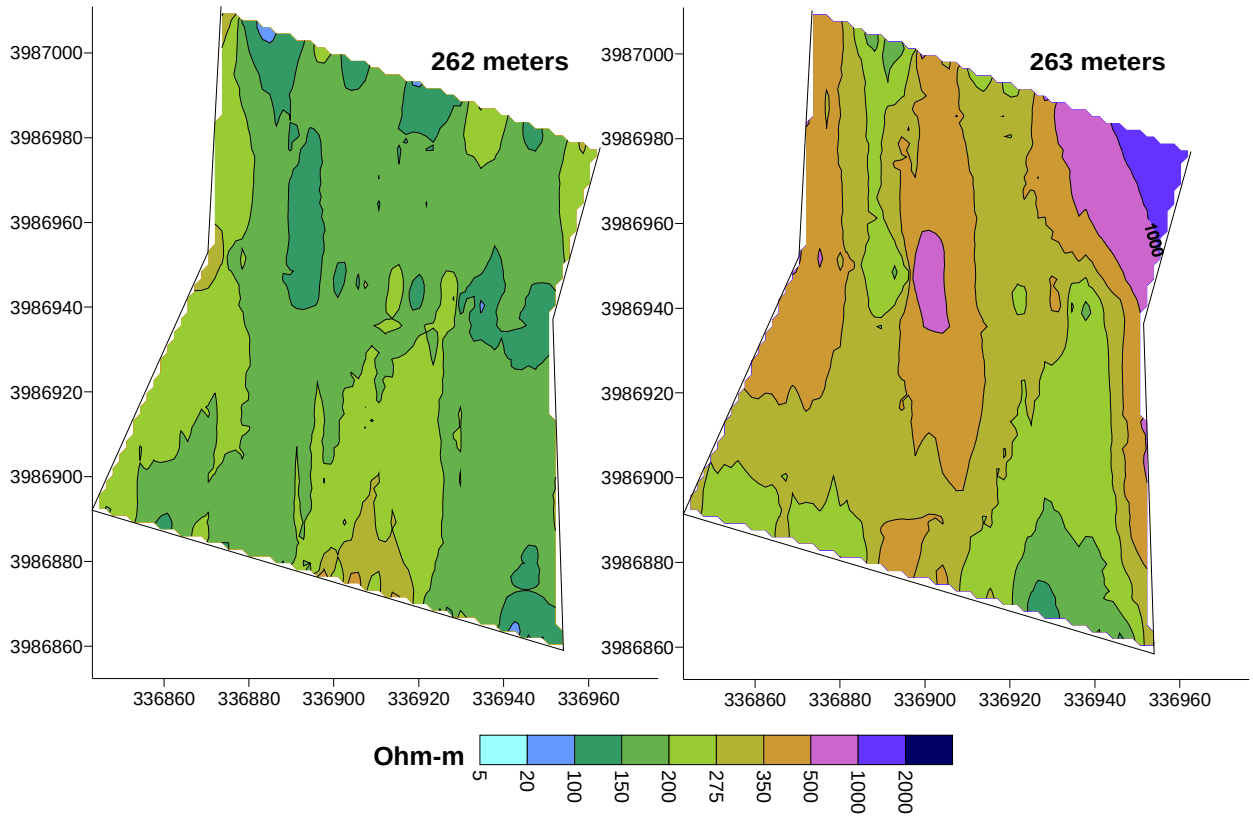


Figure 2.13. Interpolated ERI surfaces for elevation slices at the Pumpkin Hollow site. North is at top of image. Pumpkin Hollow flows south through the center of the site. Axes (m) are Northings and Eastings (UTM Zone 15N).

### *Saturated Hydraulic Conductivity*

The goal of the ERI imaging was to produce a physically-based estimate of the spatial distribution of hydraulic conductivity (*K*) within the alluvial aquifers included in the study. Three-dimensional grids of *K* were required for the understanding of flow within the alluvial system. To that end, an empirical, linear relationship between electrical resistivity, $\rho$ ($\Omega$-m), and *K* (m $d^{-1}$) was established using borehole permeameter tests at the Barren Fork Creek, Honey Creek and Flint Creek study sites (Figure 2.14):

$$K = 0.105\rho \tag{2.4}$$

The regression had a coefficient of determination ($R^2$) of 0.73 and the *F*-statistic was significant at $\alpha$ = 0.05. Since all of the alluvial floodplain sites were gravel dominated systems, the sites were similar enough in geology that the linear relationship between electrical resistivity and hydraulic conductivity was not site-specific. The interpolated ERI surfaces were based on a 2-m by 2-m grid of resistivity values and then converted to *K* using equation (2.4). The patterns revealed in the ERI interpolations were retained in *K* surfaces because the equation was a linear transformation. The positive slope of the relationship implied that areas with high resistivity also have high *K*, and that continuous high resistivity features may act as PFPs when

hydrologic conditions are appropriate (during periods of high stream flow or surface runoff). Since maximum electrical resistivity generally increased with increasing watershed area, maximum hydraulic conductivity also generally increased with increasing watershed area among the alluvial floodplain sites (Table 2.4). The maximum *K* at the Barren Fork Creek site (1752 m/d) was within the range for gravel reported by Domenico and Schwartz (1990).

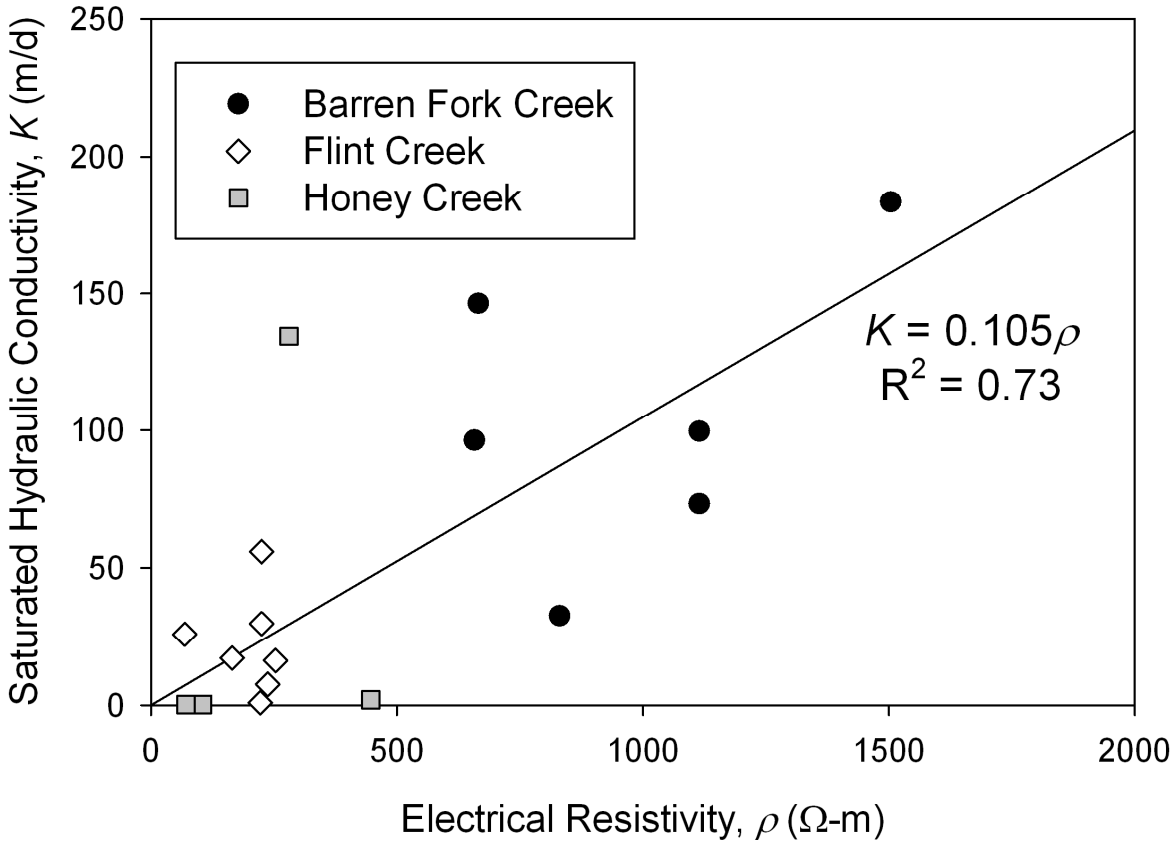


Figure 2.14. Electrical resistivity versus saturated hydraulic conductivity measured with modified borehole permeameter tests at the Barren Fork Creek, Flint Creek, and Honey Creek field sites.

Table 2.4: Summary statistics for interpolated hydraulic conductivity (*K*, m/d) at each site.

| | Mean | Standard Deviation | Minimum | Median | Maximum |
|---|---|---|---|---|---|
| Barren Fork Creek | 45 | 72 | 8 | 27 | 1750 |
| Flint Creek | 28 | 11 | 9 | 26 | 98 |
| Honey Creek | 40 | 11 | 16 | 39 | 80 |
| Pumpkin Hollow | 29 | 16 | 8 | 25 | 176 |

## Conclusions

The ERI profiles showed that the subsurface was heterogeneous at each site and areas of high electrical resistivity formed discrete, possibly continuous features in the vadose zone. Interpolations, based on variograms of resistivity, showed that resistivity within the alluvial aquifers formed patterns that were often linked to geomorphic processes. Saturated hydraulic conductivity within the alluvial aquifers was estimated by applying an empirical relationship between electrical resistivity and hydraulic conductivity. The linear relationship between electrical resistivity and hydraulic conductivity was not site-specific. The positive slope of the relationship suggested that areas of continuous high resistivity may act as zones of preferential flow within the aquifer under suitable hydrologic conditions. Among the sites, maximum electrical resistivity and hydraulic conductivity generally increased with increasing watershed area.

## References

Archie, G.E. 1942. The electrical resistivity log as an aid in determining some reservoir characteristics. *Petroleum Technology* Technical Paper 1422.

Auton, C.A. 1992. The utility of conductivity surveying and resistivity sounding in evaluating sand and gravel deposits and mapping drift sequences in northeast Scotland. *Engineering Geology* 32: 11-28.

Baines, D., D.G. Smith, D.G. Froese, and P. Bauman. 2002. Electrical resistivity ground imaging (ERGI): A new tool for mapping the lithology and geometry of channel-belts and valley-fills. *Sedimentology* 49: 441-449.

Beresnev, I.A., C.E. Hruby, and C.A. Davis. 2002. The use of multi-electrode resistivity imaging in gravel prospecting. *Journal of Applied Geophysics* 49: 245-254.

Bersezio R., M. Giudici, and M. Mele. 2007. Combining sedimentological and geophysical data for high-resolution 3-D mapping of fluvial architectural elements in the Quaternary Po Plain (Italy). *Sedimentary Geology* 202(1-2): 230-248.

Bridge, J.S. 2003. *Rivers and Floodplains: Forms, Processes, and Sedimentary Record.* Oxford, UK: Blackwell Publishing.

Crook, N., A. Binley, R. Knight, D.A. Robinson, J. Zarnetske, and R. Haggerty. 2008. Electrical resistivity imaging of the architecture of substream sediments. *Water Resources Research* 44, W00D13, doi:10.1029/2008WR006968.

Dam, D., S. Christensen, and N. B. Christensen. 2000. Characterizing the hydraulic conductivity field using electrical resistivity and inverse modeling. In *Groundwater 2000: Proceedings of the International Conference on Groundwater Research, Copenhagen, Denmark*, Bjerg P.L., P. Engesgaard, and T.D. Krom (eds). Balkema: Rotterdam, The Netherlands.

Domenico, P.A., and F. W. Schwartz. 1990. *Physical and Chemical Hydrogeology*. New York, NY: John Wiley and Sons.

Fuchs, J.W., G.A. Fox, D.E. Storm, C. Penn, and G.O. Brown. 2009. Subsurface transport of phosphorus in riparian floodplains: Influence of preferential flow paths. *Journal of Environmental Quality* 38(2): 473-484.

Gourry, J-C., F. Vermeersch, M. Garcin, and D. Girot. 2003. Contribution of geophysics to the study of alluvial deposits: a case study in the Val d'Avaray area of the River Loire, France. *Journal of Applied Geosciences* 54: 35-49.

Green, R.T., R.V. Klar, and J.D. Prikryl. 2005. Use of integrated geophysics to characterize paleo-fluvial environments, *Geotechnical Special Publication 138: Site Characterization and Modeling*, ASCE, New York, NY.

Halihan, T., S. Paxton, I. Graham, T. Fenstemaker, and M. Riley. 2005. Post-remediation evaluation of a LNAPL site using electrical resistivity imaging. *Journal of Environmental Modeling* 7: 283-287.

Heeren, D.M., R.B. Miller, G.A. Fox, D.E. Storm, A.K. Fox, and A.R. Mittelstet. 2010a. Impact of preferential flow paths on stream and alluvial groundwater interaction. In *Proc. ASCE EWRI World Environmental and Water Resources Congress*. Reston, Va.: American Society of Civil Engineers.

Heeren, D.M., R.B. Miller, G.A. Fox, D.E. Storm, C.J. Penn, and T. Halihan. 2010b. Preferential flow path effects on subsurface contaminant transport in alluvial floodplains. *Transactions of the ASABE* 53(1): 127-136.

Isaaks E.H., and R.M. Srivastava. 1989. *An Introduction to Applied Geostatistics*. New York, N.Y.: Oxford University Press.

Jacobson, R.B., and K.B. Gran 1999. Gravel sediment routing from widespread, low-intensity landscape disturbance, Current River Basin, Missouri. *Earth Surface Processes and Landforms* 24: 897-917.

Lesmes, D.P, and S.P. Friedman. 2005. Relationship between the electrical and hydrogeological properties of rocks and soils. In *Hydrogeophysics*, Rubin, Y., and S.S. Hubbard (eds). Springer: Dordrecht, The Netherlands.

Loke, M.H., and T. Dahlin. 2002. A comparison of the Gauss–Newton and quasi-Newton methods in resistivity imaging inversion. *Journal of Applied Geophysics* 49: 149–162.

Mazac, O., W.E. Kelly, and I. Landa. 1985. A hydrological model for relations between electrical conductivity ad hydraulic properties of aquifers. *Journal of Hydrology* 79: 1-19.

McNeill, J.D. 1980. Electrical Conductivity of Soils and Rocks. Technical Note TN-5, Geonics Limited, Ontario, Canada.

Menjoulet, B.C., K.R. Brye, A.L. Pirani, B.E. Haggard, and E.E. Gbur. 2009. Runoff water quality from broiler-litter-amended tall fescue in response to natural precipitation in the Ozark Highlands. *Journal of Environmental Quality* 38: 1005-1017.

Miller, R.B., D.M. Heeren, G.A. Fox, T. Halihan, D.E. Storm, and A.R. Mittelstet. 2010. Use of multi-electrode resistivity profiling to estimate vadose-zone hydraulic properties of preferential flow paths in alluvial floodplains. In *Proc. ASCE EWRI World Environmental and Water Resources Congress*. Reston, Va.: American Society of Civil Engineers.

Smith, R.C., and D.B. Sjogren. 2006. An evaluation of electrical resistivity imaging (ERI) in Quaternary sediments, southern Alberta, Canada. *Geosphere* 2(6): 287-298.

U.S. Bureau of Reclamation (USBR). 1985. *Ground Water Manual: A Water Resources Technical Manual Revised Reprint.* Denver, CO. U.S. Department of the Interior, Bureau of Reclamation.

# CHAPTER 3
# SUBSURFACE HETEROGENEITY AND TRANSIENT STORAGE

## Abstract

A better understanding of stream-aquifer interactions is needed for both estimating contaminant transport in alluvial stream systems and water policy. Assuming homogeneity in alluvial aquifers is convenient, but limits our ability to accurately predict stream-aquifer interactions in alluvial floodplains. More information is needed on focused, as opposed to diffuse, groundwater discharge/recharge to streams and the magnitude and role of transient storage in alluvial aquifers, especially relative to changes in stream stage. The objective of this project was to document and quantify the effect of flow heterogeneity (i.e., focused or preferential flow pathways, PFPs) and transient storage on groundwater flow patterns relative to changes in stream stage using flow divergence and direction. Monitoring was performed adjacent to the Barren Fork Creek and Honey Creek in northeastern Oklahoma. Based on results from subsurface electrical resistivity mapping, observation wells were installed in PFPs and non-PFP subsoils. Water levels in the wells were recorded real-time using pressure transducers for a period of six weeks, which included multiple high flow events. Divergence was used to quantify heterogeneity in hydraulic conductivity and flow direction was used to assess the potential for large-scale transient storage. The PFPs appeared to act as divergence zones allowing stream water to quickly enter the groundwater system, or as flow convergence zones draining a large groundwater area. Maximum divergence or convergence occurred with maximum rates of change in stream stage. Flow directions in the groundwater changed considerably between base and high flows, suggesting that the floodplains acted as a transient storage zone, rapidly storing and releasing water during passage of a storm hydrograph. During storm events at both sites, the average groundwater direction changed by at least 90° from the average groundwater direction during baseflow. The procedures in this project provide methodologies for quantifying subsurface heterogeneity, focused recharge/discharge, and transient storage in groundwater for alluvial floodplains. This project has important implications relative to the impact of large scale (i.e., beyond near-streambed) and stage-dependent storage on contaminant movement through alluvial stream systems and management activities in floodplains. Groundwater models of these alluvial floodplains should account for the non-random nature of heterogeneity in hydraulic conductivity, as well as the fact that some PFPs may only become activated after a minimum stream stage is reached.

## Introduction

Simplifying assumptions are a necessity in describing the natural environment. For example, Cardenas (2009) modeled stream-aquifer interactions within meander bands assuming homogenous hydraulic conductivity in the alluvial aquifer. However, assuming homogeneity limits our ability to accurately predict stream-aquifer interactions in alluvial floodplains. In fact, the Committee on Hydrologic Sciences of the National Research Council (NRC, 2004) identified several areas for further work in regard to groundwater fluxes across interfaces. The NRC committee specifically identified the need to determine the relative importance of diffuse versus focused recharge/discharge in hydro-geologic settings. Additional work is needed to document the occurrence of focused recharge and discharge relative to changes in stream stage.

It is well known that deposits of coarse alluvium in floodplains result in complex hydrologic pathways (Naiman et al., 2005). Distal floodplain areas can be linked to modern channel flows by paleochannels, i.e. linear deposits of coarse-grained sediments (Stanford and Ward, 1992; Poole et al., 1997, 2002; Amoros and Bornette, 2002; Naiman et al., 2005). Local or regional conditions can lead to circumstances where subsurface transport may be important (Turner and Haygarth, 2000; Lacas et al., 2005; Fuchs et al., 2009). Subsurface nutrient transport is promoted by spatial variability in hydraulic conductivity (Carlyle and Hill, 2001), preferential flow pathways (McCarty and Angier, 2001; Polyakov et al., 2005; Fuchs et al., 2009), and limited sorption capacity in riparian zone soils (Cooper et al., 1995; Carlyle and Hill, 2001; Polyakov et al., 2005). Tellam and Lerner (2009) suggest electrical resistivity and piezometers with pressure loggers as potential methods for better characterizing sediment distributions and solute transport in these systems.

For example, phosphorus transport to streams has been assumed to primarily take place in surface runoff, resulting in a high emphasis on riparian buffer zones as a conservation practice. Because buffers adjacent to streams primarily address the commonly observed and more easily understood surface runoff transport mechanism (Reichenberger et al., 2007; Sabbagh et al., 2009), their effectiveness may be limited if a transport pathway through the subsurface circumvents the surface trapping objectives of the riparian buffer (Cooper et al., 1995; Lacas et al., 2005). Previous work (Fuchs et al., 2009) on the Barren Fork Creek in northeastern Oklahoma demonstrated that subsurface transport of phosphorus was significant in localized preferential flow paths (PFPs). Subsequent work (Chapter 2; Miller et al., 2010b) mapped the extent of the subsurface PFPs with electrical resistivity equipment. A series of low resistivity structures that were roughly parallel to the current stream channel were separated by higher resistivity features. Low resistivity areas were interpreted as relict cut-off stream channels which had been filled with fine sediments (i.e., sand, silt and clay) and gravel having low electrical resistivity. The higher resistance areas, including the PFP, were interpreted to be buried gravel-dominated lateral or mid-channel bars, which were highly resistant to electrical current but highly conductive to water flow.

The importance of spatial heterogeneity in soils has been recognized, but quantifying parameter heterogeneity, such as hydraulic conductivity, has proven difficult. Rooij and Stagnitti (2000) performed solute leaching experiments on laboratory soil columns and collected drainage from 300 discrete compartments. The variable amounts of solute collected indicated convergence and divergence of flow lines in the vadose zone, which was used to "…quantify the nature and severity of flow heterogeneity and preferential flow." Divergence of pore flow velocity has been incorporated into groundwater contaminant transport modeling (Kavvas and Karakas, 1995), and divergence has been observed in subsurface flow models due to heterogeneity in anisotropy (Kumar et al., 2009). However, the divergence of the water table gradient using field data has not been used to characterize heterogeneity of hydraulic conductivity in unconfined aquifers.

It is also hypothesized that highly conductive alluvial systems are transient storage zones for nutrients, acting as a sink during high flow and a source during base flow. However, limited data have been presented that documents and quantifies the transient nature of groundwater in alluvial floodplains, other than near streambed hyporheic flow. Limited work has been done to investigate transient storage relative to shifts in surface and subsurface flow conditions (Zarnetske et al., 2007).

Therefore, the objective of this project was to document and quantify the impact of flow heterogeneity (i.e., PFPs) on groundwater flow patterns relative to changes in stream stage using flow divergence and direction. This project strengthens our current understanding of flow and contaminant interaction between streams and alluvial aquifers and can be used to help

quantify the efficiency of conservation practices in alluvial floodplains. This project utilized data sets of two instrumented floodplain sites in the Ozark ecoregion of Oklahoma, but such results may be applicable for gravel bed systems worldwide.

## Materials and Methods

### *Barren Fork Creek and Honey Creek Floodplain Sites*

The alluvial floodplain sites were located in the Ozark region of northeastern Oklahoma. The Barren Fork Creek site (Figures 2.6 and 3.1a, latitude: 35.90°, longitude: -94.85°) was immediately downstream of the Eldon Bridge U.S. Geological Survey (USGS) gage station 07197000. With a watershed size of 845 $km^2$, the Barren Fork Creek site had a median daily flow of 3.6 $m^3$ $s^{-1}$. The Honey Creek site (Figures 2.7 and 3.1b, latitude: 36.54°, longitude: -94.70°) was also located immediately downstream of a USGS gage station 07189542. As a smaller order stream, Honey Creek site had a 0.54 $m^3$ $s^{-1}$ median daily flow and a 150 $km^2$ watershed.

Both floodplain sites consisted of alluvial gravel deposits underlying a mantle of topsoil (Razort gravelly loam). Topsoil thickness ranged from 0.5 to 1.0 m at the Barren Fork Creek site and from 0.1 to 0.5 m at the Honey Creek site. Soil hydraulic studies on these soil types have shown that subtle morphological features can lead to considerable differences in hydraulic conductivity (Sauer and Logsdon, 2002). The riparian area on Honey Creek was located on the inside of a meander bend, an area likely to be aggradational. Located on the outside of a meander bend, the stream is actively eroding away the study area along the Barren Fork Creek. Fuchs et al. (2009) described some of the soil and hydraulic characteristics of the Barren Fork Creek floodplain site, including estimates of hydraulic conductivity for the gravel subsoil between 140 and 230 m $d^{-1}$ based on falling head trench tests.

### *Observation Well Installation and Long Term Monitoring*

Assuming a positive correlation between electrical resistivity and hydraulic conductivity, observation well locations were selected both in PFPs and in non-PFP subsoils (Figure 3.1), based on previous electrical resistivity results (Chapter 2; Miller et al., 2010a,b). Using a Geoprobe Systems drilling machine (6200 TMP, Kejr, Inc., Salina, KS), observation wells were installed in the alluvial floodplains with a 2 to 3 m screened section at the base. Depth to refusal ranged from 4.0 m to greater than 5.0 m at the Barren Fork Creek site and from 2.5 to 3.5 m at the Honey Creek site. Well locations were surveyed using a TOPCON HiperLite Plus global positioning system configured with a base station and rover unit (4 cm accuracy). These data were corrected for positional errors using the National Geodetic Survey Online Positioning User Service (OPUS). Since the water table elevation data were more sensitive to measurement error than horizontal position, a laser level was used to determine the elevation at the top of each well (1 cm accuracy).

(a) Barren Fork Creek

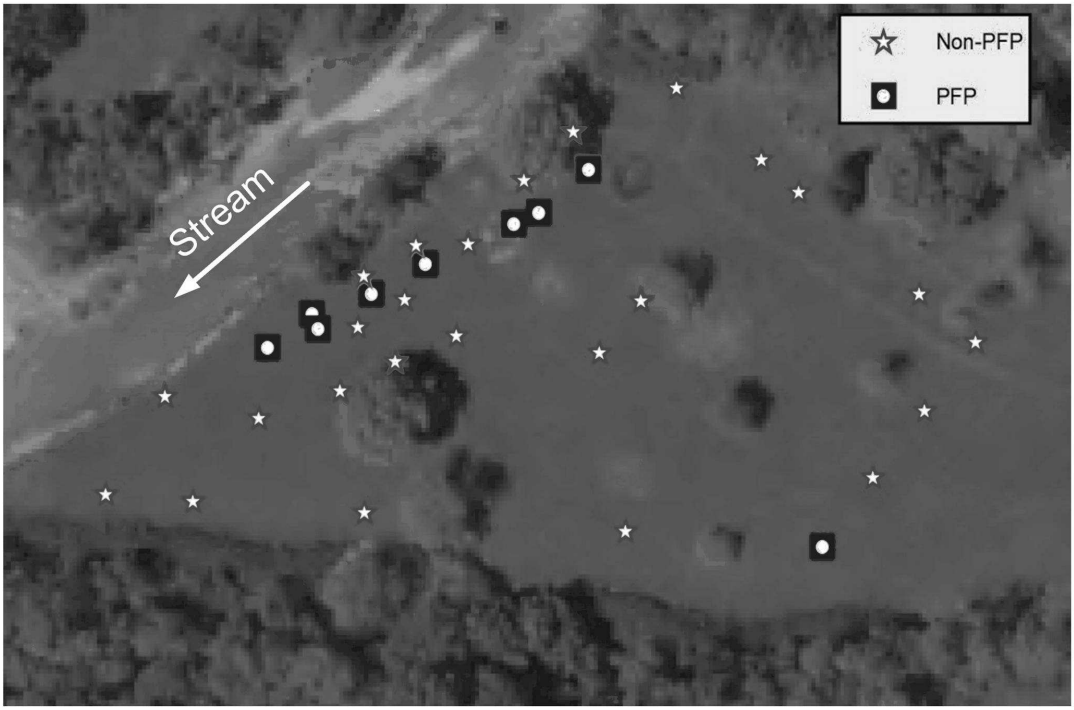


(b) Honey Creek

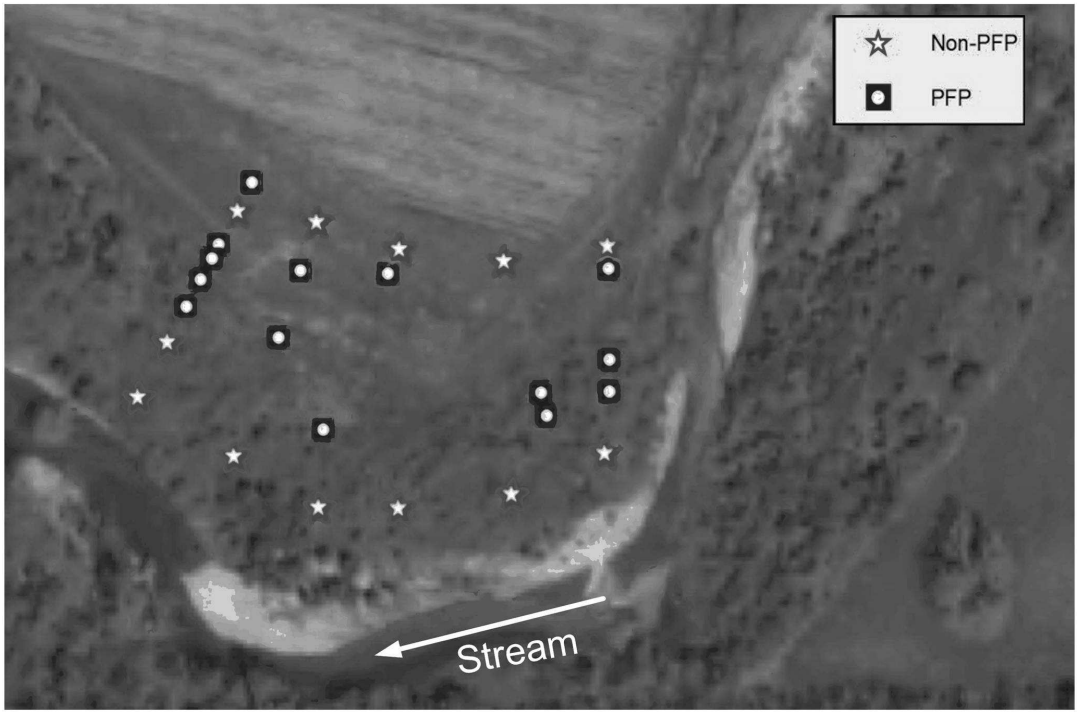


Figure 3.1. (a) Barren Fork Creek site, located near Tahlequah, OK, and (b) Honey Creek site, located near Grove, OK, showing preferential flow path (PFP) and non-PFP observation well locations. The white arrows indicate stream flow direction.

At each site, twenty-four observation wells were instrumented with automated water level loggers (HoboWare, Onset Computer Corp., Cape Cod, MA) to monitor water pressure and temperature at five minute intervals from April 3 to May 14, 2009. One logger was placed above the water table at each site to account for changes in atmospheric pressure. Reference water table elevations, obtained with a water level indicator, were then calculated. The logger data were processed with HoboWare Pro software, which accounted for changes in atmospheric pressure as well as changes in water density due to temperature. The local USGS gage stations were used to analyze stream stage.

### *Divergence as an Indicator of Subsurface Heterogeneity*

Water table elevation data were analyzed with Matlab (The Mathworks, Natick, MA). Using 30-minute intervals, a cubic interpolation was performed to determine the head for points in a two-dimensional well field grid. Contour maps were plotted with equipotential lines using 2-cm spacing. The gradient (L $L^{-1}$) of the scalar head field was calculated for each point in space using the following equation (Hunt, 1995):

$$\vec{i} = \nabla h = \frac{\partial h}{\partial x}\hat{x} + \frac{\partial h}{\partial y}\hat{y} \tag{3.1}$$

where $\vec{i}$ is the gradient vector and *h* is the head (i.e., water table elevation). Streamlines were calculated as everywhere-tangent to the gradient, or perpendicular to contour lines of *h*. The divergence of the gradient vector field was calculated using the following equation (Hunt, 1995):

$$div(\vec{i}) = \nabla \bullet \vec{i} = \frac{\partial i_x}{\partial x} + \frac{\partial i_y}{\partial y} \tag{3.2}$$

where div($\vec{i}$) is the divergence of $\vec{i}$. The operator div($\vec{i}$) is a scalar quantity with units of $L^{-1}$, and is essentially a measure of the change in gradient per unit length.

The divergence of a velocity vector field represents sources and sinks. With units of $T^{-1}$, div($\vec{v}$) represents the net flux (outflow minus inflow) through the surface of a unit volume. Due to continuity, the divergence of the velocity vector field for an incompressible fluid with no change in storage (e.g. saturated material) must be zero (Hunt, 1995). This also applies to a two-dimensional representation of an unconfined aquifer if the change in water table elevation over time is negligible. Velocity can be related to the gradient by:

$$\vec{v} = \frac{K}{\phi}\vec{i} \tag{3.3}$$

where $\vec{v}$ is the pore velocity, *K* is saturated hydraulic conductivity, and $\varphi$ is porosity. Assuming *K* and $\varphi$ are homogenous, then

$$div(\vec{v}) = \frac{\partial \frac{K}{\phi} i_x}{\partial x} + \frac{\partial \frac{K}{\phi} i_y}{\partial y} = \frac{K}{\phi}\left[\frac{\partial i_x}{\partial x} + \frac{\partial i_y}{\partial y}\right] = \frac{K}{\phi} div(\vec{i}) \tag{3.4}$$

If div($\vec{v}$) is zero, then div($\vec{i}$) must also be zero for an incompressible fluid with no change in storage. If div($\vec{i}$) is non-zero, then *K* and/or $\varphi$ must be heterogeneous, or the change in water

table elevation over time must be significant. We hypothesized that when the change in water table elevation over time was small (e.g. base flow conditions), the magnitude of div($\vec{i}$) was an indicator of the degree of aquifer heterogeneity at a point in space. Since heterogeneity in *K* was much greater than heterogeneity in $\varphi$ (Kavvas and Karakas, 1995), it was assumed that *K* was the dominant source of heterogeneity affecting the divergence data.

A positive div($\vec{i}$) represents a higher gradient leaving a control volume than entering it. Perhaps this can be best illustrated with a case study. Consider a shallow unconfined aquifer with the water table illustrated in Figure 3.2. Arrows are streamlines showing the direction of flow, which are perpendicular to the contour lines. Assuming that the aquifer can be adequately represented by two-dimensional flow and that there is no change in storage, flow between two streamlines must be constant throughout that streamtube due to conservation of mass. In case (a), since the streamtubes have a constant area, the decreasing gradient must be caused by an increasing *K*. The control volume has a unit width and a unit length, and the arrows represent the gradient vector on each side. While an $\vec{i}$ of 0.001 m m$^{-1}$ would be more reasonable, values near 10 m m$^{-1}$ were chosen for clarity of demonstration. The divergence would be calculated as div($\vec{i}$) equal to -4 m$^{-1}$. A negative value for divergence indicates convergence. As this example demonstrates, gradient convergence indicates flow from an area of low *K* to an area of high *K*. Case (b) is an example where the gradient is constant but the width of the stream tubes is increasing. Again, since flow must be constant within a streamtube, the increasing area must be caused by a decreasing *K*. Here, div($\vec{i}$) in the volume element is 9.5 m$^{-1}$. A positive divergence indicates flow from high *K* to low *K*.

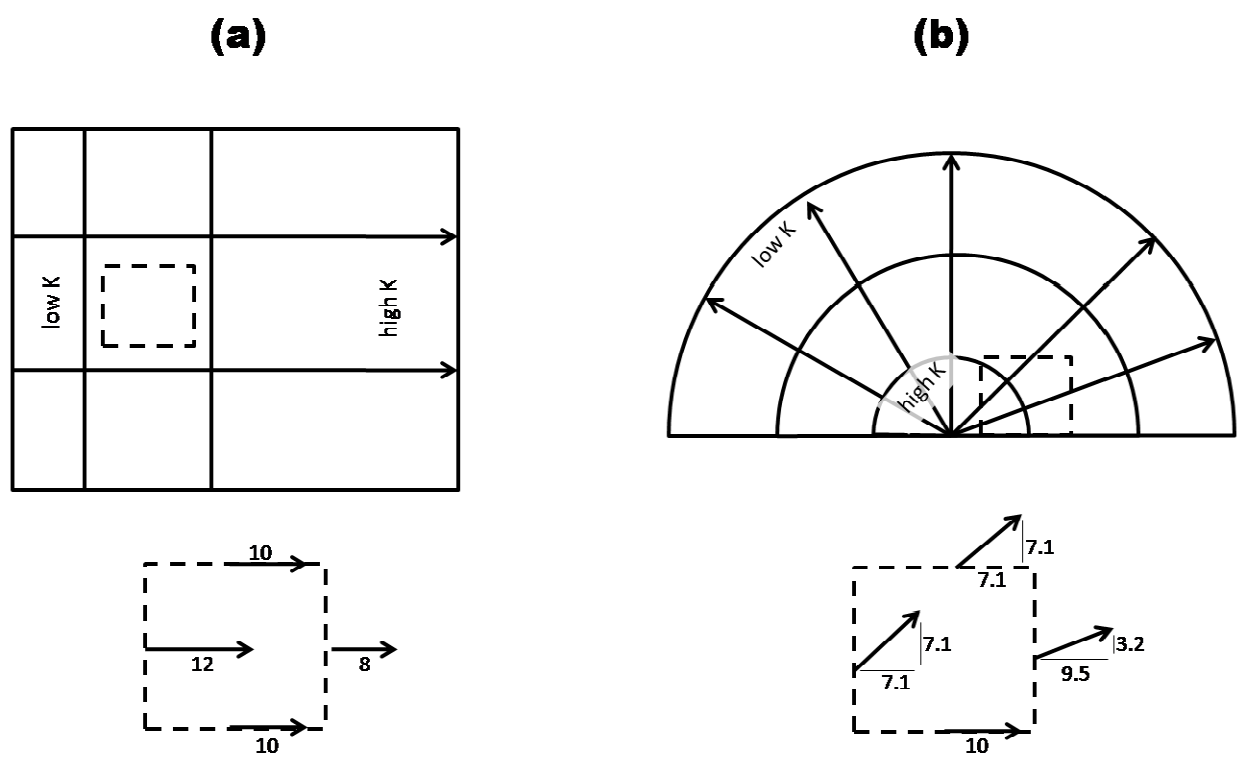


Figure 3.2. Case study for divergence calculations. Contour lines are water table elevations and arrows are streamlines. The gradient vectors are shown on each side of the control volumes. (a) Flow convergence, div($\vec{i}$) = -4 m$^{-1}$, and (b) flow divergence, div($\vec{i}$) = 9.5 m$^{-1}$.

Statistics of the div($\vec{i}$) were derived using the mean, median, standard deviation, and 5th and 95th percentiles. These statistics were correlated to the river stage during the six week monitoring period.

### *Direction as an Indicator of Transient Storage*

The magnitude (*R*) and direction (θ) of the groundwater flow gradient at each point in the two-dimensional well field grid was derived using the following equations:

$$R = \sqrt{\left(\frac{\partial h}{\partial x}\right)^2 + \left(\frac{\partial h}{\partial y}\right)^2} \tag{3.5}$$

$$\theta = \tan^{-1}\left(\frac{\partial h / \partial y}{\partial h / \partial x}\right) \tag{3.6}$$

The arctangent function was in the range of – θ/2 to θ/2 radians. The direction (θ) in radians was then converted to a 0° to 360° scale with the appropriate conversion factor for each quadrant. Statistics of the *R* and θ were derived using the mean, median, standard deviation, and 5th and 95th percentiles, and these statistics were correlated to the stage during the six week monitoring period. Polar plots of the *R* and θ were created for specific flow events at both the Barren Fork Creek and Honey Creek field sites to investigate the change in the groundwater flow direction under baseflow and the rising limb, peak, and recession limb of streamflow hydrographs.

## Results and Discussion

### *Water Table Elevations and Streamlines*

Patterns in the water table elevation contour plots and streamline plots at each site remained relatively similar during baseflow conditions, but changed during high flow events. Plots for baseflow conditions and at two points during the largest flow event at each site were selected to illustrate the range of flow patterns in the dataset (Figures 3.3 and 3.4). The highest gradients in the alluvial aquifer occurred during the rising limb of the hydrographs, when the stream stage was rising most quickly. The impact of aquifer heterogeneity could be seen qualitatively in the contour and streamline plots. For example, a PFP can be seen along the Barren Fork Creek (Figure 3.3b) providing an inlet for stream water to enter the groundwater system. This area of focused recharge appears to be at point (80 m, 60 m), which is the location of the PFP that was studied previously (Fuchs et al., 2009; Heeren et al., 2010). Intuitively, the highest water table elevation should be at the top-center of the contour plot, at the up-gradient end of the stream; however, the highest water table elevation was in the PFP, where stream water could most readily enter the alluvial aquifer. At other times, the contour patterns indicated flow convergence zones (bottom center of Figure 3.3d,f), where a PFP appeared to be draining a large area of groundwater. At the Honey Creek site, there was a PFP that activated during the rising limb of flood events (Figure 3.4b,e), providing a convergence zone that drained a large area of groundwater to the northwest. The location of this PFP was consistent with previous electrical resistivity data at this site (Chapter 2; Miller et al., 2010a,b).

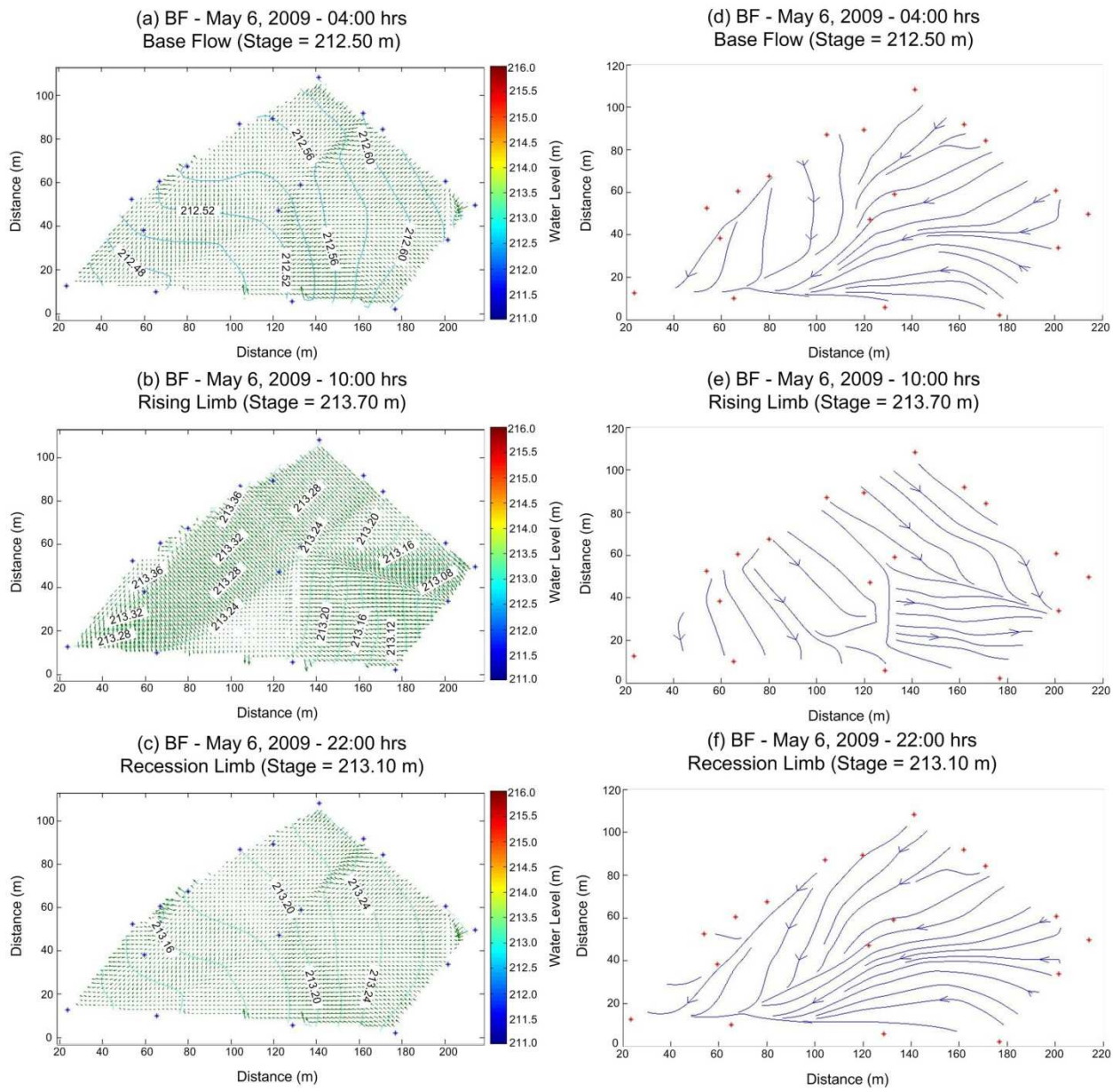


Figure 3.3. Water table elevation contour plots (a, b, and c) and streamlines (d, e, and f) for the Barren Fork Creek (BF) site during base flow (a and d), rising limb (b and e), and recession limb (c and f) of a streamflow hydrograph on May 6, 2009. Arrow vectors in the background indicate the magnitude and direction of the water table gradient. The Barren Fork Creek is located at the top left corner of the plot.

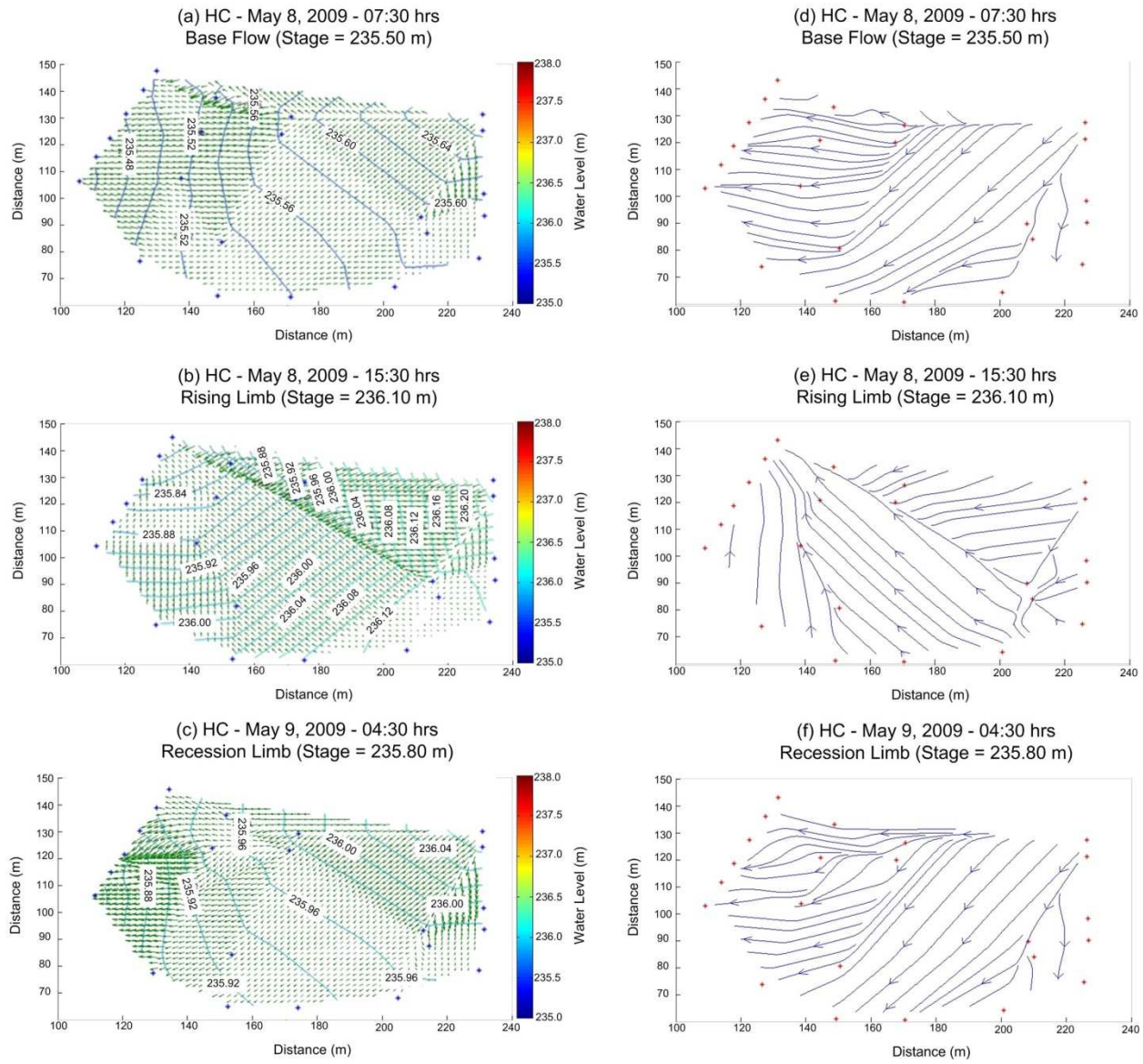


Figure 3.4. Water table elevation contour plots (a, b, and c) and streamlines (d, e, and f) for the Honey Creek (HC) site during base flow (a and d), rising limb (b and e), and recession limb (c and f) of a streamflow hydrograph on May 8-9, 2009. Arrow vectors in the background indicate the magnitude and direction of the water table gradient. Honey Creek is located around the bend at the bottom of the plot.

An interesting observation based on the water table elevation data was that the Barren Fork Creek was a losing stream at this field site, even during base flow and recession limb conditions (Figure 3.3). This illustrated the complexity of stream-aquifer interactions in these coarse gravel alluvial aquifers. We hypothesize a flow pattern where water regularly left the stream at one point within the study area, traveled through the aquifer, and reentered further downstream outside of the study area. This would be equivalent to a large-scale hyporheic flow path, with its activity dependent on stream stage. It is also possible that a sinkhole exists in the aquifer, drawing water out of the stream-aquifer system. Schlottmann et al. (2000) report that water from Cave Springs Branch (also in the Eastern Oklahoma Ozarks) may flow underneath a large surface divide to Honey Creek.

### *Divergence as an Indicator of Subsurface Heterogeneity*

Aquifer heterogeneity was quantified with divergence data which was a composite of radial flow (Figure 3.2b) and changing gradient along a flow path (Figure 3.2a). The results indicated that these effects often happen together. For example, a PFP that creates a divergence zone results in both radial flow and increasing gradient along the flow paths. The mean divergence data were plotted over time relative to the stream stage at both the Barren Fork Creek and the Honey Creek field sites (Figure 3.5).

During baseflow conditions, divergence provided a direct measure of aquifer heterogeneity since the change in water table elevation over time was small. At the Barren Fork Creek site, divergence during baseflow correlated well with stream stage. For example, during baseflow divergence became positive whenever the stream stage declined past 212.0 m. These divergence data also exhibited a negative correlation with stream stage at the Honey Creek site during baseflow conditions. As the water table declined, layers of aquifer material became unsaturated and no longer affected flow patterns.

During high flow events, the change in water table elevation over time may have become significant, in which case these divergence data would reflect both aquifer heterogeneity and change in storage (i.e., water table elevation). This was a confounding factor at the Honey Creek site. For example, on the rising limb of the May 8$^{th}$ event the mean divergence decreased to $-9 \times 10^{-5}$ $m^{-1}$ (a large convergence), followed by an increase in divergence to $6 \times 10^{-5}$ $m^{-1}$, before returning to baseflow levels of divergence (Figure 3.5). On the rising limb, measured divergence due to the rapidly changing water table would be negative. Since the mean divergence was negative during the rising limb, we were unable to determine whether it was primarily due to aquifer heterogeneity or the rapidly rising water table.

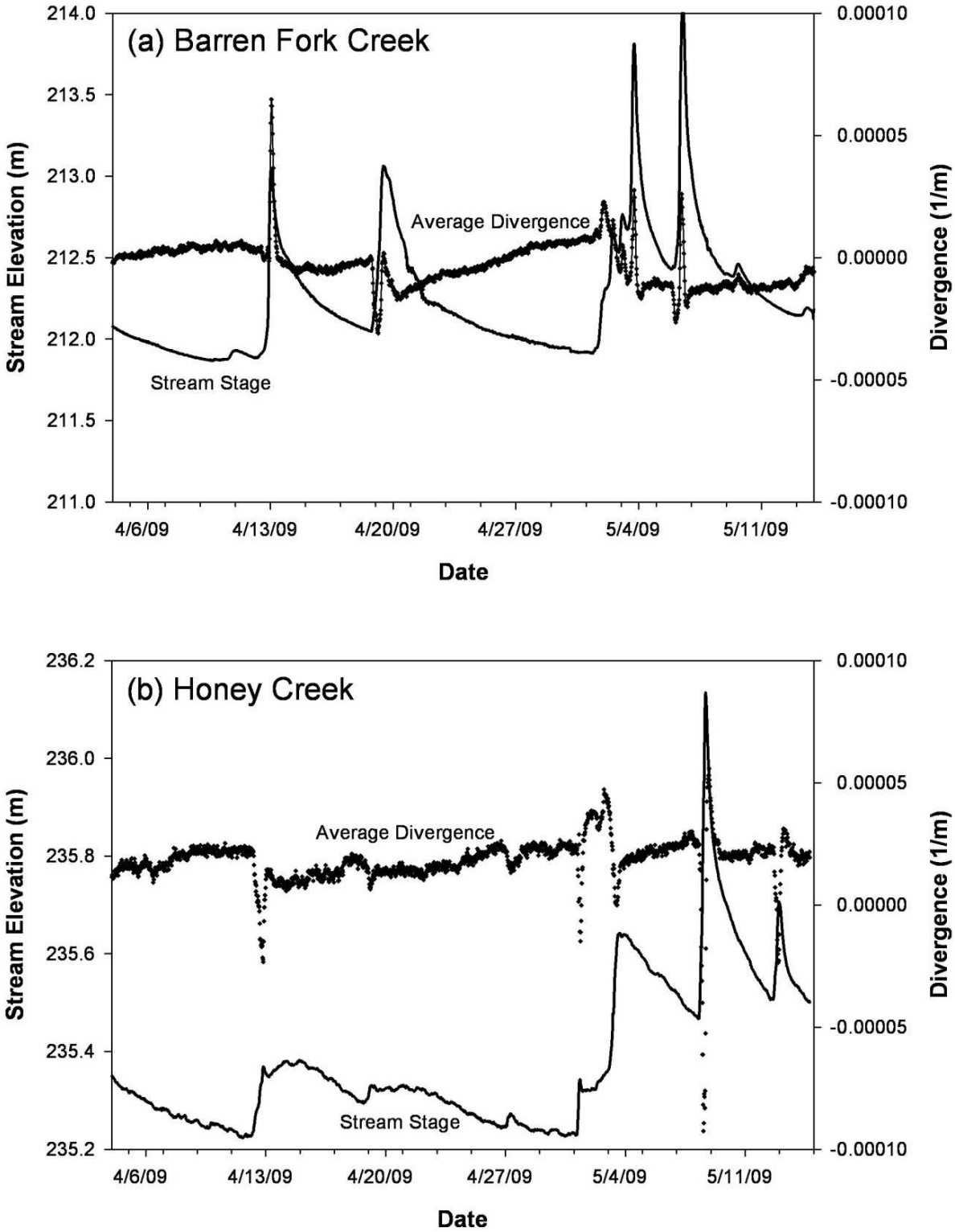


Figure 3.5. Divergence data for the Barren Fork Creek site (a) and the Honey Creek site (b). For scale, the May 6 event on the Barren Fork Creek had a peak flow of 250 $m^3 s^{-1}$, a 1.3 year recurrence interval event. The May 8 event on Honey Creek had a peak flow of 18 $m^3 s^{-1}$, a 1.7 year recurrence interval event.

However, divergence data were not confounded during high flow events at the Barren Fork Creek site. Since the mean divergence was positive during the rising limb of high flow events, i.e. the rising water table contributed to gradient convergence, the impact of aquifer heterogeneity (divergence) was dominant over change in storage effects (convergence). Mean divergence levels in the groundwater approached $6 \times 10^{-5}$ $m^{-1}$ (Figure 3.5) during the rising limb of high flow events due to a PFP connected to the stream. This divergence zone, which allowed stream water to quickly enter the groundwater system, was the same PFP observed in the water table elevation data (Figure 3.3b). The activity of a convergence zone at the southwest corner of the site (Figure 3.3f) caused the mean divergence to decrease to $-3 \times 10^{-5}$ $m^{-1}$ on the recession limb of high flow events at the Barren Fork Creek site.

It appeared that both the convergence zone PFP and the divergence zone PFP at the Barren Fork Creek site could be active at the same time. At baseflow both were active, but which one had the dominant effect on the mean divergence depended on the water table elevation. At higher stream stage, the convergence zone had a greater impact on groundwater flow, resulting in a negative mean divergence. At lower stream stages during baseflow, the divergence zone had a greater impact, resulting in a positive mean divergence.

### *Direction as an Indicator of Transient Storage*

The average groundwater flow direction at each floodplain site also changed considerably between baseflow and storm events (Figure 3.6). At the Barren Fork Creek field site, the average direction in the floodplain was approximately southwest ($200^o$ to $220^o$) during baseflow conditions, but changed to a southeastern direction (300° to 320°) during large flow events (Figure 3.7). At the Honey Creek floodplain site, the average groundwater direction was southwest (210° to 220°) (i.e., across the meander bend and directed back towards the stream) during baseflow conditions. During storm events, the average direction changed to northwest (i.e., 130° to 150° or away from the meander bend) (Figure 3.8). The statistical range in groundwater direction increased across both of the two-dimensional well grids during flow events (Figures 3.7 and 3.8), suggesting that the flow patterns in these floodplains became more complex during high stream stage.

The changes in average groundwater direction indicated the occurrence of transient storage within the floodplain: groundwater flow direction changed as water moved rapidly into the floodplain during the rising limb of the streamflow hydrograph and then returned to its original average direction as water drained through a preferential flow pathway during the recession of the hydrograph (Figures 3.7 and 3.8). Similar to the flow divergence, the change in the direction at both field sites appeared to be a function of the rate of change in the stream stage, with higher rates of change correlating to greater variations in the average groundwater direction compared to the direction under baseflow conditions. In fact, the maximum deviation in average groundwater gradient from the average gradient under baseflow conditions occurred slightly before the peak of the streamflow hydrograph at both sites. The average groundwater gradient after the peak shifted quickly back to the average gradient during baseflow conditions (Figures 3.7 and 3.8).

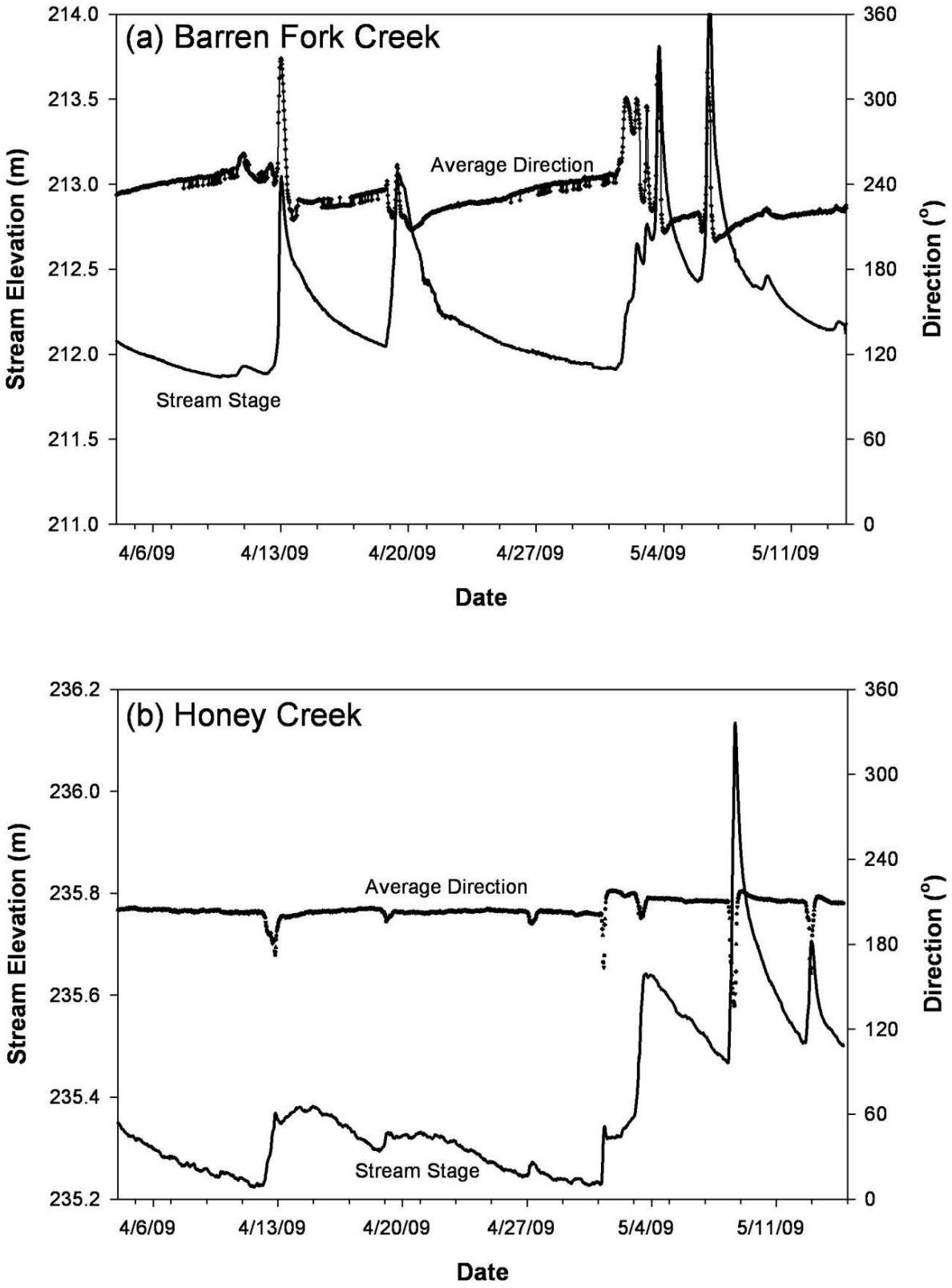


Figure 3.6. Average direction of the hydraulic gradient at the (a) Barren Fork and (b) Honey Creek field sites from April 4, 2009 to May 14, 2009.

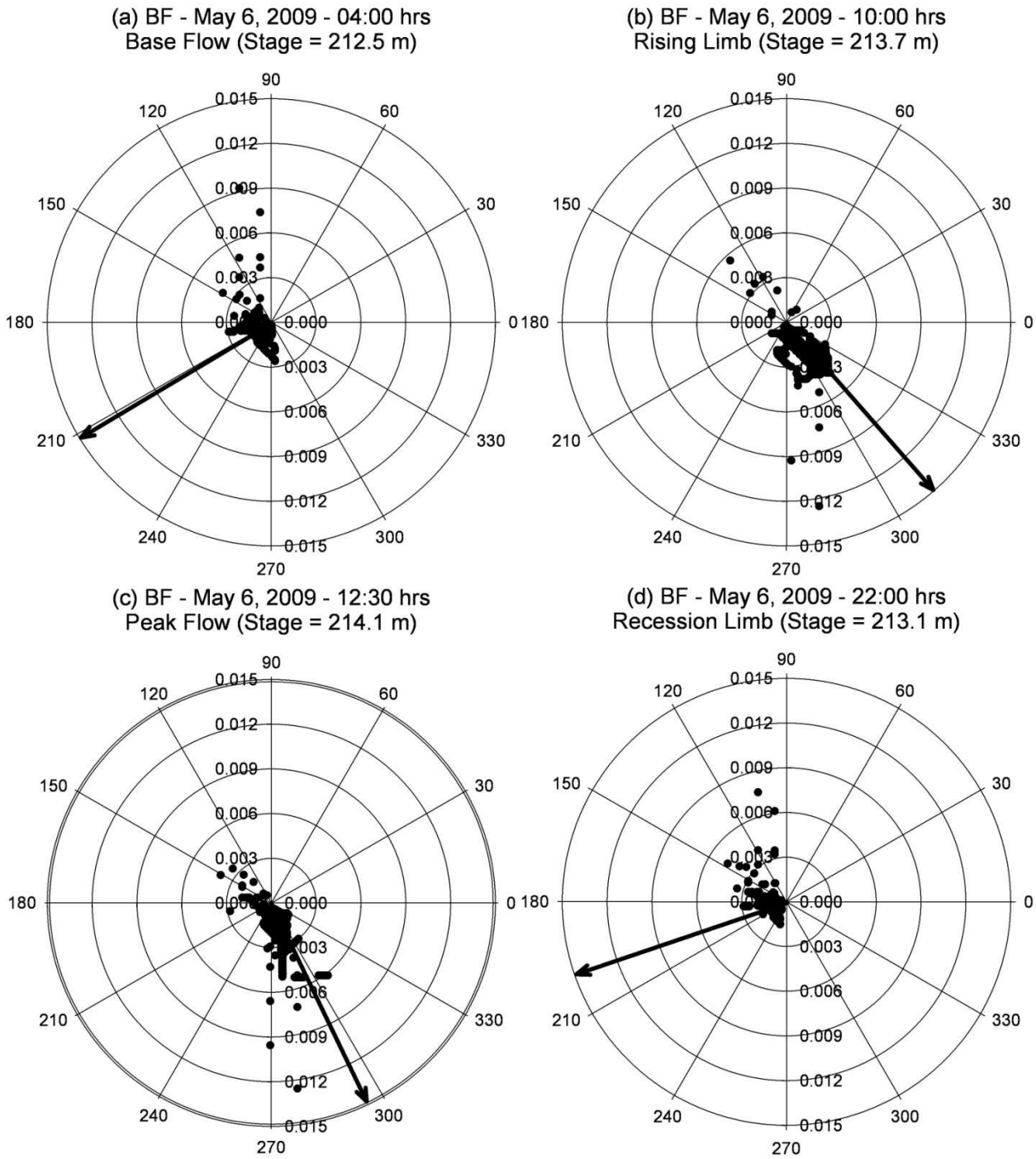


Figure 3.7. Polar plots of the hydraulic gradients during a hydrograph at the Barren Fork Creek (BF) field site on May 6, 2009. These polar plots are constructed with the magnitude and direction of the groundwater gradient for all points in the floodplain grid. The red line indicates the direction of the average groundwater gradient. (a) Base flow with an average groundwater gradient of 0.001 m/m at 211°, (b) rising limb with an average groundwater gradient of 0.003 m/s at 314°, (c) peak flow with an average groundwa ter gradient of 0.002 m/m at 295°, and (d) recession limb with an average groundwater gradient of 0.001 at 200°.

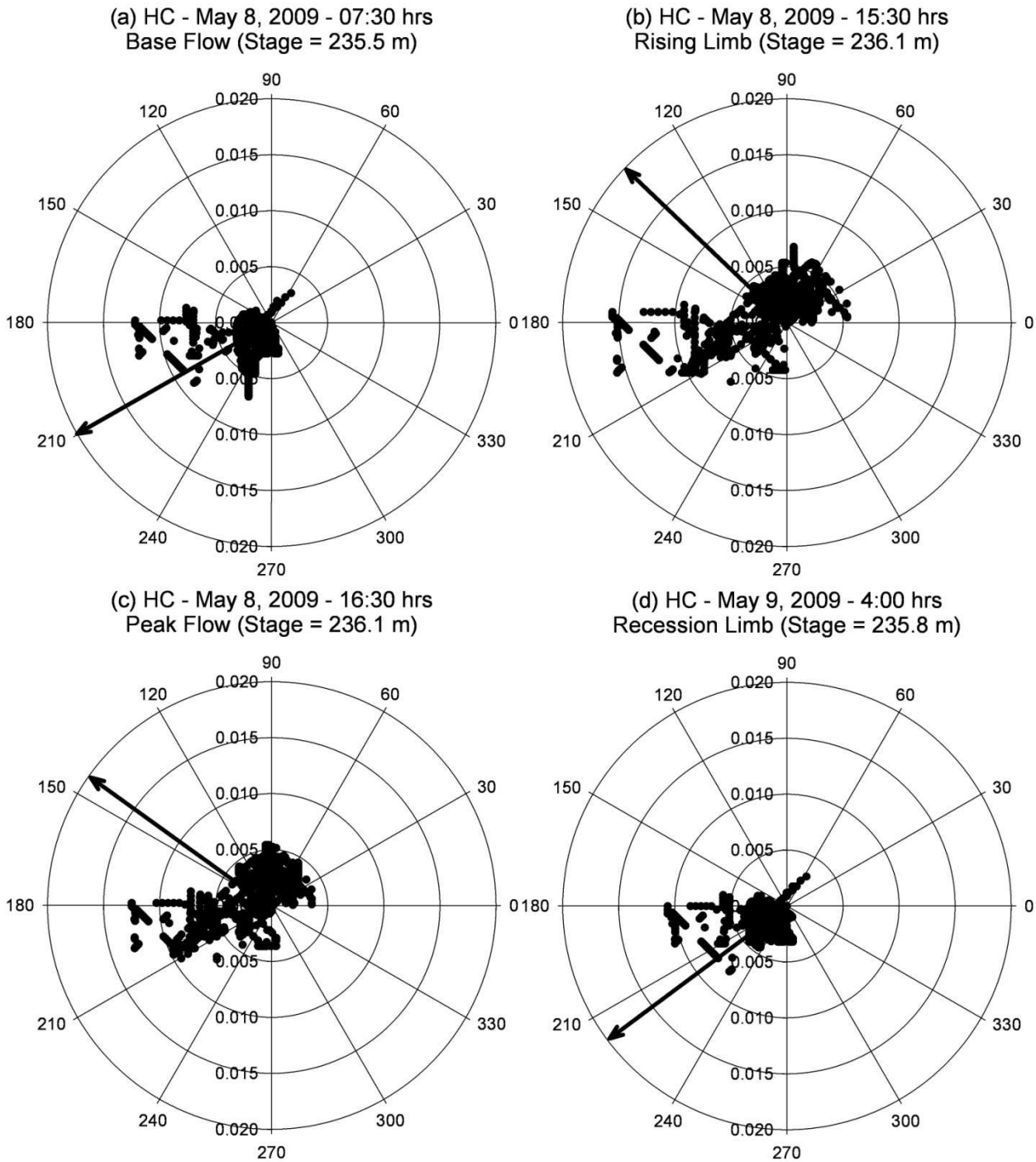


Figure 3.8. Polar plots of the hydraulic gradients during a hydrograph at the Honey Creek (HC) field site on May 8-9, 2009. These polar plots are constructed with the magnitude and direction of the groundwater gradient for all points in the floodplain grid. The red line indicates the direction of the average groundwater gradient. (a) Base flow with an average groundwater gradient of 0.003 m/m at 210°, (b) rising limb with an average groundwater gradient of 0.004 m/s at 136°, (c) peak flow with an average groundwa ter gradient of 0.003 m/m at 145°, and (d) recession limb with an average groundwater gradient of 0.003 at 217°.

### *Project Implications*

As discussed by Packman and Bencala (2000), the surface and subsurface hydrological interactions in these alluvial floodplains can be viewed from two different perspectives. The first is viewing the interaction from the stream. From this viewpoint, the interaction is commonly idealized using a transient storage model that simulates hyporheic storage in an aggregate fashion as a well-mixed but immobile system (Bencala and Walters, 1983). Harvey et al. (1996) and others have suggested this idealization captures rapid hyporheic transport (i.e., near streambed exchange) but cannot capture exchange with the more extensive alluvium. The groundwater divergence and direction results in this project further verify these conclusions and more intensely emphasize the importance of considering stream exchanges beyond the near-streambed zone (i.e., larger-scale transient storage) relative to changes in stream stage. Changes in discharge and stream stage are suggested to influence near-streambed transient storage (D'Angelo et al., 1993; Harvey and Bencala, 1993; Morrice et al., 1997; Worman et al., 2002; Zarnetske et al., 2007; Stofleth et al., 2008). However, as noted by Zarnestke et al. (2007), "…the overall understanding of how they [perturbations in discharge, elevation of channel stage, and water table] correlate to in-channel and hyporheic storage dynamics is still unclear", especially for larger-scale interactions with the alluvium. The presence of large-scale transient storage at high stream stage may have a direct impact on the transport of in-stream contaminant loads as the stream water interacts with the alluvial groundwater in floodplains throughout the watershed. Future work should be devoted to creating models capable of handling both the near-streambed and larger-scale transient storage to quantify implications of this larger-scale exchange on solute and contaminant transport in stream systems during both base flow and high flow conditions.

The second perspective is viewing the surface-subsurface interaction from the subsurface, which considers hyporheic exchange as the mixing of stream-derived and aquifer-derived water. This perspective relies heavily on the use of numerical groundwater flow models to describe reach-scale groundwater flow pathways (Packman and Bencala, 2000; Poole et al., 2006). Particle tracking models may be used to determine the extent of penetration of stream-derived water into the aquifer (Wroblicky et al., 1998). The stream is commonly idealized as a boundary that derives subsurface flow. Of course any modeling effort is dependent on the ability to adequately parameterize input data and specify the appropriate boundary conditions. Also, groundwater heads are typically measured throughout the study area to calibrate the model. The most sensitive parameter in groundwater flow models and the subject of most calibration effort is the aquifer hydraulic conductivity. The divergence and direction results from the two floodplain studies reported in this project indicate the necessity of considering horizontal zones of aquifer heterogeneity and anisotropy within alluvial floodplains to adequately simulate larger-scale PFPs over a range of water table elevations. Heterogeneity has been modeled by assuming a distribution of hydraulic conductivity and that the distribution is randomly distributed in space (Gotovac et al., 2009). However, the non-random nature of the heterogeneity has been confirmed by variograms performed on hydraulic conductivity data at these alluvial sites (Chapter 2; Miller et al., 2010b). These PFPs are hypothesized to be buried gravel bars, resulting in long, continuous zones of high conductivity (Chapter 2; Heeren et al., 2010). Also, groundwater heads measured for flow calibration should be measured during both baseflow and high stream stage events when the PFPs activate. It is important to appropriately identify potential PFPs prior to installation of observation wells for monitoring groundwater levels. Electrical resistivity imaging was used in this project to locate observation well sites at areas of potential flow convergence and divergence. Neglecting PFPs and their stage-dependent activation may limit the amount of useful information derived from groundwater flow models due to an inappropriate representation of the flow system.

## Summary and Conclusions

The assumptions of uniform, homogeneous stream/aquifer interaction and only localized, near-streambed hyporheic interactions were not appropriate in the studied alluvial floodplains. The activity of preferential flow pathways depended on the elevation of the water table and the interaction between the stream and the groundwater. It appeared that preferential flow pathways acted as divergence zones, allowing stream water to quickly enter the groundwater system, or as flow convergence zones draining a large groundwater area. Without properly locating observation wells within the pathways, general groundwater monitoring may have never indicated this preferential flow and transport. A method was developed to quantify aquifer heterogeneity using divergence of the water table gradient. During base flow conditions, non-zero results indicated areas of spatial heterogeneity in saturated hydraulic conductivity consistent with previous work (Chapter 2; Fuchs et al., 2009). During high flow events, divergence was a measure of both aquifer heterogeneity and the rapidly changing water table elevation (aquifer storage). At the Barren Fork Creek site, stream water consistently flowed into the alluvial aquifer, even during base flow conditions. Transient storage occurred in these alluvial floodplains systems as highlighted by the fact that the average groundwater flow direction at each floodplain site changed considerably between baseflow and storm events. Such transient storage may have a direct impact on the transport of in-stream contaminant loads as the stream water interacts with the alluvial groundwater along floodplains throughout the watershed. Transient zone storage models should be modified to consider this larger scale (i.e., beyond near-streambed) and stage-dependent storage. Furthermore, more work needs to be performed in additional alluvial floodplain sites with coarse, gravel material to document the occurrence of these rapid exchange flow pathways and their impact on contaminant fate and transport.

## References

Amoros, C., and G. Bornette. 2002. Connectivity and biocomplexity in waterbodies of riverine floodplains. *Freshwater Biology* 47: 761-776.

Bencala, K.E., and R.A. Walters. 1983. Simulation of solute transport in a mountain pool-and-riffile stream: A transient storage zone model. *Water Resources Research* 19: 718-724.

Cardenas, M.B. 2009. Stream-aquifer interactions and hyporheic exchange in gaining and losing sinuous streams. *Water Resources Research* 45: W06429, doi: 10.1029/2008WR007651.

Carlyle, G.C., and A.R. Hill. 2001. Groundwater phosphate dynamics in a river riparian zone: Effects of hydrologic flow paths, lithology, and redox chemistry. *Journal of Hydrology* 247: 151-168.

Cooper, A.B., C.M. Smith, and M.J. Smith. 1995. Effects of riparian set-aside on soil characteristics in an agricultural landscape: Implications for nutrient transport and retention. *Agriculture, Ecosystems, and Environment* 55: 61-67.

D'Angelo, D.J., J.R. Webster, S.V. Gregory, and J.L. Meyer. 1993. Transient storage in Appalachian and Cascade mountain streams as related to hydraulic characteristics. *Journal of the North American Benthological Society* 12: 223-235.

Fuchs, J.W., G.A. Fox, D.E. Storm, C. Penn, and G.O. Brown. 2009. Subsurface transport of phosphorus in riparian floodplains: Influence of preferential flow paths. *Journal of Environmental Quality* 38(2): 473-484.

Gotovac, H., V. Cvetkovic, and R. Andricevic. 2009. Flow and travel time statistics in highly heterogeneous porous media. *Water Resources Research* 45: W07402, doi: 1029/2008WR007168.

Harvey, J.W., B.J. Wagner, K.E. Bencala. 1996. Evaluating the reliability of the stream tracer approach to characterize stream-subsurface water exchange. *Water Resources Research* 32: 2441-2451.

Heeren, D.M, R.B. Miller, G.A. Fox, D.E. Storm, T. Halihan, and C.J. Penn, 2010. Preferential flow effects on subsurface contaminant transport in alluvial floodplains. *Transactions of the ASABE* 53(1): 127-136.

Hunt, B.W. 1995. *Fluid mechanics for Civil Engineers*. Dept. of Civil Engineering, University of Canterbury, Christchurch, New Zealand.

Kavvas, M.L., and A. Karakas. 1995. On the stochastic theory of solute transport by unsteady and steady groundwater flow in heterogeneous aquifers. *Journal of Hydrology* 179: 321-351.

Kumar, M., C.J. Duffy, and K.M. Salvage. 2009. A second-order accurate, finite volume-based, integrated hydrologic modeling (FIHM) framework for simulation of surface and subsurface flow. *Vadose Zone Journal* 8: 873-890.

Lacas, J.-G., M. Voltz, V. Gouy, N. Carluer, and J.-J. Gril. 2005. Using grassed strips to limit pesticide transfer to surface water: A review. *Agronomy for Sustainable Development* 25: 253-266.

McCarty, G., and J. Angier. 2001. Impact of preferential flow pathways on ability of riparian wetlands to mitigate agricultural pollution. In: *2nd International Symposium on Preferential Flow: Water Movement and Chemical Transport in the Environment*, Bosch, D., and K. King, (Eds.). American Society of Agricultural Engineers, St. Joseph, Mich., 53-56.

Miller, R.B., D.M. Heeren, G.A. Fox, T. Halihan, D.E. Storm, and A.R. Mittelstet. 2010a. Use of multi-electrode resistivity profiling to estimate saturated- and vadose-zone hydraulic properties of preferential flow paths in alluvial floodplains in the Ozark region of Eastern Oklahoma. In: *Proceedings of the ASCE EWRI World Environmental and Water Resources Congress*, ASCE, Reston, Va.

Miller, R.B., D.M. Heeren, G.A. Fox, D.E. Storm, T. Halihan, and A.R. Mittelstet. 2010b. Geophysical mapping of preferential flow paths across multiple floodplains. ASABE Paper No. 1008730, ASABE, St. Joseph, Mich.

Morrice, J.A., H.M. Valett, C.N. Dahm, and M.E.Campana. 1997. Alluvial characteristics, groundwater-surface water exchange and hydrologic retention in headwater streams. *Hydrological Processes* 11: 253-267.

Naiman, R.J., H. Decamps, and M.E. McClain. 2005. Catchments and the physical template. In: *Riparia: Ecology, Conservation, and Management of Streamside Communities*, Elsevier Academic Press, Boston, Mass., 19-48.

National Research Council (NRC), Committee on Hydrologic Science (COHS). 2004. Groundwater Fluxes across Interfaces. The National Academies Press, Washington, D.C.

Packman, A.I., and K.E. Bencala. 2000. Modeling surface-subsurface hydrological interactions. In: *Streams and Ground Waters*, Jones, J.B., and P.J. Mulholland (eds). Academic Press, San Diego, CA, 46-77.

Polyakov, V., A. Fares, and M.H. Ryder. 2005. Precision riparian buffers for the control of nonpoint source pollutant loading into surface water: A review. *Environmental Review* 13: 129-144.

Poole, G.C., J.A. Stanford, C.A. Frissell, and S.W. Running. 2002. Three-dimensional mapping of geomorphic controls on flood-plain hydrology and connectivity from aerial photos. *Geomorphology* 48: 329-347.

Poole, G.C., R.J. Naiman, J. Pastor, and J.A. Stanford. 1997. Uses and limitations of ground penetrating RADAR in two riparian systems. In: *Groundwater/Surface Water Ecotones: Biological and Hydrological Interactions and Management Options*, Gibert, J., J. Mathieu, and F. Fournier (Eds.). Cambridge University Press, Cambridge, England, 140-148.

Poole, G.C, J.A. Standford, S.W. Running, and C.A. Frissell. 2006. Multiscale geomorphic drivers of groundwater flow paths: subsurface hydrologic dynamics and hyporheic habitat diversity. *Journal of the North American Benthological Society* 25(2): 288-303.

Reichenberger, S., M. Bach, A. Skitschak, and H.-G. Frede. 2007. Mitigation strategies to reduce pesticide inputs into ground- and surface water and their effectiveness: A review. *Science of the Total Environment* 384: 1-35.

Rooij, G.H., and F. Stagnitti. 2000. Spatial variability of solute leaching: Experimental validation of a quantitative parameterization. *Soil Science Society of America Journal* 64: 499-504.

Sabbagh, G.J., G.A. Fox, A. Kamanzi, B. Roepke, and J.Z. Tang. 2009. Effectiveness of vegetative filter strips in reducing pesticide loading: Quantifying pesticide trapping efficiency. *Journal of Environmental Quality* 38(2): 762-771.

Sauer, T.J., and S.D. Logsdon. 2002. Hydraulic and physical properties of stony soils in a small watershed. *Soil Science Society of America Journal* 66: 1947-1956.

Schlottmann, J.L., R. Tanner, and M. Samadpour. 2000. Reconnaissance of the hydrology, water quality, and sources of bacterial and nutrient contamination in the Ozark Plateaus Aquifer System and Cave Springs Branch of Honey Creek, Delaware County, Oklahoma, March 1999 – March 2000. Water Resources Investigations Report 00-4210. Reston, Va.: U.S. Geological Survey.

Stanford, J.A., and J.V. Ward. 1992. Management of aquatic resources in large catchments: Recognizing interaction between ecosystem connectivity and environmental disturbance. In: *Watershed Management*, Naiman, R.J. (Ed.). Springer-Verlag, New York, N.Y., 91-124.

Stofleth, J.M., F.D. Shields, Jr., and G.A. Fox. 2008. Hyporheic and total storage exchange in small sand-bed streams. *Hydrological Processes* 22: 1885-1894.

Tellam, J.H., and D.N. Lerner. 2009. Management tools for the river-aquifer interface. *Hydrological Processes* 23: 2267-2274.

Turner, B.L., and P.M. Haygarth. 2000. Phosphorus forms and concentrations in leachate under four grassland soil types. *Soil Science Society of America Journal* 64(3): 1090-1099.

Worman, A., A.I. Packman, H. Johansson, and K. Jonsson. 2002. Effect of flow-induced exchange in hyporheic zones on longitudinal transport of solutes in streams and rivers. *Water Resources Research* 38(1): doi:10.1029/2001WR000769.

Wroblicky, G.W., M.E. Campana, H.M. Valett, and C.N. Dahm. 1998. Seasonal variation in surface-subsurface water exchange and lateral hyporheic area of two stream-aquifer systems. *Water Resources Research* 34: 317-328.

Zarnetske, J.P., M.N. Gooseff, T.R. Brosten, J.H. Bradford, J.P. McNamara, and W.B. Bowden. 2007. Transient storage as a function of geomorphology, discharge, and permafrost active layer conditions in Arctic tundra streams. *Water Resources Research* 43: W07410, doi:10.1029/2005WR004816.

# CHAPTER 4
# PHOSPHORUS CONCENTRATIONS IN PFP AND NON-PFP GROUNDWATER

## Abstract

While surface runoff is considered to be the primary transport mechanism for phosphorus (P), subsurface transport through coarse subsoil to gravel bed streams may be significant and represent a source of P not alleviated by current conservation practices (e.g., riparian buffers). Previous work has documented P transport in a preferential flow path (PFP) identified as a buried gravel bar. It is hypothesized that PFPs, if connected to the soil surface, provide a rapid and efficient method of transporting P, and that these alluvial features are transient storage zones for nutrients, acting as a sink during high flow and a source during baseflow. The objective of this project was to document P concentrations in alluvial groundwater both in PFP and non-PFP subsoils. Long-term monitoring was performed at floodplain sites adjacent to the Barren Fork Creek and Honey Creek in northeastern Oklahoma. Based on results from subsurface electrical resistivity mapping, observation wells were installed both in PFPs and in non-PFP subsoils. P samples were obtained from the observation wells and in the stream to document P concentration gradients over time. The PFPs that rapidly transported P had groundwater total P concentrations that mimicked the stream and exceeded 0.20 mg/L during some high flow events. The pathways with rapid P transport did not necessarily correlate to subsurface zones of high hydraulic conductivity. Pathways of high hydraulic conductivity must be connected to the surface water source and be hydraulically activated for preferential transport to occur.

## Introduction

The Ozark ecoregion of Missouri, Arkansas, and Oklahoma is approximately 62,000 $km^2$ and is characterized by karst topography, including caves, springs, sink holes, and losing streams. The erosion of carbonate bedrock (primarily limestone) by slightly acidic water has left a large residuum of chert gravel in Ozark soils, with floodplains generally consisting of coarse chert gravel overlain by a mantle of gravelly loam or silt loam. Topsoil depth in the floodplains ranged from 1 to 300 cm in the Oklahoma Ozarks, and generally increased with increasing stream order. Karst topography adds complexity to the potential pathways for contaminant transport in the Ozark ecoregion (Neill et al., 2003; Davis et al., 2005).

Increased nutrient loads result in several adverse impacts on surface water quality, including excessive algal growth, fish kills, polluted drinking water, and taste and odor issues. Scientists and engineers need to identify critical nutrient source areas and transport mechanisms within a catchment in order to protect and enhance drinking water systems, recreation activities, and aquatic ecosystems. Nitrogen is a concern, but phosphorus (P) is generally considered the most limiting nutrient in most surface water systems (Daniel et al., 1998). In addition, excessive soil P concentrations can increase potential for P transport to surface waters or leaching into the groundwater, exacerbating the problem.

Countries throughout the world have spent billions of dollars restoring and protecting riparian buffer zones adjacent to stream systems to reduce sediment, nutrient, and pesticide transport to streams from upland areas and alluvial floodplains. Buffer strip effectiveness becomes an issue

if a transport pathway through the subsurface is significant (Cooper et al., 1995; Lacas et al., 2005), since buffers primarily address the commonly observed and more easily understood surface runoff transport mechanism (Lacas et al., 2005; Popov et al., 2005; Reichenberger et al., 2007; Poletika et al., 2009; Sabbagh et al., 2009). Subsurface transport may be important due to local or regional conditions (Lacas et al., 2005), even for a highly sorbing contaminant such as P (Turner and Haygarth, 2000; Fuchs et al., 2009).

Subsurface P transport is a less studied and understood transport mechanism compared to transport by surface runoff, although numerous studies have reported subsurface P transport, including fields with tile drainage (Turner and Haygarth, 2000; Djodjic et al., 2004; Kleinman et al., 2004; Nelson et al., 2005; Andersen and Kronvang, 2006; Hively et al., 2006). For example, Kleinman et al. (2004) noted that P leaching is a significant, but temporally and spatially variable transport pathway. Djodjic et al. (2004) suggested that soils with high infiltration rates, e.g. due to macroporosity, possess reduced buffer capacity for P and therefore studies should not depend on soil test P or soil P sorption estimates alone to determine leaching potential. From research on four grassland soils, Turner and Haygarth (2000) documented that subsurface P transport, primarily in the dissolved form, can occur at concentrations that could cause eutrophication. When assessing long-term risk of P loss from waste-amended soils, Nelson et al. (2005) indicated that P leaching and subsurface transport should be considered. Andersen and Krovang (2006) developed a Danish P Index that incorporated leaching and tile drains as potential P transport pathways. Developing a model for total dissolved P (TDP) in a dairy farm watershed, Hively et al. (2006) considered transport in both baseflow and surface runoff. In addition, other researchers are beginning to emphasize colloidal P transport in the subsurface, as P adsorbs to small particles capable of being transported through soil pore spaces.

There have been several studies conducted in which observation wells were used to monitor the flow of nutrients in alluvial floodplains (Vanek, 1993; Carlyle and Hill, 2001; Fuchs et al., 2009; Heeren et al., 2010b). A study by Cooper et al. (1995) showed a high P availability for groundwater transport due to saturation of the riparian zone. Monitoring 12 wells in a lake riparian zone, Vanek (1993) noted groundwater P concentrations ranging from 0.4 to 11 mg/L with an average of 2.6 mg/L. Thompson and McFarland (2010) observed high soil P levels in streambank sediments near the water table, thought to have been transferred there by flow from the surface water into the alluvial aquifer. Carlyle and Hill (2001) monitored the behavior of P in the subsurface in a river riparian zone and suggested that riparian areas can become saturated with P. They documented higher soluble reactive P (SRP) concentrations (0.10 to 0.95 mg/L) in areas having soils with higher hydraulic conductivities buried under topsoils. Due to the increased redox potential, they suggested that riparian areas might actually be contributing to the release of P.

Even though surface runoff has shown higher concentrations in many field studies, subsurface flow with low P concentrations but occurring over a long time period may still significantly contribute to the total nutrient load of a surface water body. The above findings show that there is a potential for focused subsurface nutrient transport through preferential pathways, also called paleochannels. Exchange of water and P between the stream and the gravel subsoils is distributed across the entire river channel but enhanced in these preferential pathways (Malard et al., 2002). There is a need for additional studies devoted to understanding both groundwater flow patterns and P transport capacity through the subsurface of alluvial floodplains.

The objective of this project was to document P concentrations in alluvial groundwater both in PFP and non-PFP subsoils. Long-term monitoring was performed at floodplain sites adjacent the Barren Fork Creek and Honey Creek in northeastern Oklahoma, and it is hypothesized that similar hydrogeologic conditions exist in gravel bed streams and their associated shallow alluvial aquifers worldwide.

# Materials and Methods

## *Alluvial Floodplain Sites*

The alluvial floodplain sites were located in the Ozark region of northeastern Oklahoma. The Barren Fork Creek site (Figures 2.6 and 3.1a, latitude: 35.90°, longitude: -94.85°) was immediately downstream of the Eldon Bridge U.S. Geological Survey (USGS) gage station 07197000. With a watershed size of 845 $km^2$, the Barren Fork Creek site had a median daily flow of 3.6 $m^3$ $s^{-1}$. The Honey Creek site (Figures 2.7 and 3.1b, latitude: 36.54°, longitude: -94.70°) was also located immediately downstream of a USGS gage station (07189542). As a smaller order stream, the Honey Creek site had a 0.54 $m^3$ $s^{-1}$ median daily flow and a 150 $km^2$ watershed.

The Barren Fork Creek site was a hay field with a soil test P (STP) of 33 mg/kg (59 lb/ac) and had not received fertilizer for several years. The Honey Creek study site was composed of both forest and grassland. Adjacent to a tree farm, the area had received fertilizer in the past resulting in an STP of 60 mg/kg (106 lb/ac). The riparian area on Honey Creek was located on the inside of a meander bend, an area likely to aggradational. The study area at the Barren Fork Creek was located on the outside of a meander bend and was being eroded away by the stream. The soils of both floodplain sites were classified as Razort gravelly loam underlain with alluvial gravel deposits. Topsoil thickness ranged from 0.5 to 1.0 m at the Barren Fork Creek site and from 0.1 to 0.5 m at the Honey Creek site. Soil hydraulic studies on these soil types have shown that subtle morphological features can lead to considerable differences in soil water flow rates (Sauer and Logsdon, 2002). Fuchs et al. (2009) described some of the soil and hydraulic characteristics of the Barren Fork Creek floodplain site, including estimates of hydraulic conductivity for the gravel subsoil between 140 and 230 m $d^{-1}$ based on falling head trench tests.

## *Observation Well Installation*

Assuming a positive correlation between electrical resistivity and hydraulic conductivity, observation well locations were located in PFPs and in non-PFP subsoils (Figure 3.1), based on electrical resistivity results (Chapter 2; Miller et al., 2010a,b). Using a Geoprobe Systems drilling machine (6200 TMP, Kejr, Inc., Salina, KS), observation wells were installed in the alluvial floodplains with a 2 to 3 m screened section at the base. Depth to refusal ranged from 4.0 m to greater than 5.0 m at the Barren Fork Creek site and from 2.5 to 3.5 m at the Honey Creek site.

## *Phosphorus Sampling and Testing*

Water samples from observation wells were collected during multiple high flow events (Figure 4.1) from the top of the water table (i.e., upper 10 cm) using a peristaltic pump. High flow events were of particular interest because stream P concentrations generally increase with streamflow in these watersheds (Storm et al., 2009). Samples were stored on ice and transported back to the laboratory for analysis. Samples were digested with the sulfuric acid-nitric acid method (Pote et al., 2009). Total P concentrations were determined colorimetrically (Murphy and Riley, 1962; EPA Method 365.2) with a spectrophotometer (Spectronic 21D, Milton Roy, Ivyland, PA). Contour plots of total P concentration were generated with Matlab (The Mathworks, Natick, MA).

A cubic interpolation was performed to determine the P concentration for grid points in the two-dimensional well field with a contour interval of 0.01 mg/L P. Data from the local USGS gage stations were also used in the analysis.

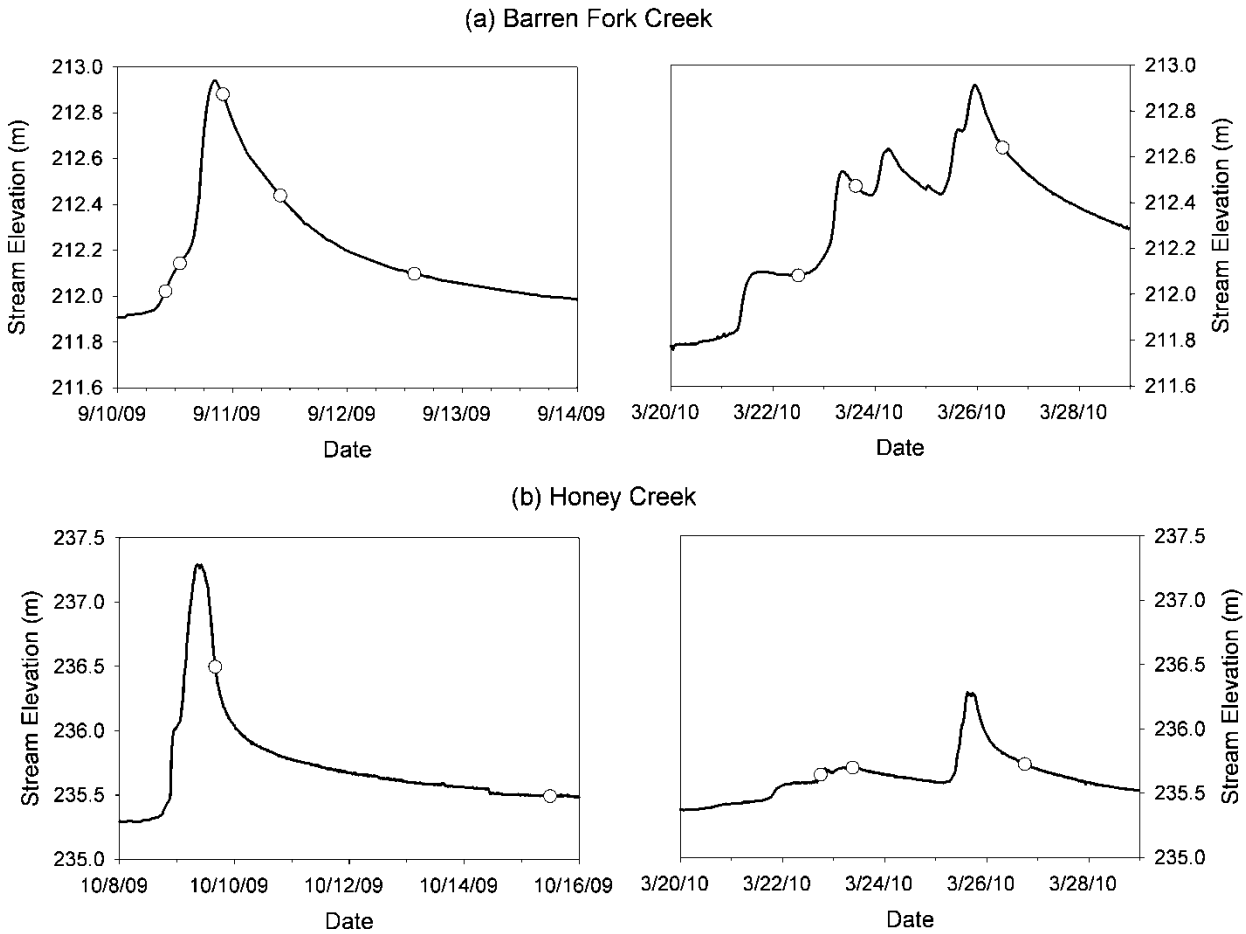


Figure 4.1. Hydrographs for the (a) Barren Fork Creek and (b) Honey Creek field sites. Circles designate dates of P sampling from the observation wells and creeks.

## Results and Discussion

### *Phosphorus Concentrations*

Contour plots of stream and groundwater total P concentrations at the Barren Fork Creek and Honey Creek field sites are shown in Figures 4.2 to 4.4 for two high flow events. During baseflow conditions, groundwater P concentrations were typically 0.01 to 0.04 mg/L and 0.02 to 0.06 mg/L at the Barren Fork Creek and Honey Creek field sites, respectively. The P concentrations were generally highest where stream water was entering the groundwater system, and decreased with distance down-gradient from the stream. Groundwater flow is generally to the southwest at both sites (Chapter 3; Heeren et al., 2010a). This is likely due to sorption of the P onto the fine material in the gravel. Fuchs et al. (2009) reported a mass of P sorbed per unit mass of soil at complete surface coverage of 125 mg $kg^{-1}$ and a binding energy

of 0.048 L $mg^{-1}$ for a Langmuir Isotherm performed on the fine material (i.e. < 2.0 mm) in the alluvial aquifer at the Barren Fork Creek site. Even though total P concentrations decreased as stream water moved through the aquifer due to sorption and dilution, transient storage was occurring in the alluvial aquifer as seen in the significant levels of P leaving the study area (and presumably re-entering the stream).

During high flow events, the maximum P concentrations measured in the groundwater were as high as 0.20 mg/L at the Barren Fork Creek site and 0.25 mg/L at the Honey Creek field site. In the groundwater adjacent to the creeks, a retarded migration of P into the alluvial groundwater was observed (Figures 4.2 to 4.4). However, in PFPs, rapid transport of P occurred in the groundwater system with concentrations at or near the P concentration in the creeks during larger storm events when the PFPs activated. For example, well 28 at the Barren Fork Creek site (in the southeast corner of Figure 3.1 and 4.2c,d), 100 m from the stream, had P concentrations similar to the stream P concentration. Well 28 was located adjacent to an abandoned stream channel that runs along the bluff; it is possible that the PFP is a buried lateral gravel bar. This would be consistent with observations in Chapter 3. Although only a fraction of the PFP wells had high P concentrations, high heterogeneity can result in situations where the main portion of the flow occurs in a few flow paths (Gotovac et al., 2009). It is hypothesized that high hydraulic conductivity combined with a high P concentration may result in a significant P load.

To determine whether P concentrations varied with depth at the Barren Fork Creek site, low-flow sampling (with the peristaltic pump) was used on March 23, 2010, to collect samples at both the top of the water table and 2.0 m below the water table. (Sampling with depth was not performed at the Honey Creek site due to the shallow depth of the aquifer.) In most wells, P concentrations were similar at both depths. However, in well 28 (in the southeast corner of Figure 4.3b), the 2-m sample had a P concentration of 0.19 mg/L (compared to 0.04 mg/L at the top of the water table), which approached the level of P in the stream. These concentrations suggested that this PFP was at a particular elevation, near the bottom of the aquifer. The high concentrations in well 28 in Figure 4.2 were likely from the higher pumping rate that was used in 2009, resulting in mixing of groundwater from different depths within the observation well. Since the high flow events were similar in magnitude at the Barren Fork Creek site (Figure 4.1), this PFP was activated during both events. Honey Creek had significantly more activity in PFPs in 2009 due to the 6-yr recurrence interval event, compared to the less than 2-yr recurrence interval events in 2010.

Suspended colloids and sediment often possess particulate P; therefore high total P concentrations tended to correlate with samples that were visibly cloudy. Due to the shallow depth of water in the wells at the Honey Creek site, it was difficult to determine when the cloudiness was due to suspended colloids in the groundwater and when it was due to agitated sediment from the bottom of the well.

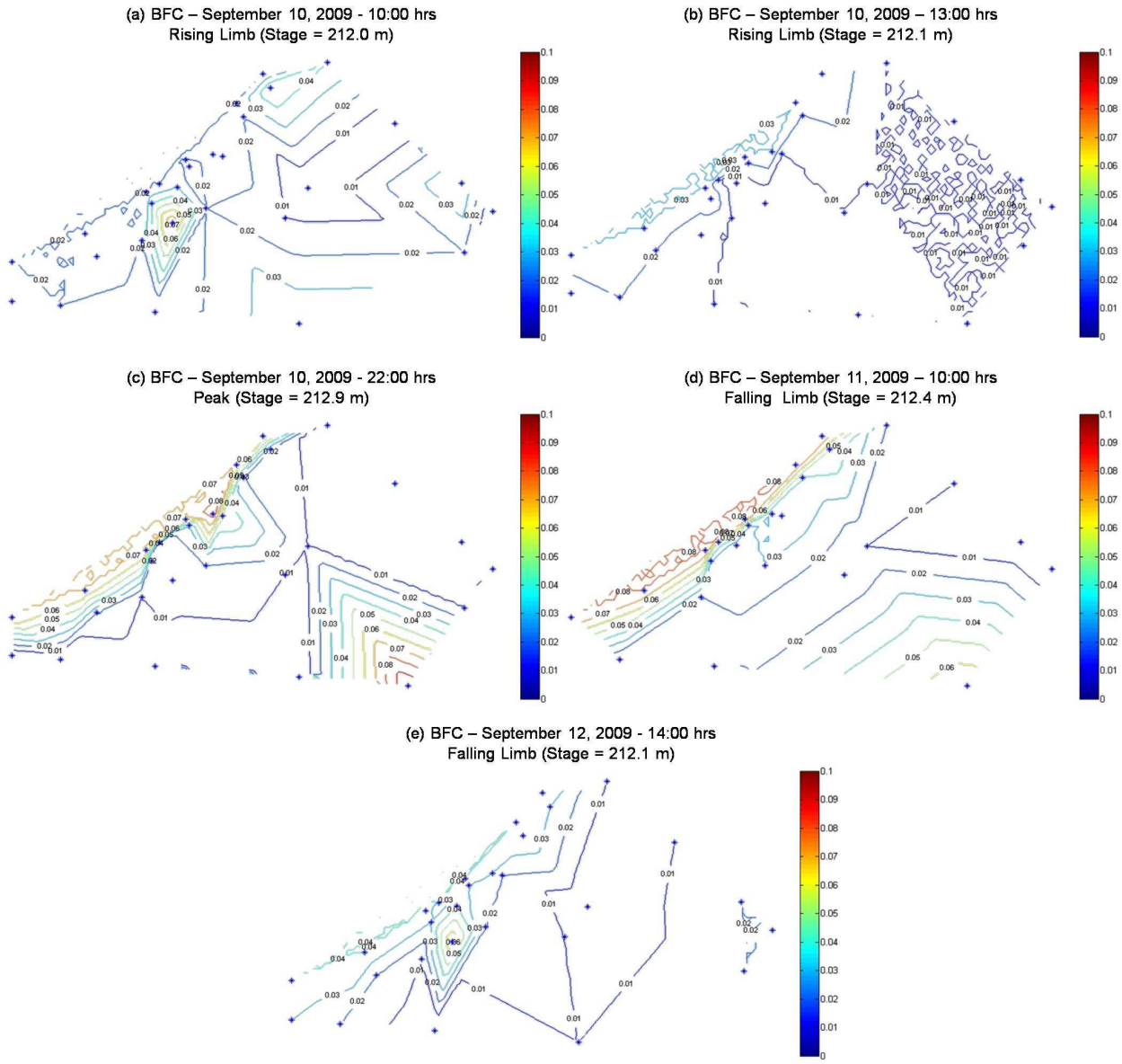


Figure 4.2. Total P concentration (mg/L as P) contour plots for the Barren Fork Creek (BFC) for the September 10, 2009, high flow event. Maximum flow was 86 $m^3 s^{-1}$, a 1.1-yr recurrence interval event.

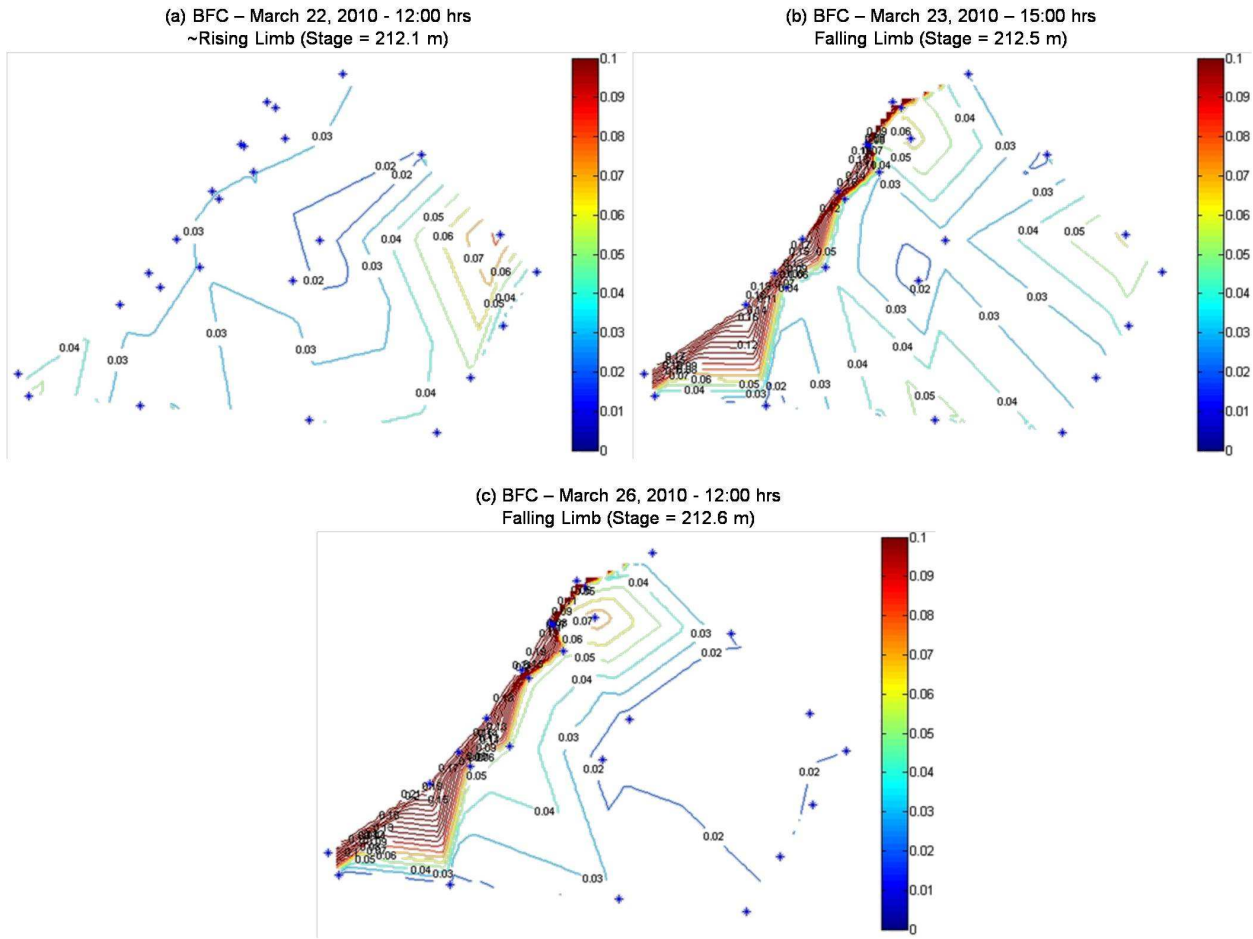


Figure 4.3. Total P concentration (mg/L as P) contour plots for the Barren Fork Creek (BFC) for the March 23 and March 25, 2010, flow events. The maximum flow for the March 23, 2010, event (a and b) was 48 $m^3 s^{-1}$, a 1.05 year recurrence interval event. The maximum flow for the March 25, 2010, event (c) was 85 $m^3 s^{-1}$, a 1.1-yr recurrence interval event.

Groundwater total P concentrations were also summarized by the median and interquartile range (Table 4.1). A general linear model was used to analyze differences between PFP and non-PFP wells, but the differences were statistically different in only one of the four datasets (Table 4.2). These results suggested that although the PFP wells were located in zones of high hydraulic conductivity, flow capacity was not the only condition necessary for significant P transport. Zones of high conductivity must be connected (i.e., not isolated by low conductivity material) and hydrologically activated (e.g., water table reaching a minimum elevation) for preferential flow to occur. Finally, the preferential flow must be connected to a P source (e.g., high concentrations in the stream or leaching from the soil surface) to be transporting P. Therefore, it is not surprising that only a fraction of the PFP wells had high P concentrations. The general linear model was also used to compare differences between wells close to the stream and wells far from the stream, and found the distance from the stream to be a statistically significant variable in two of the four data sets. This is consistent with the observation of P generally moving into the aquifer but with the movement retarded due to sorption.

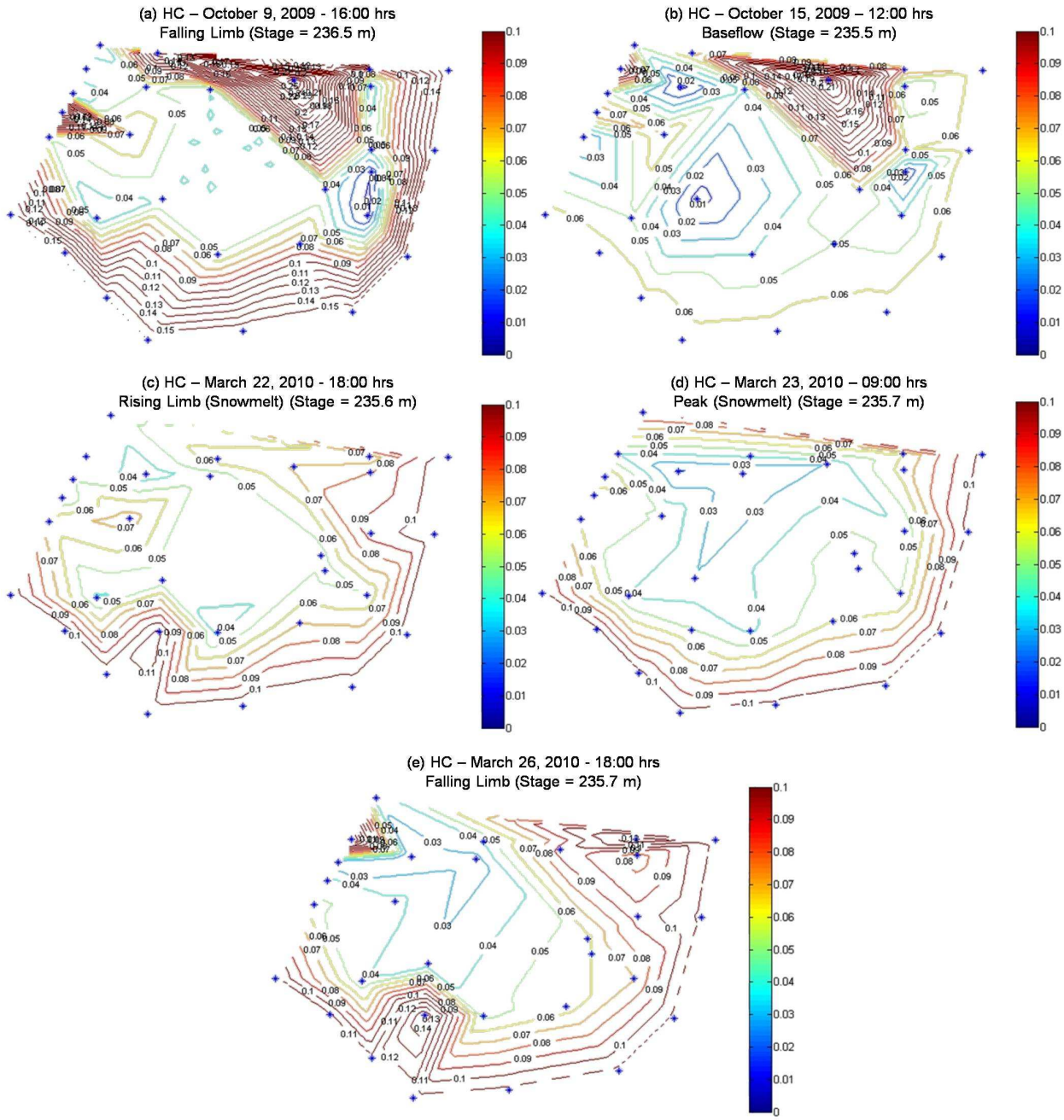


Figure 4.4. Total P concentration (mg/L as P) contour plots for Honey Creek (HC) for the October 9, 2009, and March 23 and March 25, 2010, flow events. The maximum flow for the October 9, 2009, event (a and b) was 81 $m^3$ $s^{-1}$, a 6 year recurrence interval event. The maximum flow for the March 23, 2010, event (c and d) was 6.1 $m^3$ $s^{-1}$, a 1.1 year recurrence interval event. The maximum flow for the March 25, 2010, event (e) was 24 $m^3$ $s^{-1}$, a 1.7-yr recurrence interval event.

Table 4.1. Total phosphorus concentrations (mg/L as P). Groundwater concentrations are characterized by the median and interquartile range (IQR).

| Site | Date | Runoff Source | Hydrograph | Groundwater Median | Groundwater IQR | Stream |
|---|---|---|---|---|---|---|
| Barren Fork Creek | 9/10/09A | Rainfall | Rising Limb | 0.02 | 0.03 | 0.02 |
| | 9/10/09B | Rainfall | Rising Limb | 0.01 | 0.01 | 0.03 |
| | 9/10/09C | Rainfall | Peak | 0.01 | 0.02 | 0.07 |
| | 9/11/09 | Rainfall | Falling Limb | 0.02 | 0.03 | 0.08 |
| | 9/12/09 | Rainfall | Falling Limb | 0.02 | 0.02 | 0.04 |
| | 3/22/10 | Snowmelt | ~Rising Limb | 0.03 | 0.01 | 0.03 |
| | 3/23/10 | Snowmelt | Falling Limb | 0.04 | 0.02 | 0.20 |
| | 3/26/10 | Rainfall | Falling Limb | 0.02 | 0.03 | 0.21 |
| Honey Creek | 10/09/09 | Rainfall | Falling Limb | 0.05 | 0.03 | 0.16 |
| | 10/15/09 | Rainfall | Baseflow | 0.05 | 0.03 | 0.07 |
| | 3/22/10 | Snowmelt | Rising Limb | 0.05 | 0.02 | 0.11 |
| | 3/23/10 | Snowmelt | Peak | 0.05 | 0.02 | 0.10 |
| | 3/26/10 | Rainfall | Falling Limb | 0.05 | 0.04 | 0.11 |

Table 4.2. Comparison of total phosphorus concentrations between PFP and non-PFP observation wells, and between wells close to the stream and wells far from stream. Probability (p) from a General Linear Model with $p<0.05$ being significant.

| Site | Year | Probability Distance From Stream | Probability PFP v. non-PFP |
|---|---|---|---|
| Barren Fork Creek | 2010 | 0.000 | 0.000 |
| Barren Fork Creek | 2009 | 0.528 | 0.169 |
| Honey Creek | 2010 | 0.006 | 0.532 |
| Honey Creek | 2009 | 0.285 | 0.161 |

## Summary and Conclusions

During baseflow conditions, groundwater P concentrations were typically 0.01 to 0.06 mg/L. During high flow events, the maximum P concentrations measured in the groundwater were as high as 0.20 mg/L at the Barren Fork Creek site and 0.25 mg/L at the Honey Creek site. In the general groundwater system adjacent to the creek, a slow migration of P into the alluvial groundwater was observed. However, in preferential flow pathways, rapid transport of P was possible in the groundwater system with concentrations at or near the P concentration in the streams during large storm events when the PFPs activated. Without properly locating observation wells within the pathways, general groundwater monitoring may have never indicated this preferential flow and transport. The pathways with rapid P transport did not necessarily correlate to subsurface zones of high hydraulic conductivity. Pathways of high hydraulic conductivity must be hydraulically activated for preferential flow to occur and must be connected to the surface water source for preferential transport of P to occur. High P levels at the soil surface would be another possible source for preferential transport, but that transport mechanism was not studied in this project.

This project shows that PFPs can transport water and P rapidly from the stream through the groundwater system, but more work needs to be done to characterize runoff P leaching through the topsoil, its connectivity to the PFPs, and its rapid movement to the stream bypassing riparian buffers. Such results emphasize the sporadic nature of focused recharge/discharge in these systems and more work should be devoted to understanding the occurrence and activation of alluvial preferential flow pathways.

## References

Andersen, H.E., and B. Kronvang. 2006. Modifying and evaluating a P index for Denmark. *Water, Air, and Soil Pollution* 174(1-4): 341-353.

Carlyle, G.C., and A.R. Hill. 2001. Groundwater phosphate dynamics in a river riparian zone: Effects of hydrologic flow paths, lithology, and redox chemistry. *Journal of Hydrology* 247: 151-168.

Cooper, A.B., C.M Smith, and M.J. Smith. 1995. Effects of riparian set-aside on soil characteristics in an agricultural landscape: Implications for nutrient transport and retention*. Agriculture, Ecosystems, and Environment* 55: 61-67.

Daniel, T.C., A.N. Sharpley, and J.L. Lemunyon. 1998. Agricultural phosphorus and eutrophication: A symposium overview. *Journal of Environmental Quality* 27: 251-257.

Davis, R.K., S. Hamilton, and J. Van Brahana. 2005. *Escherichia Coli* survival in mantled karst springs and streams, Northwest Arkansas Ozarks, USA. *Journal of the American Water Resources Association* 41(6): 1279-1287.

Djodjic,F., B. Katarina, and L. Bergstrom. 2004. Phosphorus leaching in relation to soil type and soil phosphorus content. *Journal of Environmental Quality* 33: 678–684.

Fuchs, J.W., G.A. Fox, D.E. Storm, C. Penn, and G.O. Brown. 2009. Subsurface transport of phosphorus in riparian floodplains: Influence of preferential flow paths. *Journal of Environmental Quality* 38(2): 473-484.

Gotovac, H., V. Cvetkovic, and R. Andricevic. 2009. Flow and travel time statistics in highly heterogeneous porous media. *Water Resources Research* 45: W07402, doi: 10.1029/2008WR007168.

Heeren, D.M., R.B. Miller, G.A. Fox, D.E. Storm, A.K. Fox, and A.R. Mittelstet. 2010a. Impact of preferential flow paths on stream and alluvial groundwater interaction. In *Proc. ASCE EWRI World Environmental and Water Resources Congress*. Reston, Va.: American Society of Civil Engineers.

Heeren, D.M., R.B. Miller, G.A. Fox, D.E. Storm, C.J. Penn, and T. Halihan. 2010b. Preferential flow path effects on subsurface contaminant transport in alluvial floodplains. *Transactions of the ASABE* 53(1): 127-136.

Hively, W.D., P. Gerard-Marchant, and T.S. Steenhuis. 2006. Distributed hydrological modeling of total dissolved phosphorus transport in an agricultural landscape II. Dissolved phosphorus transport. *Hydrology and Earth Systems Sciences* 10(2): 263-276.

Kleinman, P.J.A., B.A. Needelman, A.N. Sharpley, and R.W. McDowell. 2004. Using soil phosphorus profile data to assess phosphorus leaching potential in manured soils. *Soil Science Society of America Journal* 67(1): 215-224.

Lacas, J.-G., M. Voltz, V. Gouy, N. Carluer, and J.-J. Gril. 2005. Using grassed strips to limit pesticide transfer to surface water: A review. *Agronomy for Sustainable Development* 25: 253-266.

Malard, F., K. Tockner, M.J. Dole-Oliver, and J.V. Ward. 2002. A landscape perspective of surface-subsurface hydrological exchanged in river corridors. *Freshwater Biology* 47: 621-640.

Miller, R.B., D.M. Heeren, G.A. Fox, T. Halihan, D.E. Storm, and A.R. Mittelstet. 2010a. Use of multi-electrode resistivity profiling to estimate saturated- and vadose-zone hydraulic properties of preferential flow paths in alluvial floodplains in the Ozark region of Eastern Oklahoma. In *Proc. ASCE EWRI World Environmental and Water Resources Congress*. Reston, Va.: American Society of Civil Engineers.

Miller, R.B., D.M. Heeren, G.A. Fox, D.E. Storm, T. Halihan, and A.R. Mittelstet. 2010b. Geophysical mapping of preferential flow paths across multiple floodplains. ASABE Paper No. 1008730. St. Joseph, Mich.: ASABE.

Murphy, J., and J.P. Riley. 1962. A modified single solution method for the determination of phosphate in natural waters. *Analytica Chimica Acta* 27: 31-36.

Neill, H., M. Gutierrez, and T. Aley. 2003. Influences of agricultural practices on water quality of Tumbling Creek cave stream in Taney County, Missouri. *Environmental Geology* 45: 550-559.

Nelson, N.O., J.E. Parsons, and R.L. Mikkelson. 2005. Field-scale evaluation of phosphorus leaching in acid sandy soils receiving swine waste*. Journal of Environmental Quality* 34(6): 2024-2035.

Poletika, N.N., P.N. Coody, G.A. Fox, G.J. Sabbagh, S.C. Dolder, and J. White. 2009. Chlorpyrifos and atrazine removal from runoff by vegetated filter strips: Experiments and predictive modeling. *Journal of Environmental Quality* 38(3): 1042-1052.

Pote, D.H., T.C. Daniel, and P.B. DeLaune. 2009. Total phosphorus and total dissolved phosphorus in water samples. In *Methods of Phosphorus Analysis for Soils, Sediments, Residuals, and Waters*, 113-114. J.L. Kovar and G.M. Pierzynski, eds. Blacksburg, Va.: SERA-IEG 17, Virginia Tech University.

Popov, V.H., P.S. Cornish, and H. Sun. 2005. Vegetated biofilters: the relative importance of infiltration and adsorption in reducing loads of water-soluble herbicides in agricultural runoff. *Agriculture, Ecosystems, and Environment* 114: 351–359.

Reichenberger, S., M. Bach, A. Skitschak, and H.-G. Frede. 2007. Mitigation strategies to reduce pesticide inputs into ground- and surface water and their effectiveness: a review. *Science of the Total Environment* 384: 1-35.

Sabbagh, G.J., G.A. Fox, A. Kamanzi, B. Roepke, and J.Z. Tang. 2009. Effectiveness of vegetative filter strips in reducing pesticide loading: Quantifying pesticide trapping efficiency. *Journal of Environmental Quality* 38(2): 762-771.

Sauer, T.J., and S.D. Logsdon. 2002. Hydraulic and physical properties of stony soils in a small watershed. *Soil Science Society of America Journal* 66: 1947–1956.

Storm, D.E., P.R. Busteed, A.R. Mittelstet, and M.J. White. 2009. Hydrologic modeling of the Oklahoma/Arkansas Illinois River Basin using SWAT 2005. Final Report submitted to the Oklahoma Department of Environmental Quality. Biosystems and Agricultural Engineering Department, Division of Agricultural Sciences and Natural Resources, Oklahoma State University, October 8, 2009.

Thompson, C.A., and A.M.S. McFarland. 2010. Effects of surface and groundwater interactions on phosphorus transport within streambank sediments. *Journal of Environmental Quality* 39: 548-557.

Turner, B.L., and P.M. Haygarth. 2000. Phosphorus forms and concentrations in leachate under four grassland soil types. *Soil Science Society of America Journal* 64 (3): 1090-1099.

Vanek, V. 1993. Transport of groundwater-borne phosphorus to Lake Bysjon, South Sweden. *Hydrobiologia* 251(1-3): 211-216.

# CHAPTER 5
# COMPARISON OF SUBSURFACE AND SURFACE RUNOFF PHOSPHORUS TRANSPORT

## Abstract

There have been countless studies on phosphorus (P) contributions from surface runoff, but studies comparing the contribution of surface versus subsurface P are limited, as subsurface transport is often considered negligible. Previous work has shown that the transport of P in the gravelly subsurface at two sites in northeast Oklahoma can be significant, especially in preferential flow paths (PFPs), hypothesized to be buried gravel bars. The objective of this project was to quantify, based on field data, the subsurface P transport capacity on an annual load basis, and compare this estimated subsurface load to the surface runoff load from simulations with the Pasture Phosphorus Management Calculator (PPM Plus). Ozark ecoregion study sites adjacent to the Barren Fork Creek and Honey Creek, neither of which have received litter applications or extensive cattle production in the past decade, were instrumented with observation wells. Groundwater levels and P concentrations were monitored for several months. Using Monte Carlo simulations based on appropriate statistical distributions derived from these data, the mean subsurface P load traveling through the groundwater with a single PFP was estimated to be 0.12 kg $yr^{-1}$ and 0.02 kg $yr^{-1}$ for the Barren Fork Creek and Honey Creek field sites, respectively. Computer simulations were performed using PPM Plus based on current site conditions (i.e., no fertilization or cattle grazing), resulting in average total P surface runoff loads of 0.46 kg $yr^{-1}$ for the Barren Fork Creek site and 0.67 kg $yr^{-1}$ for the Honey Creek site. Simulations were also performed based on typical intensive pasture management for the region with poultry litter application and cattle grazing. These simulations resulted in total P runoff loads of 14.0 kg $yr^{-1}$ at the Barren Fork Creek site and 9.8 kg $yr^{-1}$ at the Honey Creek site, an order of magnitude greater than the estimated subsurface P transport capacities on low intensity agricultural fields. Subsurface P contribution with a single PFP was significant compared to surface runoff for the low intensity agricultural fields. These results indicated that the subsurface P capacity of alluvial floodplains in the Ozark ecoregion was at least $10^{-2}$ to $10^{-1}$ kg $yr^{-1}$, although the capacity may be higher in cases with greater numbers of PFPs and where the subsurface is connected to a larger P source. Further work needs to address sites with phosphorus fertilizer application and cattle grazing, quantifying P leaching through the topsoil and potentially higher subsurface P loads.

## Introduction

Phosphorus (P) is a necessary nutrient for terrestrial and aquatic plants, yet over-application of organic and/or inorganic fertilizers to agricultural fields can result in elevated Soil Test Phosphorus (STP) levels and can lead to eutrophication in receiving streams and reservoirs (NRCS, 1994). One such area of concern is eastern Oklahoma and western Arkansas where poultry litter is often applied based on nitrogen requirements, resulting in excessive P application (White, 2007). Sharpley at al. (2003) have noted that feed imported to support concentrated poultry production has resulted in a net increase of nutrients in the region. After export of poultry products, what remains in the region is nutrient rich poultry litter, which is bulky and expensive to export. Therefore, the poultry litter is applied to nearby pastures as an

inexpensive fertilizer, and over time results in elevated STP with an increasing risk of P loss to streams and reservoirs.

Nonpoint source P pollution became a major focus in the 1970's and 1980's, after it was discovered that reducing point source pollution did not significantly improve water quality in many watersheds (Crowder and Young, 1988). Unlike point source loads, nonpoint source load reduction is much more difficult and complex (Sims and Sharpley, 2005). The design and implementation of agricultural conservation practices to reduce P in runoff, such as buffer strips, riparian zones, terracing, and cover crops, are site specific and may be difficult to implement as economic, social, and political considerations affect farmers' willingness to adopt and maintain these practices (Sharpley et al*.,* 2003; Sims and Sharpley, 2005).

Like in the 1970's and 1980's where the focus was on the easily measurable and reducible point sources, implementation of riparian buffer zones and other conservation practices currently focus on the more easily understood and observable surface runoff mechanism (Lacas et al., 2005; Popov et al*.*, 2005; Reichenberger et al., 2007; Poletika et al*.*, 2009; Sabbagh et al., 2009). Although conservation practices can reduce P in surface runoff, the movement of subsurface P and its contribution to the receiving stream system may need to be considered. Studies have shown that subsurface nutrient transport can be significant in soils with spatially variable hydraulic conductivity (Carlyle and Hill, 2001), preferential flow pathways (McCarty and Angier, 2001; Polyakov et al., 2005; Fuchs et al., 2009; Heeren, et al., 2010a), and limited soil sorption capacity (Cooper et al., 1995; Carlyle and Hill, 2001; Polyakov et al., 2005). For example, Storm et al*.* (2009) used Soil and Water Assessment Tool (SWAT) (Arnold et al*.,* 1998) to model the Illinois River basin in eastern Oklahoma and western Arkansas. They estimated 7% of nonpoint source P contributions were derived from baseflow compared to 22% due to surface runoff from application of poultry litter.

The objective of this project was to compare subsurface P flux from two field sites in northeastern Oklahoma (Barren Fork Creek and Honey Creek) to the surface runoff P loads based on simulations of the Pasture Phosphorus Management Calculator (PPM Plus) (White, 2007; White et al., 2009; White et al., 2010). Based on long term monitoring of water elevation and P concentrations at the two field sites, the subsurface P capacity was quantified and compared to the total P surface runoff loads predicted by PPM Plus.

## Materials and Methods

### *Barren Fork Creek and Honey Creek Floodplain Sites*

The two floodplain sites were located in the Ozark ecoregion of northeastern OK. The Barren Fork Creek (Figures 2.6 and 3.1a, latitude: 35.90°, longitude: -94.85°) and Honey Creek sites (Figures 2.7 and 3.1b, latitude: 36.54°, longitude: -94.70°) were immediately downstream of U.S. Geological Survey (USGS) gage stations 07197000 and 07189542, respectively. With a watershed size of 845 $km^2$, the Barren Fork Creek site had a median daily flow of 3.6 $m^3 s^{-1}$. As a smaller order stream, Honey Creek site had a 0.54 $m^3 s^{-1}$ median daily flow and a 150 $km^2$ watershed. Both floodplain sites consisted of alluvial gravel deposits underlying a mantle of topsoil (Razort gravelly loam). The Barren Fork site's topsoil thickness ranged from 0.5 to 1.0 m with a STP of 33 mg/kg. The alluvial floodplain consisted of a hay field with no fertilizer applied in recent years and had an area of 2.7 ha with a 0.004% slope. The site at Honey Creek had a topsoil thickness ranging from 0.1 to 0.5 m and a higher STP level of 60 mg/kg due to historical poultry litter application. It consisted of 3.2 ha with a 0.01% slope; 1.5 ha was forest along the stream and the remainder was hay field.

### *Subsurface P Sampling*

Based on geophysical mapping of the subsurface, twenty-four observation wells were located and installed at each site (Figure 3.1). Assuming a positive correlation between electrical resistivity and saturated hydraulic conductivity (*K*), the well locations were selected in both PFP and non-PFP subsoils (Chapter 2; Miller et al., 2010). Using a peristaltic pump, groundwater samples were collected during high flow events. Samples were preserved on ice, transported back to the laboratory and digested based on the sulfuric acid-nitric acid method (Pote et al., 2009). Total phosphorus concentrations were determined colorimetrically (Murphy and Riley, 1962; EPA Method 365.2) with a spectrophotometer (Spectronic 21D, Milton Roy, Ivyland, PA).

### *Monte Carlo Simulations to Estimate Subsurface Transport Capacity*

The subsurface P transport capacity was defined as the average subsurface load crossing the down-gradient boundary of the observation well field at each field site (i.e., the south boundary at the Barren Fork Creek site and the northwest boundary at the Honey Creek site). Each down-gradient boundary consisted of one PFP. Subsurface P load was calculated by first determining the average groundwater flow based on Darcy's Law:

$$Q = qA = \left( -K \frac{\partial h}{\partial x} \right) wd = (Ki) wd \tag{5.1}$$

where *Q* is the groundwater discharge ($L^3/T$), *q* is the Darcy velocity (L/T), *K* is the saturated hydraulic conductivity (L/T), *h* is the groundwater head (L), *x* is the spatial direction (L), *A* is the cross-sectional area ($L^2$), *w* is the width of the monitored boundary or groundwater flow domain (L), *d* is the depth of the aquifer (L), and *i* is the average groundwater gradient (L/L). Note that equation (5.1) was applied separately to the single PFP and the non-PFP groundwater domain crossing the selected boundary at each field site with their site specific width (*w*) and depth (*d*) of the aquifer domain. The P transport capacity, $m_p$, (M/T) was then calculated using the following equation:

$$m_P = Q \times TP \times n_d \tag{5.2}$$

where TP is the total P concentration ($M/L^3$) measured from observation wells in the PFP and non-PFP domains, and $n_d$ is the number of days per year in which each groundwater flow domain was activated.

Monte Carlo simulations were performed using 10,000 realizations of subsurface transport capacity due to uncertainty in several variables. The distributions and parameters of those distributions for the input variables are shown in Table 5.1. Distributions for *K* were estimated based on electrical resistivity measurements correlated to point measurements of *K* as reported in Chapter 2. A normal distribution after a power function transformation was used to quantify the *K* distribution. The aquifer width, *w*, was held constant for each field site for the non-PFP domain, but varied for the PFP domain based on a uniform distribution. The *w* of the PFP was varied since ERI data was not available for the entire floodplain site; therefore, the *w* of the PFP may be smaller or larger than estimated based on the available data. The distribution for *d* was assumed uniform for both PFP and non-PFP domains. Differences in *d* between the PFPs and non-PFPs were identified based on electrical resistivity mapping of high *K* zones at each field site (Chapter 2; Miller et al., 2010). The non-PFP domain was assumed active for 365 days; therefore a fixed value was used for these calculations. The PFP activity was quantified based

on the minimum stream stage that resulted in PFP activation during the study period (Chapter 4; Heeren et al., 2010b). This parameter distribution was derived from 60 yr and 11 yr of daily mean streamflow measurements by the U.S. Geological Survey (USGS) at the Barren Fork Creek and Honey Creek sites, respectively. For the Barren Fork Creek and Honey Creek field sites, this stage corresponds to flows of 43 and 5.7 $m^3 s^{-1}$, respectively. A lognormal distribution was used for $n_d$ for PFP activation. Transport capacity or load was therefore highly dependent on $n_d$. Uniform distributions were also used for *i* and TP with unique *i* and TP for the PFPs and non-PFPs. The *i* and TP distributions were derived from the groundwater level data and P concentrations measured in the observation well fields with higher *i* and TP for the PFP domains due to their activation during storm events (Chapter 3 and 4; Heeren et al., 2010b).

Table 5.1. Distributions and their statistics for input parameters used in the Monte Carlo simulations at both the Barren Fork Creek (BFC) and Honey Creek (HC) field sites. Note that unique distributions were used for the single preferential flow pathway (PFP) and the non-preferential flow (non-PFP) domain.

| Parameter | Site | Flow Domain | Distribution | Statistics |
|---|---|---|---|---|
| Saturated Hydraulic Conductivity (m/d) | BF | Non-PFP | Normal after power function ($\lambda^a$ =-0.62) | $\mu_x^b$=0.13; $\sigma_x^b$=0.04 |
| | | PFP | Normal after power function (λ=-0.62) | $\mu_x$=0.13; $\sigma_x$=0.04 |
| | HC | Non-PFP | Normal after power function (λ=0.23) | $\mu_x$=2.3; $\sigma_x$=0.17 |
| | | PFP | Normal after power function (λ=0.23) | $\mu_x$=2.3; $\sigma_x$=0.17 |
| Groundwater Gradient (m/m) | BFC | Non-PFP | Uniform | Min=0.0005; Max=0.0015 |
| | | PFP | Uniform | Min=0.0015; Max=0.0025 |
| | HC | Non-PFP | Uniform | Min=0.0005; Max=0.0015 |
| | | PFP | Uniform | Min=0.0015; Max=0.0025 |
| Aquifer Depth (m) | BFC | Non-PFP | Uniform | Min=2.0; Max=3.0 |
| | | PFP | Uniform | Min=1.5; Max=2.5 |
| | HC | Non-PFP | Uniform | Min=0.25; Max=1.0 |
| | | PFP | Uniform | Min=0.5; Max=1.5 |
| Domain Width (m) | BFC | Non-PFP | Fixed | 150 |
| | | PFP | Uniform | Min=5.0; Max=10 |
| | HC | Non-PFP | Fixed | 65 |
| | | PFP | Uniform | Min=2.0; Max=4.0 |
| Total Phosphorus Concentration (mg/L) | BFC | Non-PFP | Uniform | Min=2.0; Max=3.0 |
| | | PFP | Uniform | Min=1.5; Max=2.5 |
| | HC | Non-PFP | Uniform | Min=0.25; Max=1.0 |
| | | PFP | Uniform | Min=0.5; Max=1.5 |
| Activity (d) | BFC | Non-PFP | Fixed | 365 |
| | | PFP | Lognormal | $\mu_x$=2.19; $\sigma_x$=1.02 |
| | HC | Non-PFP | Fixed | 365 |
| | | PFP | Lognormal | $\mu_x$=1.34; $\sigma_x$=1.17 |

[a] λ = exponent for the power transformation of the original distribution.

[b] $\mu_x$ , $\sigma_x$ = mean and standard deviation for the normal and lognormal distributions.

### *PPM Plus Simulations*

PPM Plus is a software tool which predicts the average amount of P and sediment lost from an agricultural field in Oklahoma (White, 2007; White et al., 2009; White et al., 2010). It predicts the average annual P and sediment load delivered to the nearest stream from a single agricultural field using a region-specific, 15-yr weather period. PPM Plus can be used to simulate a myriad of management options by accounting for detailed field characteristics and land management. PPM Plus is based on Soil and Water Assessment Tool (SWAT) (Arnold et al., 1998); a product of more than 30 years of model development by the U.S. Department of Agriculture, Agricultural Research Service. Models like SWAT are primarily used by highly trained specialists and are too complex for use by most conservation and nutrient management planners. PPM Plus simplifies the operation of SWAT to put the predictive power of one of our best water quality models into the hands of people who make daily decisions that affect water quality. Therefore, due to its ease of use and applicability, PPM Plus was selected to estimate the average annual P loss from the two field sites (Table 5.2).

Table 5.2. High and low intensity agricultural production scenario PPM Plus inputs for the Barren Fork Creek and Honey Creek field sites.

| Input Parameter | Barren Fork Creek | Honey Creek |
|---|---|---|
| | *Inputs Common to Both Scenarios* | |
| Land Use | Pasture | Pasture |
| Field Area (ha) | 2.7 | 1.7 |
| Riparian Buffer Area (ha) | 0 | 1.5 |
| Riparian Buffer Width (m) | 0 | 53 |
| Field Slope (%) | 0.004 | 0.01 |
| Field Slope Length (m) | 120 | 120 |
| Distance to Stream (m) | 0 | 0 |
| Mehlich III STP (mg/kg) | 30 | 66 |
| Soil Type | Razort Gravelly Loam | Razort Gravelly Loam |
| Forage Type | Mixed Warm and Cool Season Grasses | Mixed Warm and Cool Season Grasses |
| | *Low Intensity Agricultural Production Scenario* | |
| Grazing Density (AU/acre) | 0 | 0 |
| Management Operation | Hay - August | Hay - August |
| | *High Intensity Agricultural Production Scenario* | |
| Grazing Density (AU/ha) | 1.2 | 1.2 |
| Grazing Duration | 365 Days with Supplemental Feed | 365 Days with Supplemental Feed |
| Forage Management | Optimally Managed | Optimally Managed |
| Fertilization | 6 Mg/ha Poultry Litter March 1 | 6 Mg/ha Poultry Litter March 1 |

PPM Plus was parameterized for the Barren Fork Creek and Honey Creek field sites for two scenarios (Table 5.2). The first scenario represented low intensity agricultural production for pasture without any cattle grazing, which was the current land use. The only agricultural activity was hay removal scheduled for August. The second scenario represented high-intensity agricultural production for pasture with a high stocking rate of 1.2 animal units (AU) per ha and a 6 Mg/ha poultry litter application rate in March to meet the nitrogen requirements for a 9000 kg $ha^{-1}$ forage yield goal (Zhang et al., 2009).

## Results and Discussion

Based on the Monte Carlo simulations, the estimated mean total subsurface P load transport capacity (i.e., annual load) of the non-PFP flow domain at the Barren Fork Creek field site was 0.10 kg $yr^{-1}$. This compared to a mean of 0.02 kg $yr^{-1}$ from the single PFP. The total P load from surface runoff based on the PPM Plus simulations was 0.46 kg $yr^{-1}$ from the current conditions and 14.0 kg $yr^{-1}$ with litter application and cattle grazing (Figure 5.1a). At the Honey Creek site, the estimated mean subsurface P transport capacity (i.e., annual load) was 0.02 kg $yr^{-1}$, respectively, in the non-PFP domain and 0.0005 kg $yr^{-1}$ in the single PFP. These results compared to 0.67 kg $yr^{-1}$ of surface P runoff based on current site conditions and 9.8 kg $yr^{-1}$ of surface P runoff with poultry litter application and cattle grazing (Figure 5.1b).

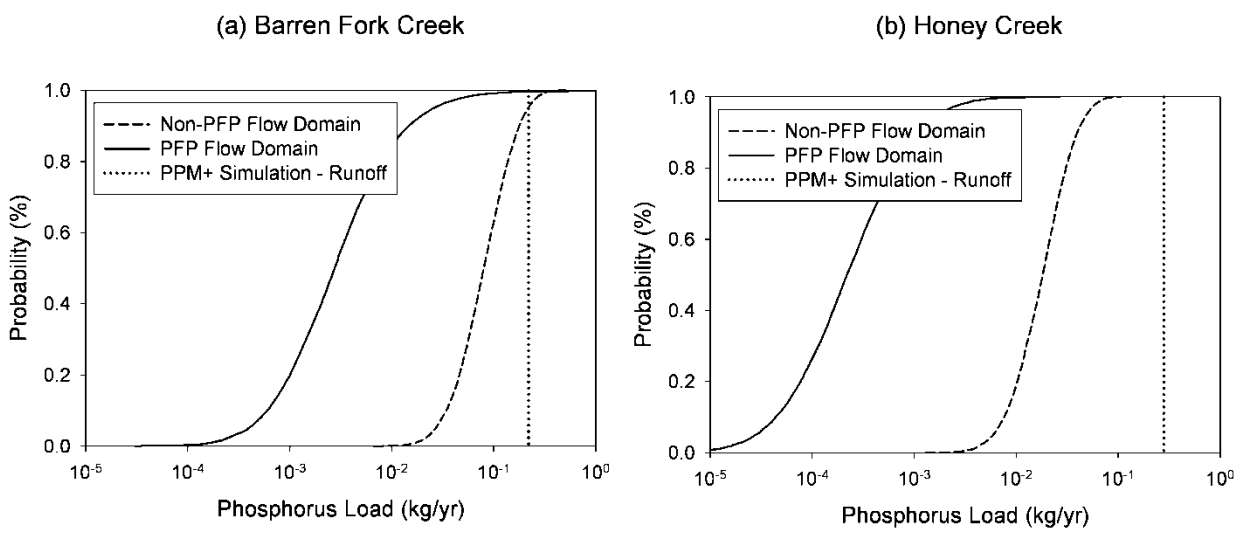


Figure 5.1. Total phosphorus load capacity of subsurface with a single PFP based on Monte Carlo simulations and total phosphorus loads of surface runoff based on PPM Plus simulations at the Barren Fork Creek and Honey Creek field sites. Note that the PFP flow domain consists of a single PFP at the boundary of the ground water system. PFP = preferential flow pathways; non-PFP = non-preferential flow.

The Honey Creek site had a smaller subsurface P transport capacity due to a smaller aquifer cross-sectional area (both in terms of *d* and *w*) and *K* than the Barren Fork Creek site. As the stream order increased, *d* and *K* increased due to larger gravel deposits. The size of the PFP was larger at the Barren Fork Creek site making the P load higher than at Honey Creek, the smaller order stream.

These results demonstrated that the subsurface P capacity was in the same order of magnitude relative to the surface runoff P load at the current site conditions, yet was small compared to the simulation with poultry litter application and cattle grazing. Though the total P capacity was small in the single PFP due to the small area and number of days active, it may provide rapid transport from the ground surface to the aquifer and then from the aquifer to the stream. In areas where there is a larger number (and area) of PFPs or during years where the PFP remains active for longer periods of time, the PFPs may provide a larger P transport capacity. For example, the P load transport capacity at the 99th percentile of the Monte Carlo simulations was 0.10 kg $yr^{-1}$ in the single PFP at the Barren Fork Creek, or over 25% of the surface runoff P load from the current conditions. The Illinois River, the stream which both creeks are tributaries of, may have a deeper aquifer, higher *K*, and larger PFPs than the Barren Fork Creek, resulting in a higher subsurface P capacity. Therefore, as the stream order increases, the significance of subsurface P capacity and PFPs may also increase.

These results indicated that the subsurface P capacity of alluvial floodplains in the Ozark ecoregion was at least $10^{-2}$ to $10^{-1}$ kg $yr^{-1}$. The capacity may be higher in cases where the subsurface is connected to a larger source of P. The field data used in this analysis did not include P concentrations in alluvial aquifers below floodplains with poultry litter application or cattle production. Further work is needed to quantify P leaching through the surface topsoil, potentially resulting in additional subsurface P loads.

## Conclusion

Research has shown that subsurface P contributions can be significant in soils with spatial variability in hydraulic conductivity, preferential flow pathways, and limited sorption capacity in riparian zone soils. This study estimated subsurface P transport capacity as quantified by annual P load crossing the outflow boundary of two groundwater systems, with uncertainty parameters quantified through Monte Carlo simulations. The subsurface P transport capacity was compared to surface runoff loads based on simulations of the PPM Plus. Results suggested that the subsurface P transport capacities were significant compared to surface runoff P loads at low intensity agricultural field sites. Though the subsurface contributions were small compared to the PPM Plus simulations with poultry litter and cattle grazing, the sites in this study did not have poultry litter application or cattle grazing. Therefore, the measured subsurface P transport included a relatively small amount of P leaching from the surface. Future work needs to quantify P leaching through the soil from a surface P source and determine whether this significantly elevates levels of subsurface P transport. It is hypothesized that as the stream order increases, the significance of subsurface P transport capacity and preferential flow pathways also increases.

## References

Arnold, J.G., R. Srinivasan, R.S. Muttiah, and J.R. Williams. 1998. Large area hydrologic model development and assessment part 1: Model development. *Journal of the American Water Resources Association* 34(1): 73-89.

Carlyle, G.C., and A.R. Hill. 2001. Groundwater phosphate dynamics in a river riparian zone: Effects of hydrologic flow paths, lithology, and redox chemistry. *Journal of Hydrology* 247(3-4):151-168.

Cooper, A.B., C.M. Smith, and M.J. Smith. 1995. Effects of riparian set-aside on soil characteristics in an agricultural landscape: Implications for nutrient transport and retention. *Agriculture, Ecosystems, and Environment* 55(1): 61-67.

Crowder, B., and C.E. Young. 1988. Managing farm nutrients: Tradeoffs for surface and ground water quality. Agric. Econ. Rep. 583. USDA, U. S. Gov. Print. Office, Washington, DC.

Fuchs, J.W. G.A. Fox, D.E. Storm, C. Penn, and G.O. Brown. 2009. Subsurface transport of phosphorus in riparian floodplains: Influence of preferential flow paths. *Journal of Environmental Quality* 38(2): 473-484.

Heeren, D.M., R.B. Miller, G.A. Fox, D.E. Storm, T. Halihan, and C.J. Penn. 2010a. Preferential flow effects on subsurface contaminant transport in alluvial floodplains. *Transactions of the ASABE* 53(1): 127-136.

Heeren, D.M., R.B. Miller, G.A. Fox, D.E. Storm, A.R. Mittelstet, and C.J. Penn. 2010b. Impact of preferential flow paths on alluvial groundwater flow patterns and phosphorus transport in the Ozark Ecoregion. ASABE Paper No. 1008729. St. Joseph, Mich.: ASABE.

Lacas, J.-G., M. Voltz, V. Gou, N. Carluer, and J.-J. Gril. 2005. Using grassed strips to limit pesticide transfer to surface water: A review. *Agronomy for Sustainable Development* 25(2): 253-266.

McCarty, G., and J. Angier. 2001. Impact of preferential flow pathways on ability of riparian wetlands to mitigate agricultural pollution. In *Proc. 2nd Intl. Symp. On Preferential Flow: water Movement and Chemical Transport in the Environment,* 53-56. D. Bosch and K. King. Eds. St. Joseph, Mich.: ASAE.

Miller, R.B., D.M. Heeren, G.A. Fox, D.E. Storm, T. Halihan, and A.R. Mittelstet. 2010. Geophysical mapping of preferential flow paths across multiple floodplains. ASABE Paper No. 1008730. St. Joseph, Mich.: ASABE.

Murphy, J., and J.P. Riley. 1962. A modified single solution method for the determination of phosphate in natural waters. *Analytica Chimica Acta* 27: 31-36.

NRCS (Natural Resource Conservation Service). 1994. The phosphorus index: A phosphorus assessment tool. United States Department of Agriculture, Natural Resources Conservation Service. http://nrcs.usda.gov/TECHNICAL/ECS/nutrient/pindex.html, *accessed* on April 14th, 2010.

Poletika, N.N., P.N. Coody, G.A. Fox, G.J. Sabbagh, S.C. Dolder, and J. White. 2009. Chlorpyrifos and atrazine removal from runoff by vegetated filter strips: Experiments and predictive modeling. *Journal of Environmental Quality* 38(3): 1042-1052.

Polyakov, V., A. Fares, and M.H. Ryder. 2005. Precision riparian buffers for the control of nonpoint-source pollutant loading into surface water: A review. *Environmental Review* 13(3): 129-144.

Popov, V.H., P.S. Cornish, and H. Sun. 2005. Vegetated biofilters: The relative importance of infiltration and adsorption in reducing loads of water-soluble herbicides in agricultural runoff. *Agriculture, Ecosystems and Environment* 114(2-4): 329-347.

Pote, D.H., T.C. Daniel, and P.B. DeLaune. 2009. Total phosphorus and total dissolved phosphorus in water samples. In *Methods of Phosphorus Analysis for Soils, Sediments, Residuals, and Waters*, 113-114. J.L. Kovar and G.M. Pierzynski, eds. Blacksburg, Va.: SERA-IEG 17, Virginia Tech University.

Reichenberger, S., M. Bach, A. Skitschak, and H.-G. Frede. 2007. Mitigation strategies to reduce pesticide inputs into ground- and surface water and their effectiveness: A review. *Science of the Total Environment* 384: 1-35.

Sabbagh, G.J., G.A. Fox, A. Kamanzi, B. Roepke, and J.Z. Tang. 2009. Effectiveness of vegetative filter strips in reducing pesticide loading: Quantifying pesticide trapping efficiency. *Journal of Environmental Quality* 38(2): 762-771.

Sharpley, A.N., T. Daniel, T. Sims, J. Lemunyon, R. Stevens, and R. Parry. 2003. Agricultural phosphorus and eutrophication. 2nd ed. ARS-149. USDA, Washington, DC.

Sims, J.T. and A.N. Sharpley. 2005. *Phosphorus: Agriculture and the Environment*. Agronomy Monograph No. 46. American Society of Agronomy, Crop Science Society of America, Soil Science Society of America: Madison, Wis., USA.

Storm, D.E., P.R. Busteed, A.R. Mittelstet, and M.J. White. 2009. Hydrologic modeling of the Oklahoma/Arkansas Illinois River basin using SWAT 2005: Final report submitted to the Oklahoma Department of Environmental Quality. Biosystems and Agricultural Engineering Department, Division of Agricultural Sciences and Natural Resources, Oklahoma State University, October 8, 2009.

White, M. 2007. Development and validation of a quantitative phosphorus loss assessment tool. Ph.D. Dissertation. Biosystems and Agricultural Engineering Department, Oklahoma State University: Stillwater, OK.

White, M.J., D.E. Storm, M.D. Smolen, and H. Zhang. 2009. Development of a quantitative pasture phosphorus management tool using the SWAT model. *Journal of the American Water Resources Association* 45(2): 397-406.

White, M.J., D.E. Storm, P.R. Busteed, M.D. Smolen, H. Zhang, and G.A. Fox. 2010. A quantitative phosphorus loss assessment tool for agricultural fields. *Environmental Modelling and Software* (In Press).

Zhang, H., D.W. Hamilton, and J. Payne. 2009. Using poultry litter as fertilizer. Oklahoma Cooperative Extension Service PSS-2246, Oklahoma State University. http://www.poultrywaste.okstate.edu/files/pss-2246web.pdf, Accessed April 16th, 2010.

# APPENDIX A
# QUALITY ASSURANCE REPORT

Electrical resistivity mapping was overseen by Dr. Halihan. All personnel collecting and analyzing data were trained with appropriate field and laboratory procedures. Three-dimensional mapping of the alluvial floodplain subsurface was developed at each field site.

In order to install observation wells in both PFP and non-PFP soils, wells were located based on electrical resistivity results. Without properly locating observation wells within the pathways, general groundwater monitoring may have never indicated this preferential flow and transport. Quality control for water table measurements was achieved by proper installation, calibration, operation and maintenance of pressure transducers and data loggers.

Sampling, testing, and analysis of all water samples were overseen by Dr. Penn. All field technicians were trained for proper sample handling, preventative maintenance, repeatability, and sample custody procedures. Water samples were stored in an ice box in the field and during transport back to the lab.

Samples were digested with the sulfuric acid-nitric acid method (Pote et al., 2009). Total P concentrations were determined colorimetrically (Murphy and Riley, 1962; EPA Method 365.2) with a spectrophotometer (Spectronic 21D, Milton Roy, Ivyland, PA). Samples in addition to the data presented in Chapter 4 were collected but were not considered in the analysis due to concerns about the calibration curve that was used at that time.

The precision and bias of sample handling were assessed using field blanks and duplicates. The data quality objectives for sample handling were as follows:

Table A.1. Data quality objectives.

| QC Test | Frequency | Results | Objective |
|---|---|---|---|
| Field Blanks | Once per field visit | Accuracy Bias | < 115% MDL |
| Field Duplicates | Once per field visit | Standard Deviation | ±10% |

Sample handling QC checks were performed by the analysis of one field blank per sampling event. The blank was logged into the laboratory and analyzed in the same way as the other samples. Sampling precision was checked by taking one duplicate sample per sampling event, and standard deviations were calculated from these duplicates. Results indicate that 83% of the blanks were less than 115% of a minimum detection limit (MDL) of 0.01 mg/L, and that 71% of the pairs of duplicates had a standard deviation less than 10% of their mean.

# APPENDIX B
# USDA NRCS WEB SOIL SURVEY MAPS

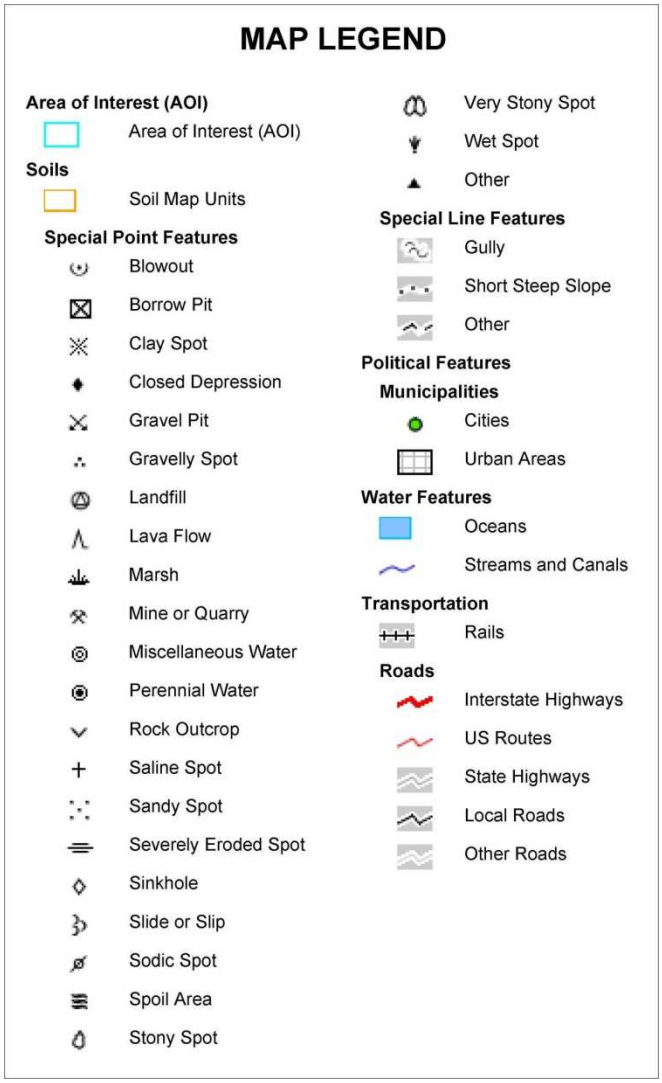

# Barren Fork Creek Site

## Map Unit Legend

| Cherokee County, Oklahoma (OK021) | | | |
|---|---|---|---|
| **Map Unit Symbol** | **Map Unit Name** | **Acres in AOI** | **Percent of AOI** |
| ClF | Clarksville stony silt loam, 20 to 50 percent slopes | 5.0 | 21.3% |
| Es | Elsah very gravelly loam, 0 to 3 percent slopes, frequently flooded | 7.4 | 31.6% |
| SgD | Britwater gravelly silt loam, 3 to 8 percent slopes | 1.3 | 5.6% |
| Sm | Healing silt loam, 0 to 1 percent slopes, occasionally flooded | 0.2 | 0.9% |
| Sn | Razort gravelly loam, 0 to 3 percent slopes, occasionally flooded | 7.8 | 33.3% |
| TrD | Shidler-Rock outcrop complex, 2 to 8 percent slopes | 1.7 | 7.3% |
| Totals for Area of Interest (AOI) | | 23.4 | 100.0% |

Sm
Es
TrD
CIF
SgD
Sn
E0770 RD
332400
332460
332520
332580
332640
332700
332760
332820
332880
332940
397480
397420
397360
397300
397240
397180
397120
N
0
50
100
200
300
Meters
0
200
400
800
1,200
Feet

# Flint Creek Site

## Map Unit Legend

| Delaware County, Oklahoma (OK041) | | | |
|---|---|---|---|
| **Map Unit Symbol** | **Map Unit Name** | **Acres in AOI** | **Percent of AOI** |
| ClF | Clarksville stony silt loam, 20 to 50 percent slopes | 1.9 | 5.9% |
| Es | Elsah very gravelly loam, 0 to 3 percent slopes, frequently flooded | 8.4 | 26.2% |
| SaB | Britwater silt loam, 1 to 3 percent slopes | 2.6 | 8.1% |
| SgD | Britwater gravelly silt loam, 3 to 8 percent slopes | 3.8 | 12.0% |
| Sm | Healing silt loam, 0 to 1 percent slopes, occasionally flooded | 4.4 | 13.9% |
| Sn | Razort gravelly loam, 0 to 3 percent slopes, occasionally flooded | 6.9 | 21.7% |
| W | Water | 3.9 | 12.2% |
| Totals for Area of Interest (AOI) | | 31.9 | 100.0% |

346260
346320
346380
346440
346500
346560
346620
4007520
4007460
4007400
4007340
4007280
4007220
4007160
4007100
Sn
ClF
Sm
Es
Es
W
SgD
Flint Creek
Sn
Sn
D0567 RD
SaB
SaB
SgD
ES
VIRGIL TALBOT MEMORIAL HWY
N
Meters
0
35
70
140
210
Feet
0
150
300
600
900

# Honey Creek Site

## Map Unit Legend

| Delaware County, Oklahoma (OK041) | | | |
|---|---|---|---|
| **Map Unit Symbol** | **Map Unit Name** | **Acres in AOI** | **Percent of AOI** |
| BhB | Doniphan gravelly silt loam, 1 to 3 percent slopes | 2.6 | 0.9% |
| CkD | Clarksville very gravelly silt loam, 1 to 8 percent slopes | 38.7 | 13.0% |
| ClE | Clarksville stony silt loam, 5 to 20 percent slopes | 2.6 | 0.9% |
| ClF | Clarksville stony silt loam, 20 to 50 percent slopes | 45.2 | 15.2% |
| SgD | Britwater gravelly silt loam, 3 to 8 percent slopes | 16.9 | 5.7% |
| Sm | Healing silt loam, 0 to 1 percent slopes, occasionally flooded | 60.6 | 20.4% |
| Sn | Razort gravelly loam, 0 to 3 percent slopes, occasionally flooded | 130.5 | 43.9% |
| Totals for Area of Interest (AOI) | | 297.2 | 100.0% |

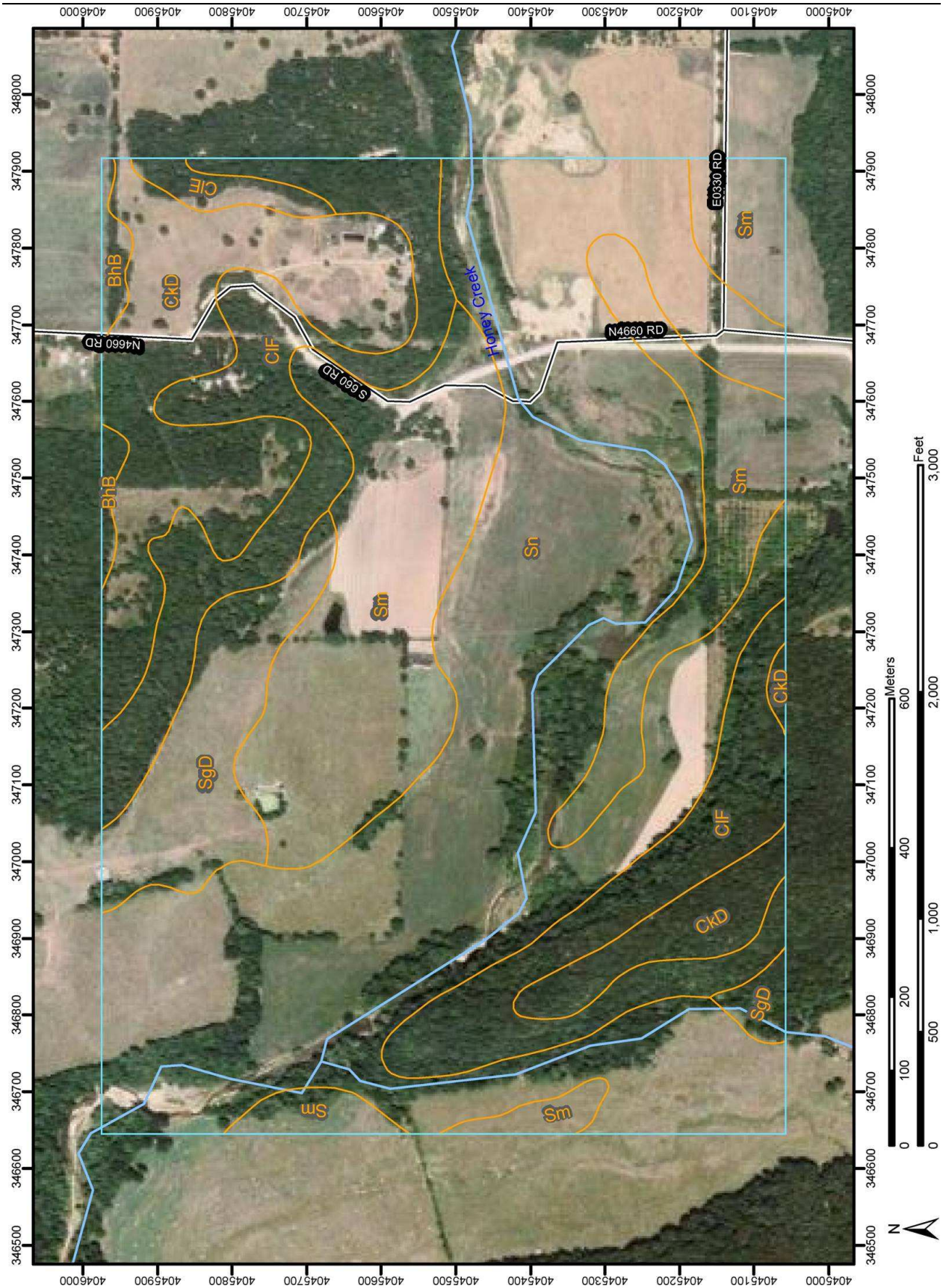
N4660 RD
S 660 RD
E0330 RD
Honey Creek
BhB
CkD
ClF
Sm
Sn
SgD
Meters
Feet
N

# Pumpkin Hollow Site

## Map Unit Legend

| Cherokee County, Oklahoma (OK021) | | | |
|---|---|---|---|
| **Map Unit Symbol** | **Map Unit Name** | **Acres in AOI** | **Percent of AOI** |
| ClF | Clarksville stony silt loam, 20 to 50 percent slopes | 13.9 | 42.9% |
| Es | Elsah very gravelly loam, 0 to 3 percent slopes, frequently flooded | 8.2 | 25.4% |
| SgD | Britwater gravelly silt loam, 3 to 8 percent slopes | 4.8 | 14.7% |
| Sn | Razort gravelly loam, 0 to 3 percent slopes, occasionally flooded | 5.5 | 17.0% |
| **Totals for Area of Interest** | | **32.4** | **100.0%** |

336780
336840
336900
336960
337020
337080
3987360
3987300
3987240
3987180
3987120
3987060
3987000
3986940
CIF
Es
Sn
Pumpkin Hollw
SgD
CIF
CIF
94° 48' 42"
94° 48' 26"
N
Map Scale: 1:2,530 if printed on A size (8.5" x 11") sheet.
Meters
0 20 40 80 120
Feet
0 50 100 200 300

# APPENDIX C
# FEMA 2009 FLOODPLAIN MAPS

## Barren Fork Creek Site

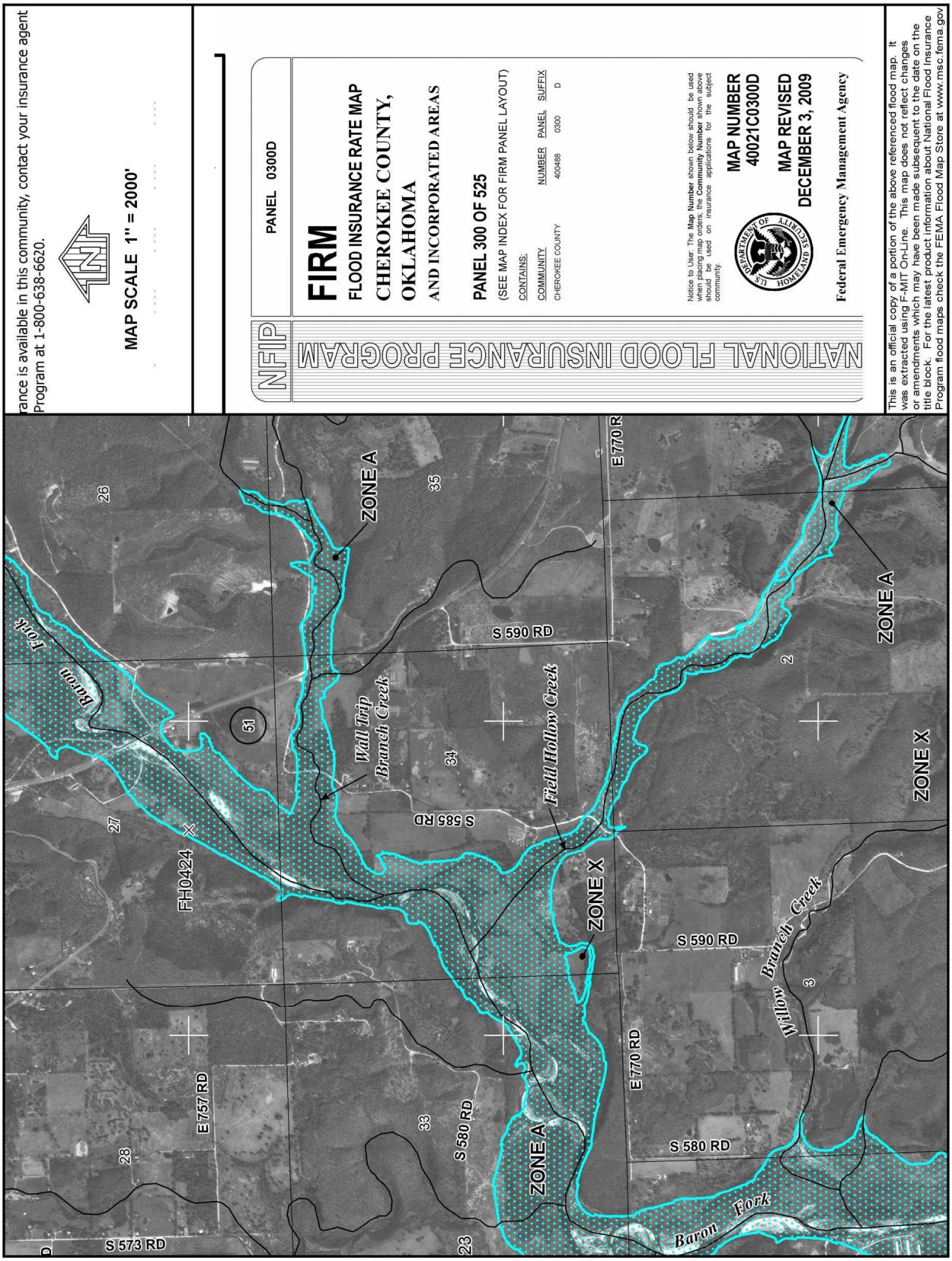

## Flint Creek Site

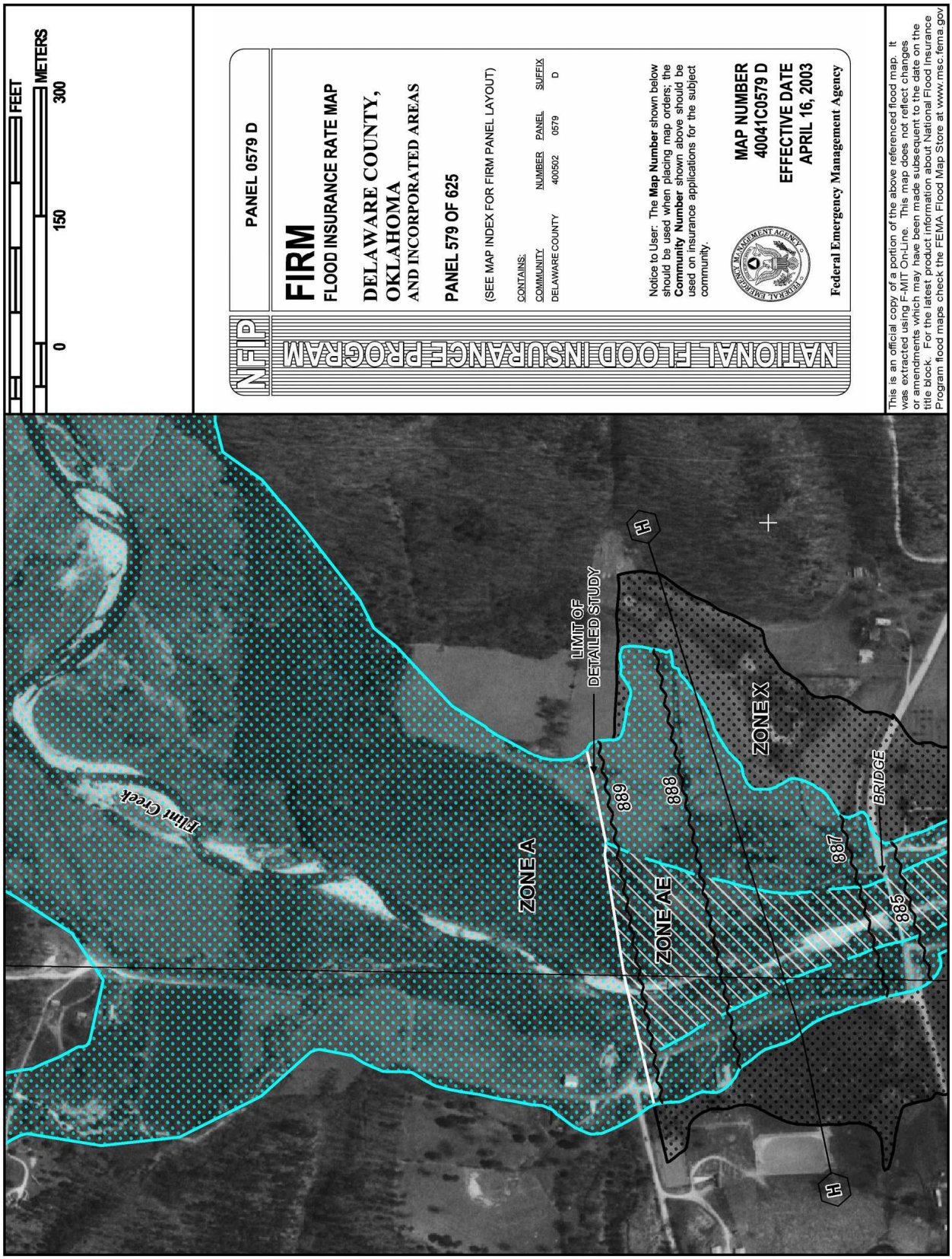

## Honey Creek Site

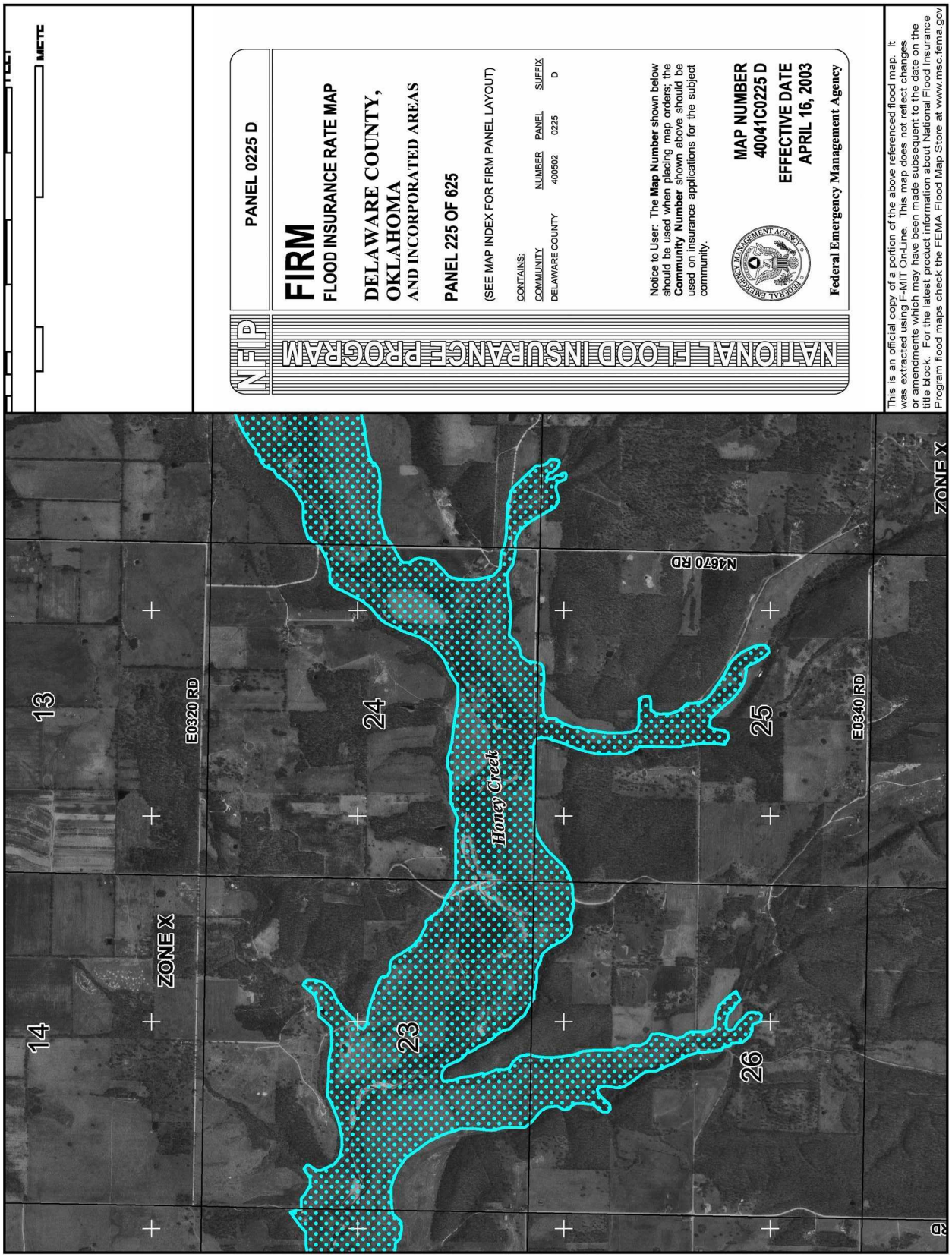
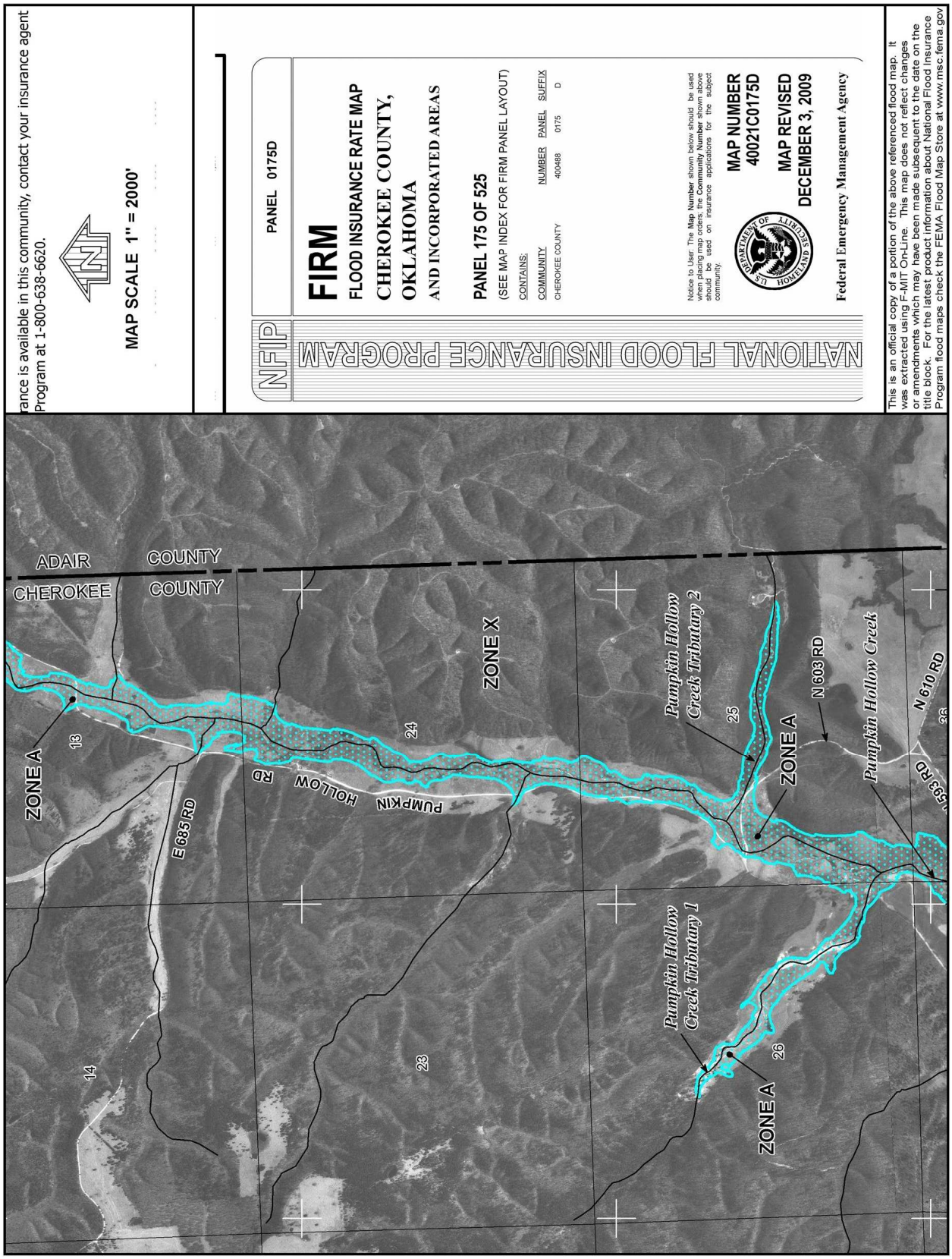
## Pumpkin Hollow Site